

University of Natural Resources and Life Sciences, Vienna

Department of Biotechnology
Institute of Applied Microbiology
Vienna Institute of Biotechnology

Effect of different sugar substrates on relevant culture parameters in a recombinant IgM production process using CHO cells

Master thesis

For obtaining the academic degree

Master of Science

Submitted by

Moritz Kramann, Bakk. techn.

Supervisor: Univ.Prof. Dr. Renate Kunert

Co-supervisor: Dr. David Reinhart

Wien, July 2015



Acknowledgements

I am much obliged to my fellow colleagues for always giving competent and helpful advice and providing constant support throughout the project.

Special thanks also goes to my family and friends who supported me during the academic studies at all times.

Abstract

About 70% of all nowadays recombinantly produced proteins are generated in CHO cells. One of the most popular protein class produced in CHO cells are immunoglobulins (antibodies). Although immunoglobulin G (IgG) is the most prominent therapeutic antibody class that is recombinantly produced, immunoglobulin M (IgM) is becoming more and more evaluated as a therapeutic and diagnostic drug due to its benefits such as higher avidity. Usually all production processes using CHO cells are based on glucose as sugar substrate. For the purpose of testing beneficial effects on the production of recombinant IgMs using CHO cells we investigated the application of alternative sugar substrates such as fructose, galactose, mannose, sucrose and trehalose in batch fermentations. The disaccharides sucrose and trehalose were of special interest, because of their protein stabilizing properties. Thus they were not only studied as substrates, but also as supplements. However, the CHO cells could not be grown on all alternative sugars, the adaption was only feasible for galactose and mannose. While mannose did not illustrate major noticeable differences, the replacement of glucose with galactose demonstrated promising impacts. A decrease in specific sugar consumption of about 50 % and the specific lactate production of about 80%, an undesirable growth inhibiting secondary metabolite, was observed when using galactose instead of glucose. Although the growth inhibiting production of lactate was minimized, the process demonstrated 33% lower growth, 33% shorter duration and 10% lower titers. The batch fermentations comparing the alternative carbon sources were conducted at 37°C and at 32°C. Running the process at reduced temperatures might lead to reduced cell metabolism, prolonged culture viability and thus ultimately to an increased recombinant IgM yield. Additionally to the product titer, the influence on important IgM quality criteria such as the isoform distribution and the glycosylation were investigated. Particularly the IgMs produced by cells grown on galactose revealed a different set of glycosylations and thus a potentially beneficial behaviour as therapeutics regarding immunological tolerance. With the purpose of designing a potentially large-scale production process, it was aimed to operate the experiments in bioreactors.

1 Table of Contents

2	Abbreviations	6
3	List of figures	9
4	List of tables	11
5	Introduction.....	12
6	Material and Methods	19
6.1	Cell Lines	19
6.2	Cultivation medium.....	19
6.3	Maintenance and cultivation conditions.....	20
6.4	Cell concentration	21
6.5	Viability.....	21
6.6	Metabolites.....	21
6.7	Adaption to different sugar sources	22
6.8	Batch experiments in shaking flasks and DASGIP module	22
6.9	Antibody quantification by ELISA.....	26
6.10	SDS-PAGE and Western Blot	28
6.11	Silver Staining.....	29
6.12	Intracellular Protein Content by Flow Cytometry	29
6.13	Glycosylation analysis by Mass Spectrometry (MS).....	31
6.14	List of Equipment and Reagents.....	32
6.15	Calculations.....	34
7	Results	36
7.1	Adaption of cell line A to alternative sugar sources	36
7.2	Batch 1 – determination of the optimal sugar concentration (cell line A).....	37
7.3	Batch 2 – investigating a potentially beneficial effect of sucrose or trehalose as supplement (cell line A)	44
7.4	Batch F49 – Comparison of different sugars in D/H medium with ProCHO5 in the DASGIP module and in shaker flasks (cell line A)	51
7.5	Batch F52 – Shaker batch experiments with temperature reduction to 32°C (cell line A).....	54
7.6	Batch F53 – Investigation of the bad performance of medium supplemented with galactose (cell line A)	63
7.7	Batch F54 – Fermentation with temperature reduction to 32°C (cell line B)	68
7.8	Batch F56 – Parameter screening in DASGIP bioreactors of cell line A.....	74
8	Discussion	78
8.1	Adaptation of cell lines to the alternative sugar substrates	78
8.2	Determination of the optimal sugar concentration.....	79
8.3	Sucrose and trehalose as supplements	79
8.4	Batch experiments and temperature reduction	79
8.5	Investigation of the bad performance of cell line A in medium supplemented with galactose	81
8.6	Product quality – isoform distribution and glycosylation	81
8.7	Mannose and galactose as alternative substrates.....	82

8.8	Batch experiments in the DASGIP module	83
9	Future perspectives	84
10	Bibliography.....	85
11	Appendix	87
11.1	Adaption of CHO cells (B) to alternative sugar substrates	87
11.2	Metabolic data for the batch F52.....	88
11.3	Metabolic data for the batch F54.....	91
11.4	Silver Staining.....	95
11.5	Cell-bank information sheets.....	96
11.6	Glycosylation analysis-report	99

2 Abbreviations

A	Galactose
BQ	Big squares
CC	Cell concentration [c/mL]
CD	Chemically defined
CDR	Complementarity determining region
CHO	Chinese hamster ovary
CS	Culture supernatant
D/H	DMEM/Ham`s F12
D0	Day of culture start
DHFR	Dihydrofolate reductase
DMEM	Dulbecco`s modified eagle medium
DO	Dissolved oxygen [% saturation]
DX	Day of culture termination
ELISA	Enzyme linked immunosorbent assay
ESI	Electron spray ionization
EtOH	Ethyl alcohol
F	Fucose
FACS	Flourescence-activated cell sorting
FITC	Fluorescin isothiocyanate
Gal	Galactose
Glc	Glucose
Gn	N-acetylgalactosamine
HEK	Human embryonic kidney
HMW	High molecular weight
HPLC	High performance liquid chromatography
HRP	Horseradish peroxidase
HS	Headspace
IgG	Immunoglobulin G
IgM	Immunoglobulin M

kDa	kilo Dalton
M	Mannose
Man	Mannose
MetOH	Methyl alcohol
MS	Mass spectrometry
MTX	Methotrexate
Na	N-acetylneuraminic acid
NAD	Nicotinamide adenine dinucleotide
NS0	Nonsecreting (mouse myeloma)
PAGE	Polyacrylamide gel electrophoresis
PBS	Phosphate-buffered saline
Pro	ProCHO5 Medium
PVDF	Polyvinylidene fluoride
qM	Specific metabolic rate [pg/c/d]
qP	Specific productivity [pg/c/d]
RO	Reverse osmosis
RPM	Rounds per minute
SA	Sialic acid
SDS	Sodium dodecylsulfate
SF	Serum free
SF125	125 mL shaking flask
STD	Standard
STY	Space time yield
T25	50 mL roux flask
TMB	Tetramethylbenzidine
UDP	Uridine diphosphate
VCC	Viable cell concentration [c/mL]
VCCD	Viable cumulative cell day [1/mL]
VCD	Viable cell day [1/mL]
w/o Glc	without glucose
WB	Western Blot

wGlc	with glucose
X	Xylose
μ	Specific growth rate [1/d]
μ_v	Viable specific growth rate [1/d]

3 List of figures

Figure 1: Structure of an IgM.....	14
Figure 2: Structures of the different sugars.	15
Figure 3: Metabolic pathway of the glycolysis.	16
Figure 4: Feeder pathways for glycolysis,.	17
Figure 5: Enzymatic reaction of pyruvate to lactate.....	18
Figure 6: Typical growth curve for CHO cells..	20
Figure 7: The course of the whole project from thawing the CHO cells to the batch experiments.....	23
Figure 8: More detailed view about the phase, where the CHO cells A have first been thawed and worked with. ...	23
Figure 9: More detailed view about the second phase, where the CHO cells A have been newly thawed and additional experiments were performed.	24
Figure 10: More detailed view about the CHO cells B that have been thawed along with the CHO cells A in the second phase.	24
Figure 11: Setup of the dilution plate.	27
Figure 12: Protein bands of the HiMark Pre-Stained HMW Protein Standard.....	29
Figure 13: The cell concentrations at the end of each passage before and after the cells have been passaged into new medium containing the alternative sugar substrates.	36
Figure 14: The viabilities at the end of each passage before and after the cells have been passaged into new medium containing the alternative sugar substrates.....	36
Figure 15: The cell concentrations as well as the viabilities over the time of the batch experiment as a comparison between the three different glucose concentrations.....	38
Figure 16: The viable cumulative cell days (VCCD) over the time of the batch experiment.....	38
Figure 17: The product titers over the time of the batch experiment as a comparison between the three different glucose concentrations.	39
Figure 18: The cell concentrations as well as the viabilities over the time of the batch experiment as a comparison between the three different galactose concentrations.	39
Figure 19: The viable cumulative cell days (VCCD) over the time of the batch experiment.....	40
Figure 20: The product titers over the time of the batch experiment as a comparison between the three different galactose concentrations.....	40
Figure 21: The cell concentrations as well as the viabilities over the time of the batch experiment as a comparison between the three different mannose concentrations.	41
Figure 22: The viable cumulative cell days (VCCD) over the time of the batch experiment.....	41
Figure 23: The product titers over the time of the batch experiment as a comparison between the three different mannose concentrations.	42
Figure 24: Consumption of glucose, galactose and mannose.....	42
Figure 25: Specific productivities as the average over the whole process..	43
Figure 26: The western blot.	44
Figure 27: Daily cell concentrations and viabilities of the shaking flasks supplemented with trehalose at different concentrations along with the control (CHO cells A).	45
Figure 28: The viable cumulative cell days (VCCD) over the time of the batch experiment.....	46
Figure 29: Daily product titers of the shaking flasks supplemented with trehalose at different concentrations along with the control (CHO cells A).....	46
Figure 30: Average specific productivities over the whole batch experiment of the shaking flasks supplemented with trehalose at different concentrations as well as the control (CHO cells A).....	47
Figure 31: Daily cell concentrations and viabilities of the shaking flasks supplemented with sucrose at different concentrations along with the control (CHO cells A).	47
Figure 32: The viable cumulative cell days (VCCD) over the time of the batch experiment.....	48

Figure 33: Daily product titers of the shaking flasks supplemented with sucrose at different concentrations along with the control (CHO cells A).....	48
Figure 34: Average specific productivities over the whole batch experiment of the shaking flasks supplemented with sucrose at different concentrations as well as the control (CHO cells A).....	49
Figure 35: Results of the western blot.	50
Figure 36: Daily cell concentrations and viabilities of the DASGIP bioreactors.	52
Figure 37: The viable cumulative cell days (VCCD) over the time of the batch experiment.....	52
Figure 38: Daily cell concentrations and viabilities of the shaking flasks..	53
Figure 39: The viable cumulative cell days (VCCD) over the time of the batch experiment.....	53
Figure 40: Daily cell concentrations and viabilities of the shaking flasks stored at 37°C as the average of the duplicates.	56
Figure 41: The viable cumulative cell days (VCCD) over the time of the batch experiment.....	56
Figure 42: Daily cell concentrations and viabilities of the shaking flasks stored at 32°C as the average of the duplicates.	57
Figure 43: The viable cumulative cell days (VCCD) over the time of the batch experiment.....	57
Figure 44: Daily titers of the shaking flasks stored at 37°C as the average of the duplicates.	58
Figure 45: Daily titers of the shaking flasks stored 32°C as the average of the duplicates.	58
Figure 46: Result of the silver staining.....	60
Figure 47: Glycan distribution.....	62
Figure 48: Illustration of different glycoforms described in this thesis.	62
Figure 49: Daily cell concentrations and viabilities as the average of the duplicates.....	64
Figure 50: The viable cumulative cell days (VCCD) over the time of the batch experiment.....	64
Figure 51: Daily titers as the average of the duplicates.	65
Figure 52: pH values for shaking flasks incubated at 7% CO ₂ and 32°C (F52) and 20% CO ₂ and 32°C (F53) over the time of the batch experiments.....	65
Figure 53: Flow cytometry results of CHO cells A from Batch F53 for intracellular heavy chains.....	67
Figure 54: Flow cytometry results of CHO cells A from Batch F53 for intracellular light chains.	67
Figure 55: Daily cell concentrations and viabilities of the shaking flasks incubated at 37°C as the average of the duplicates.	69
Figure 56: The viable cumulative cell days (VCCD) over the time of the batch experiment.....	69
Figure 57: Daily cell concentrations and viabilities of the shaking flasks incubated at 32°C as the average of the duplicates.	70
Figure 58: The viable cumulative cell days (VCCD) over the time of the batch experiment.....	70
Figure 59: Daily titers of the shaking flasks incubated at 37°C as the average of the duplicates.	71
Figure 60: Daily titers of the shaking flasks incubated at 32°C as the average of the duplicates.	71
Figure 61: Result of the silver staining.....	73
Figure 62: Daily cell concentrations and viabilities of the bioreactors.	75
Figure 63: The viable cumulative cell days (VCCD) over the time of the batch experiment.....	75
Figure 64: pH monitored over the whole process for each bioreactor.	76
Figure 65: Detailed information about the dissolved oxygen [%saturation], O ₂ and CO ₂ concentration in the headspace of each bioreactor during the fermentation.....	77

4 List of tables

<i>Table 1: Overview of the media, its sugar concentration and supplements.</i>	19
<i>Table 2: The relevant process conditions of each batch experiment.</i>	25
<i>Table 3: Sample plan for batch experiments.</i>	26
<i>Table 4: Reagents used for ELISA.</i>	26
<i>Table 5: The operating procedure of the SDS-PAGE and Western Blot in more detail.</i>	28
<i>Table 6: The detailed operating procedure of the sample preparation for Flow cytometry.</i>	30
<i>Table 7: All the equipment and reagents that were used and its purpose.</i>	32
<i>Table 8: Summary of Batch 1.</i>	43
<i>Table 9: Summary of Batch 2.</i>	49
<i>Table 10: Isoform distribution of the sucrose and trehalose supplemented approaches, control and standard.</i>	50
<i>Table 11: Summary of Batch F49.</i>	54
<i>Table 12: All product related parameters as the average of the duplicates.</i>	59
<i>Table 13: All metabolism related parameters as the average of the duplicates.</i>	59
<i>Table 14: Summary of Batch F52.</i>	60
<i>Table 15: All product related parameters as the average of the duplicates.</i>	66
<i>Table 16: All metabolism related parameters as the average of the duplicates.</i>	66
<i>Table 17: Summary of Batch F53.</i>	66
<i>Table 18: All product related parameters as the average of the duplicates.</i>	71
<i>Table 19: All metabolism related parameters as the average of the duplicates.</i>	72
<i>Table 20: Summary of Batch F54.</i>	73
<i>Table 21: Summary of Batch F56.</i>	76

5 Introduction

The successful production of recombinant proteins as therapeutics started with the generation of recombinant insulin (Humulin from Genentech) as the first recombinant protein getting market authorization in 1982. Important to mention here is, that because of the relative simplicity of the molecule it has been produced in *Escherichia coli* (Butler 2005). Bacteria such as *E. coli* are rapidly growing on simple media and are very easy genetically manipulated, hence they can generate recombinant proteins in large quantities and are considered to be an inexpensive expression technology. That is why bacterial expression systems are by far the most commonly used technology for the production of recombinant proteins of very low complexity, such as insulin. However, bacteria are not capable of advanced folding and post translational modifications (Verma et al., 1998). Yeasts as an alternative expression system can also be fast grown on simple growth media, but in contrast to bacteria, yeasts provide advanced protein folding pathways and can perform post translational modifications and are thus an attractive option for the expression of a broad range of clinically and industrially important proteins (Wood et al., 1985). But given that yeasts execute post translational modifications in a different manner compared to higher eukaryotes such as mammals and the need for recombinant proteins as therapeutics with higher complexity, led to the development of eukaryotic cell lines being capable of fulfilling these requirements. Eventually it was the human tissue plasminogen activator (tPA, Genentech) being the first recombinant protein produced in mammalian cells with market approval in 1986 (Kim et al., 2012).

Although a variety of alternative eukaryotic expression systems are available, such as insects, transgenic animals and plants, mammalian cells from the beginning on have been the main expression system. Within the mammalian cells the Chinese Hamster Ovary (CHO) cells play the most important role as the industries workhorses in the large-scale production of recombinant proteins, compared to other mammalian cell lines such as baby hamster kidney, mouse myeloma-derived NS0 or human embryonic kidney (HEK)-293 cells. CHO cells are stamped by significant technical limitations such as a low specific growth rate, low cell concentration, high energy and nutrient consumption (mainly glucose and glutamine) going hand in hand with high production of unwanted secondary metabolites (mainly lactate and ammonium), which altogether define a production process as low productive compared to microbial production processes (Altamirano et al., 2013). Nevertheless an estimated 70% of all nowadays recombinantly produced proteins are generated in CHO cells with current annual sales exceeding US\$ 30 billion worldwide (Jayapal et al., 2007). The predominance of CHO cells is based on several facts. First, they can be successfully adapted and grown in suspension, which is of great advantage for large-scale cultivation. Second, they are easy to cultivate in regulatory-friendly chemically defined (CD) and serum-free (SF) media. Third, the CHO cells are capable of performing complex and efficient post-translational modifications, which are both compatible

with and bioactive in humans. Especially the glycosylation patterns are more human-like, compared to other mammalian cell lines. Fourth, well established gene amplification systems such as the dihydrofolate reductase (DHFR)-system to overcome the typically low specific productivity of CHO cells are available. Last but not least, CHO cells have been shown to be a safe expression system for recombinant proteins for more than two decades and thus it may be easier to obtain market authorization for therapeutics produced in these cells (Kim et al., 2012) (Lai et al., 2013).

A promising class of therapeutic proteins for recombinant expression are immunoglobulin M (IgM) antibodies. IgMs are the first type of antibodies that are produced as the reaction to foreign substances by the adaptive immune system. They are characterized by their pentameric structure with ten identical epitope-binding sites per molecule, which provides a substantially higher avidity compared to other immunoglobulin types. Thereby IgMs have a higher chance of binding to foreign substances such as pathogens and are particularly effective in triggering the complement system when compared to the other immunoglobulin classes. On the other side IgMs show a lower affinity to their target and are rather known to be polyreactive. That is why during an ongoing infection a process called class-switching occurs, resulting in the production of other antibody classes (IgG, IgA, IgE, IgD), which exhibit a much higher affinity and hence effectivity (Eisen 2014). Nevertheless, IgMs are becoming more and more important as potential therapeutics and diagnostics: Although for a very long time the potential of IgMs was not completely understood, because of properties that are different to the much more popular IgGs, such as the low target affinity mentioned above, in the course of time they have been positively evaluated for their benefit as therapeutics in the mucosal environment and in serum to fight upcoming tumor cells and foreign antigens. Thus they will play a very important role in diagnosis and other clinical applications in the future (Mader et al., 2013).

Usually the natural IgMs occur as pentamers (Figure 1), but also other isoforms such as hexamers, tetramers, trimers, dimers and even as monomers have been found in the culture supernatant of recombinant cells. Thus it is not only the product titer that is of importance, but also the product quality. Since pentamers are mainly the desired product, the isoform distribution is of special interest. Thus we investigated the impact of alternative sugar substrates on the isoform distribution and additionally on the glycosylation.

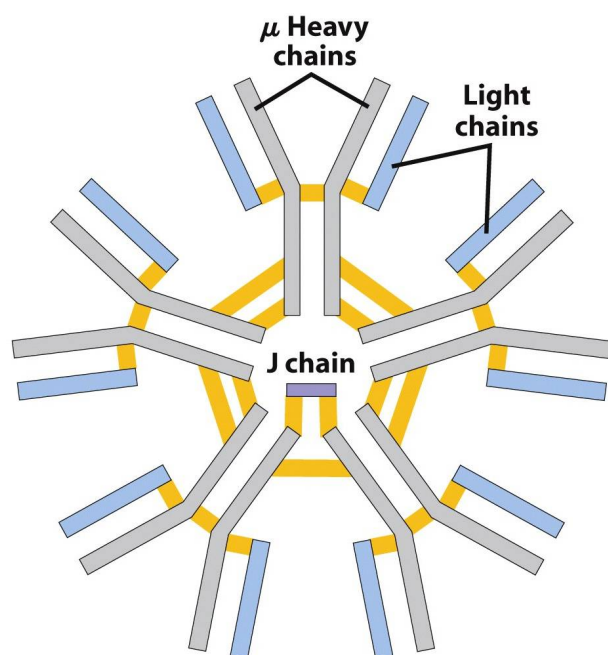


Figure 5-23
Lehninger Principles of Biochemistry, Fifth Edition
 © 2008 W.H. Freeman and Company

Figure 1: Structure of an IgM. Grey: μ heavy chain, Blue: κ light chain, Purple: J chain, Yellow: Disulfide bonds

The standard energy sources for CHO cells are mainly glucose as the carbon-source and glutamine as the nitrogen-source. Additionally to the high consumption rates, which lead to quickly reached limiting concentrations, these substrates are metabolized into the undesirable metabolites lactate and ammonium ion, respectively. The production of lactate results in medium acidification, which can be counter steered by a pH controlling system such as the addition of base to the culture. However, a consequence of this is an increase of the medium osmolality and the known negative effects of lactate on cell growth and productivity are largely due to this implication. In general, a lactate concentration below 20 mM is unproblematic, while a concentration between 20 and 40 mM negatively affects the productivity and more than 40 mM arrest the cell growth (Cruz et al., 2000). While the generation of ammonium also increases the osmolality, the adverse effects here have a bigger impact, because they are primarily due to its direct toxicity and bring the CHO cells to start suffer at concentrations from 2 to 5 mM (Schneider et al., 1996). Moreover it has been demonstrated that ammonium has an impact on the glycosylation and thus on the quality of the product (Altamirano et al., 2013).

The aim of this project was to apply different sugar substrates and investigate the effect on relevant culture parameters in batch experiments using IgM producing CHO cells. As alternative sugar substrates galactose and mannose as C4 and C2 epimers of glucose were applied. Additionally fructose as monosaccharide and bound to glucose as the disaccharide sucrose was tested as well as the disaccharide trehalose, which is made up of two glucose molecules (Figure 2).

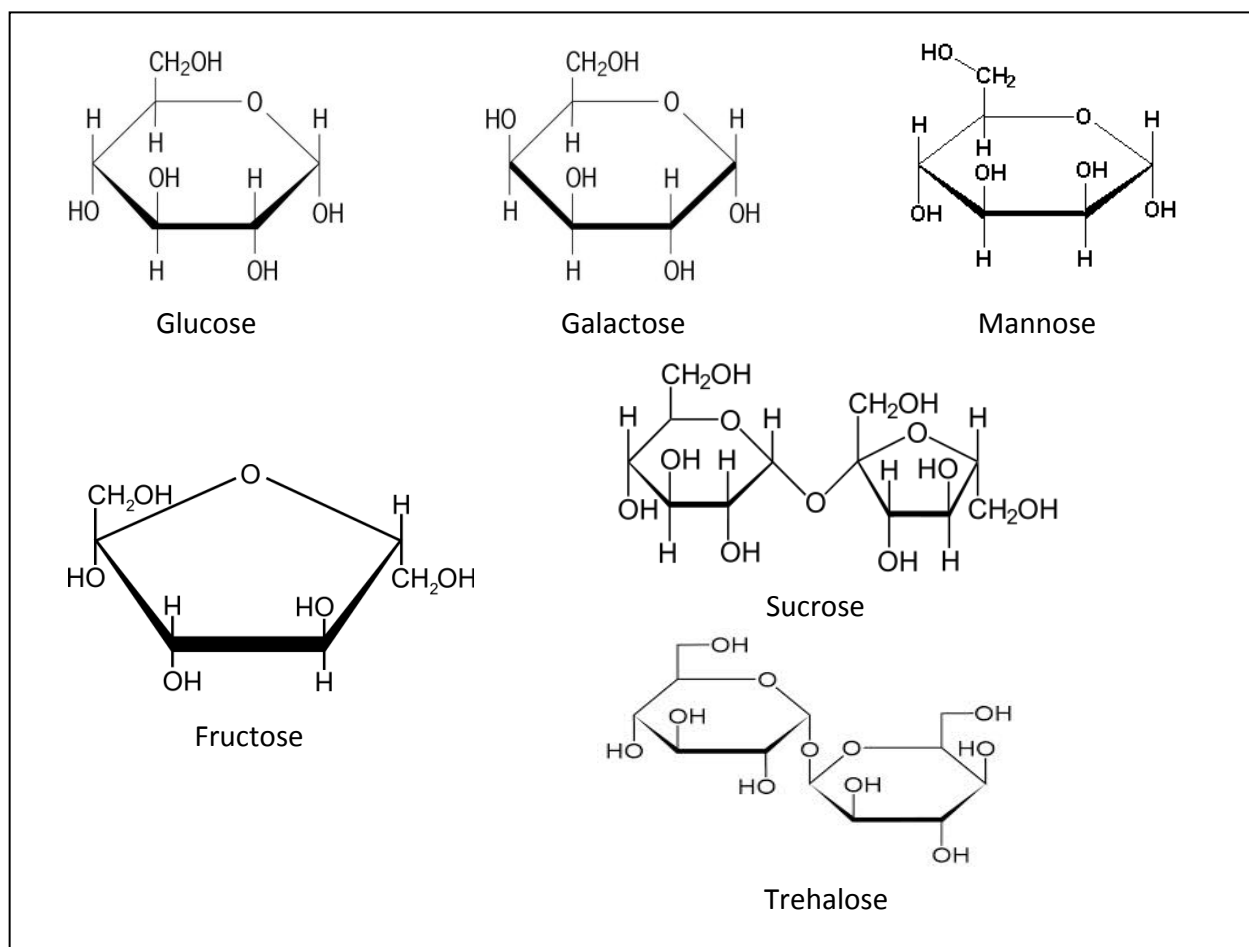


Figure 2: Structures of the different sugars.

The very prominent metabolic pathway, which is responsible for the processing of sugars, is the glycolysis (Figure 3). Glucose represents the starting point of the glycolysis and is favorably processed over alternative sugars. There are no distinct catabolic pathways for other sugar substrates, thus all sugars have to find their way into the glycolysis (Figure 4). The introduction of galactose starts with conversion into galactose-1-phosphate by the enzyme galactokinase. Then a uridine diphosphate (UDP) nucleotide group is exchanged from UDP-glucose to galactose-1-phosphate by a galactose-1-phosphate-uridylyltransferase, resulting in UDP-galactose and glucose-1-phosphate. While the UDP-galactose is converted into UDP-glucose by a UDP-galactose-epimerase, the enzyme phosphoglucumutase converts glucose-1-phosphate into glucose-6-phosphate and thus introduces it into the glycolysis.

Mannose is first phosphorylated by a mannokinase into mannose-6-phosphate, before it is introduced into the glycolysis after being transferred into fructose-6-phosphate by a phosphomannose isomerase.

The introduction of fructose begins with the conversion into fructose-1-phosphate by a fructokinase. In the next step the fructose-1-phosphate is split into glyceraldehyde and dihydroxyacetone-phosphate by a fructose-1-phosphate-aldolase. Both of these intermediate

products enter the glycolysis by eventually being processed into glyceraldehyde-3-phosphate by a triosekinase and triose-phosphate-isomerase, respectively.

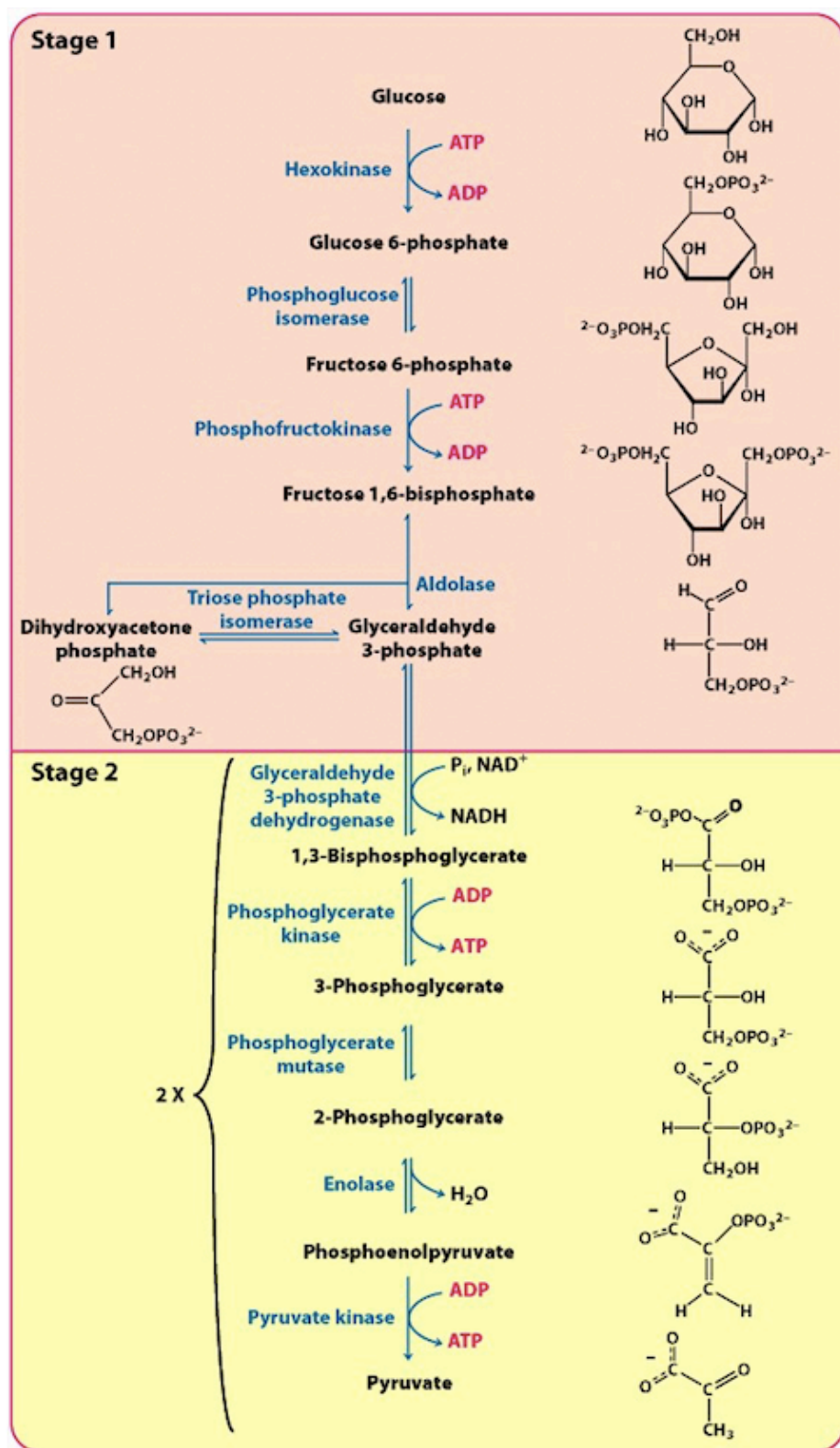


Figure 3: Metabolic pathway of the glycolysis. *Biochemistry*, seventh edition ©2012 W.H. Freeman and Company.

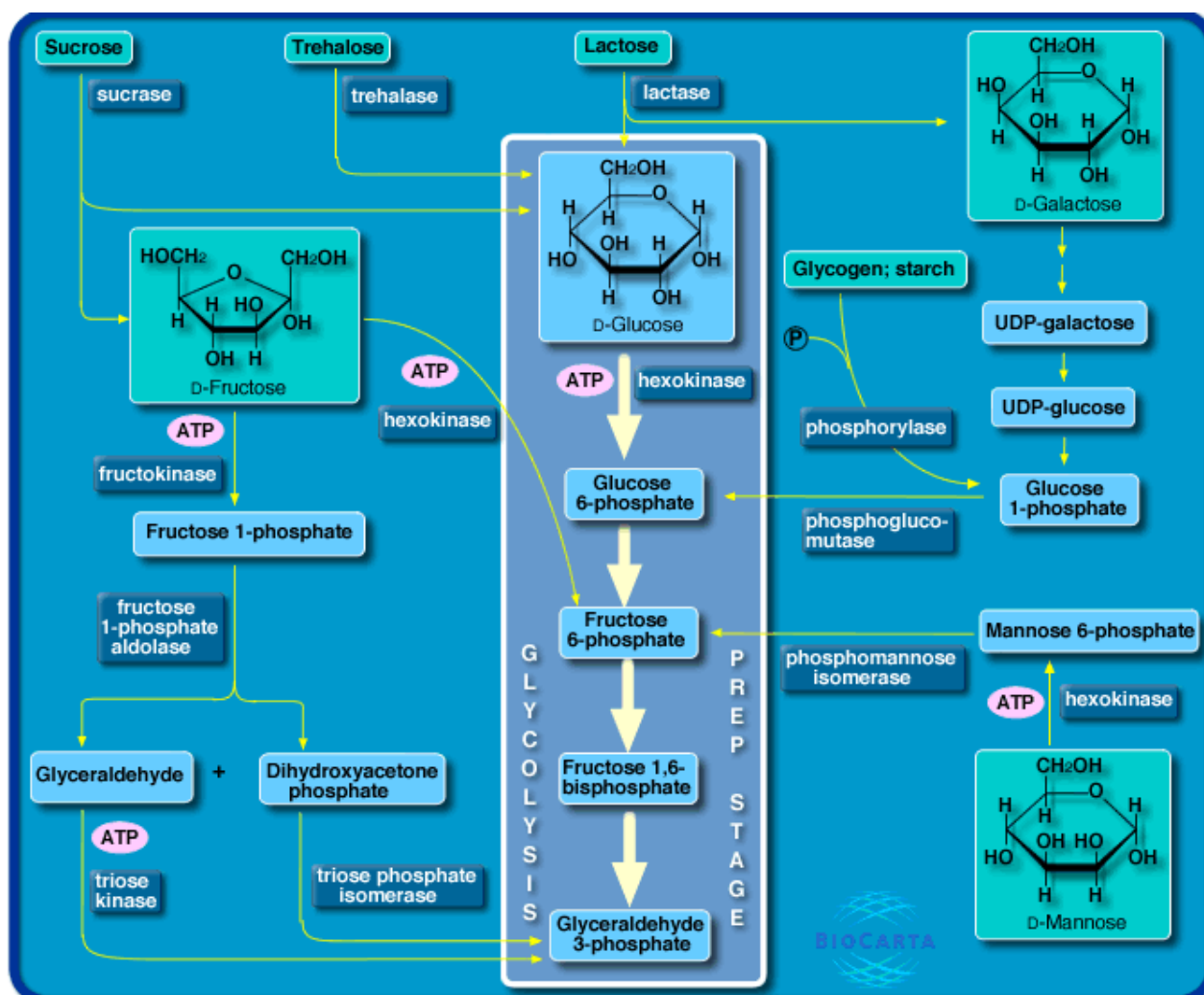


Figure 4: Feeder pathways for glycolysis, Glenn Croston (PhD), <http://www.biocarta.com/pathfiles/feederpathway.asp> [2015/06/01].

The idea, why using an alternative sugar source might be beneficial, is that they are metabolized by different pathways compared to glucose. The rapid processing of glucose leads to accumulation of pyruvate as the end product of the glycolysis and to a very high consumption of the redox mediator NAD^+ , which is essential for the glycolysis (Figure 3). Usually NAD^+ is replenished from NADH in the oxidative phosphorylation, which is the most efficient pathway in energetic terms, but it is also a rather slow process. As a consequence, NAD^+ is reconstituted from NADH by reducing pyruvate to lactate with the help of the lactate dehydrogenase (Figure 5) (Rachel Legmann 2011). Thus a slower metabolized sugar might lead to a lesser amount of lactate and minimize its adverse effects on growth and viability. Furthermore the disaccharides trehalose and sucrose have a known protein stabilizing effect (Cleland et al., 2001) (Onitsuka et al., 2014). It would be a highly sophisticated method to use a sugar substrate that simultaneously acts protein stabilizing with regard to productivity and product quality.

Moreover, as already mentioned above, the use of alternative substrates might influence the glycosylation and thus have a potentially beneficial impact on the quality of the antibody product.

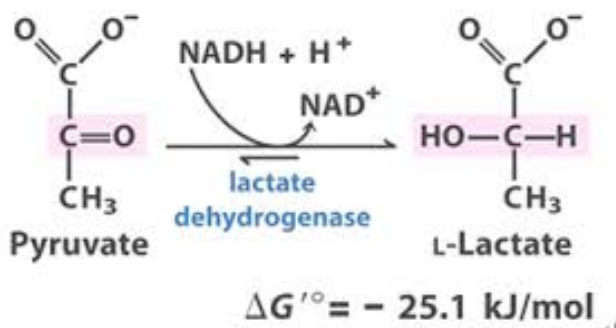


Figure 5: Enzymatic reaction of pyruvate to lactate. http://www.proteopedia.org/wiki/index.php/User:Kelly_Roark/Sandbox1 [2015/06/01]

To investigate all the mentioned aspects, several batch experiments were performed to raise and collect information to eventually make a statement of the effect of different sugar substrates on relevant culture parameters in a recombinant IgM production process using CHO cells. One of the relevant culture parameters that has been closely monitored was the cell growth by identifying the daily cell concentrations. Another one was the daily viability by determining the percentage of living cells. Additionally the concentrations of a variety of metabolites such as glucose (or alternative sugar sources), lactate, glutamine, glutamate and ammonium were enzymatically analyzed from each day of a batch process. Moreover every day a sample was taken to determine the produced amount of antibodies. Last but not least, from the day the batch experiments were terminated, samples were drawn for the analysis of the isoform distribution and/or glycosylation of the IgMs.

6 Material and Methods

6.1 Cell Lines¹

In the herein presented work, the following cell lines were all generated from the CHO DG44 host cell line using the dihydrofolate reductase (DHFR) gene amplification system. Furthermore they all grow in suspension and have previously been adapted to a 1:1 mixture of Dulbecco's Modified Eagle Medium and Ham's F12 (D/H 1:1).

- **Cell line A: IgM expressing recombinant CHO cell line**
- **Cell line B: IgM expressing recombinant CHO cell line**

6.2 Cultivation medium

All cell lines were grown in suspension and have been adapted to a 1:1 mixture of Dulbecco's Minimum Essential Medium (DMEM) and Ham's F12 medium, stated as D/H 1:1 medium. The standard D/H 1:1 medium contained glucose and was supplemented with protein-free additive (iron(III)-citrate, sodium selenite, ascorbic acid and ethanolamine dissolved in purified water, 1x in-house formulation) and soy peptone (1x in-house formulation) as nutrients, pluronic F-68 (1x in-house formulation) as protection against shear forces, L-glutamine (4 mM; Sigma-Aldrich) as energy source and methotrexate (MTX, 0.096 µM; Sigma-Aldrich) as gene amplification agent.

Table 1: Overview of the media, its sugar concentration and supplements.

Medium	Sugars	Additional supplements
D/H w/ Glc (Biochrom, Germany)	Glucose 3.151 g/L	Protein-free additive, soy peptone, pluronic, L-glutamine, MTX Additionally for batch 2: Sucrose or trehalose
D/H w/o Glc (Biowest, France)	Glucose 6 g/L Mannose 6 g/L Galactose 6 g/L	Protein-free additive, soy peptone, pluronic, L-glutamine, MTX
ProCHO5 (Lonza, Switzerland)	Glucose ≥ 8 g/L	Phenol red, L-glutamine, MTX

¹ See appendix for cell-bank information sheets

6.3 Maintenance and cultivation conditions

The routine cultures were thawed and first cultured in standard D/H 1:1 medium in T25 flasks and stored in the Heracell incubator at 37°C and 7% CO₂. The CHO cells follow a typical growth curve (Figure 6) and thus start to die after a certain period of time. To keep the cells alive, as a matter of routine, the viability and cell concentration of each culture were determined either every third or fourth day, followed by seeding the cells into new medium, which causes a continuous expansion of the cells in the exponential growth phase. This procedure is known as *splitting* and each splitting is equivalent to one passage. In the case of the T25 flasks the cultures were passaged with an aimed starting cell concentration of 2×10^5 cells/mL at a working volume of 10 mL. However, after several passages the cultures were transferred into 125 mL shaking flasks. The shaking flasks were stored in the Kuhner shaker at 140 rpm, 37°C, 7% CO₂ and 90% humidity and the cultures were passaged with a starting cell concentration of 3×10^5 c/mL at a working volume of 15 mL.

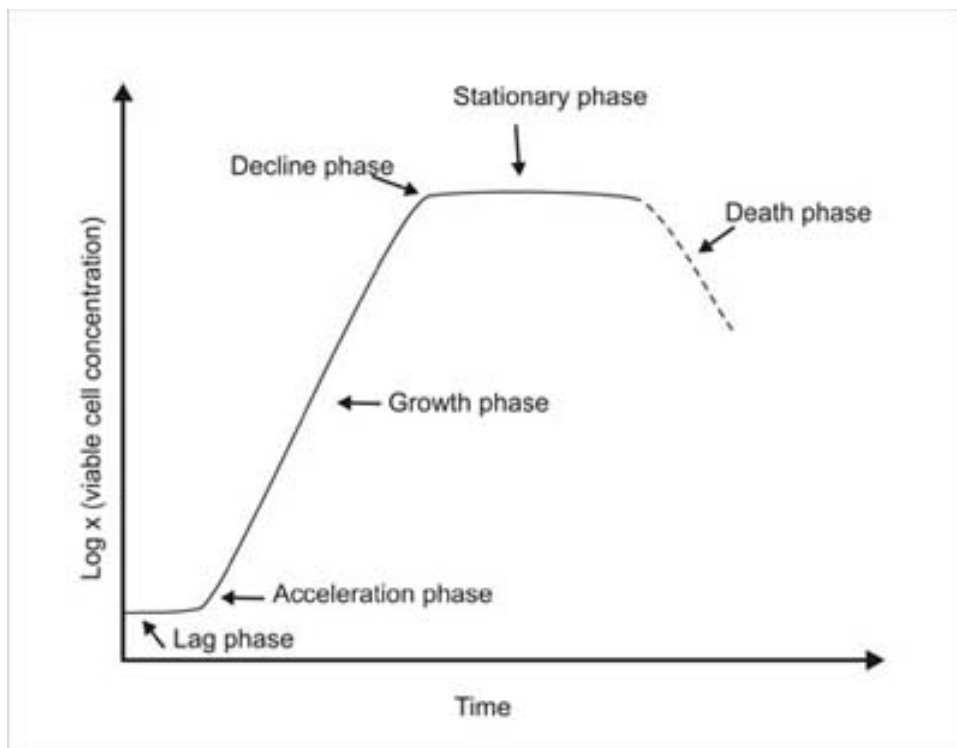


Figure 6: Typical growth curve for CHO cells. Source: A. Cunningham, Center for Biofilm Engineering, Montana State University, Bozeman, MT.

6.4 Cell concentration

The cell concentrations were determined by counting the cell nuclei using a Z2 Coulter Counter according to the manufacturer's instructions. The Coulter Counter was made up of two chambers connected by a small orifice with a specific electric current and a detector. It was counting the cell nuclei by pulling them through the orifice, with each nucleus causing an alteration in the impedance proportional to the volume of the nucleus. The change in the impedance, caused by the poorly conductive cell nuclei replacing electrolytes in the orifice, is detected and converted into a differential number. The major advantage of detecting the cell nuclei was, that cell aggregations were disrupted and properly detected. Briefly, cell suspension was centrifuged and the resulting cell pellet was resolved and incubated for 1 hour in 1 mL Coulter buffer. The sample was then analyzed and the cell concentration determined according to equation 3.

Eq. 1
$$x \left[\frac{c}{\text{mL}} \right] = \frac{a*(b+c)*d}{(e*c*f)}$$

x – Cell concentration [c/mL]
a – Differential number from Z2 Coulter-Counter [c]
b – Coulter isotone solution applied [mL]
c – Sample volume applied [mL]
d – Coulter buffer volume applied [mL]
e – Coulter factor (x 0.1)
f – Centrifuged sample volume [mL]

6.5 Viability

For the determination of the viability 100 µL sample was mixed with 20 µL 0.4% trypan blue solution, filled into a hemocytometer and at least 4 big squares (BQ) were counted. Trypan blue is only passing through the membrane in a dead cell, which thus appear to be blue. To identify the viability and the estimated cell concentration the following equations were used:

Eq. 2
$$\text{Cell concentration} \left[\frac{c}{\text{mL}} \right] = \frac{\text{number of cells counted}}{\text{number of big squares counted}} \times \text{dilution} \times 10000$$

Eq. 3
$$\text{Viability [\%]} = \frac{\text{number of living cells}}{\text{number of total cells}} \times 100$$

6.6 Metabolites

A part of the supernatant of a sample was used to measure the metabolite concentrations on a fully automated and enzyme-based device, Bioprofile 100plus, according to the manufacturer's instructions. The following metabolites were determined: glucose, lactate, glutamine, glutamate and ammonium.

Since the Bioprofile 100plus could not analyze the concentrations of the alternative sugar substrates mannose and galactose, these were determined by high performance liquid chromatography (HPLC) by Ing. Gabriela Lhota and colleagues from the analytics group under the supervision of Ao.Univ.Prof. Dipl.-Ing. Dr.nat.techn. Karola Vorauer-Uhl.

6.7 Adaption to different sugar sources

When the cultures demonstrated viabilities above 90% and sufficient cell concentrations after they experienced at least 4 passages, they were gently adapted to alternative sugar substrates. For this purpose the cultures were passaged into different shaking flasks using a glucose free D/H 1:1 medium (w/o Glc) that has been supplemented with one of either carbon source glucose, galactose, fructose, mannose, sucrose or trehalose at a concentration of 6 g/L. As a consequence, for the first passage some glucose still remained from the standard medium. In the course of time and with each further passage the glucose concentration decreased until eventually there was no glucose left and the cells were adapted on the alternative sugar substrate.

6.8 Batch experiments in shaking flasks and DASGIP module

The batch experiments were either performed in shaking flasks or in the fully automated DASGIP bioreactors. Since the shaking flasks were simply incubated in a controlled environment, while the DASGIP bioreactors could be directly controlled and monitored, the latter was expected to be superior in terms of growth, productivity and duration.

For the batch experiments the inoculum was prepared by transferring an aliquot from the routine cultures into a fresh 250 mL, 500 mL, or 1000 mL shaking flask to generate sufficient volume.

Prior to starting a batch experiments run, the cell concentrations needed to be high enough to provide the necessary inoculum concentrations and the viabilities had to be above 90%. Subsequently, a certain volume of the inoculum culture was centrifuged, followed by removing the spent medium and subsequently resolving the cell pellet in fresh medium. The cells were then incubated at specified conditions and closely monitored until the viability started to drop. Along with the increased number of dead cells, the amount of released intracellular protein degrading agents rose and would have an increased impact on the recombinantly produced proteins. Thus we set a viability of 60% as the endpoint of every batch process. In the following there is first shown an overview displaying the course of the whole project (Figure 7), followed by more detailed figures about the CHO cells leading into the different batch experiments (Figure 8, Figure 9, Figure 10).

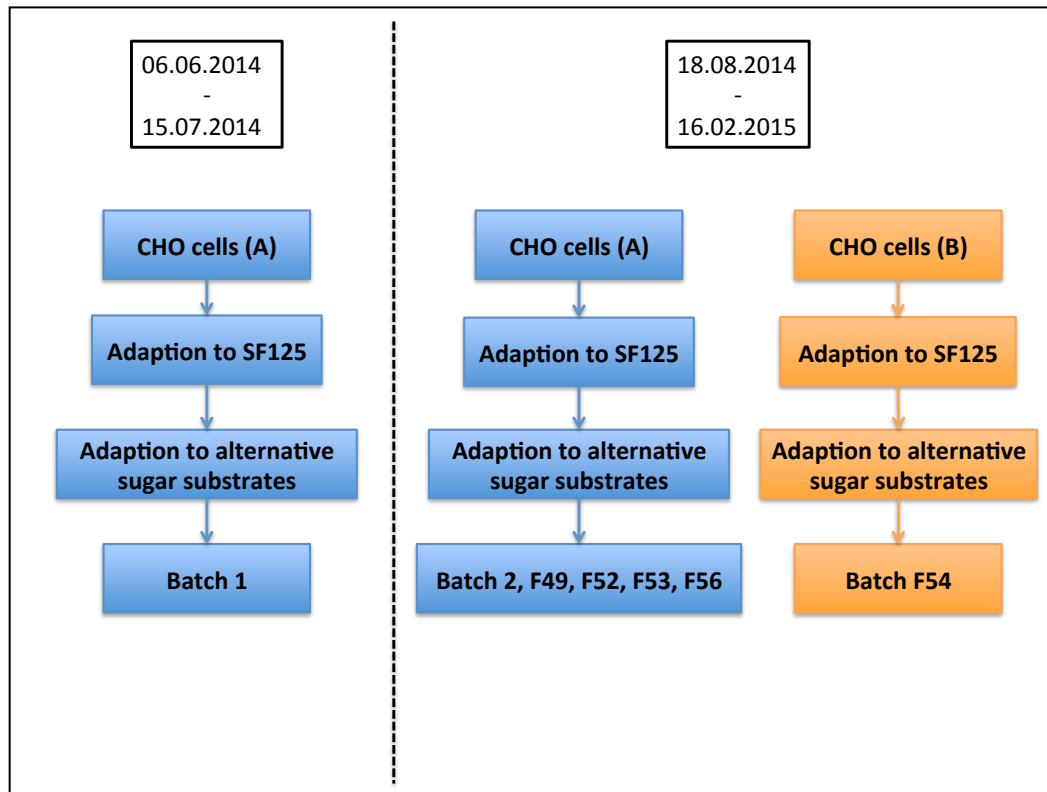


Figure 7: The course of the whole project from thawing the CHO cells to the batch experiments. On the left side the first and on the right side the second phase is displayed. SF125 – 125 mL shaking flasks

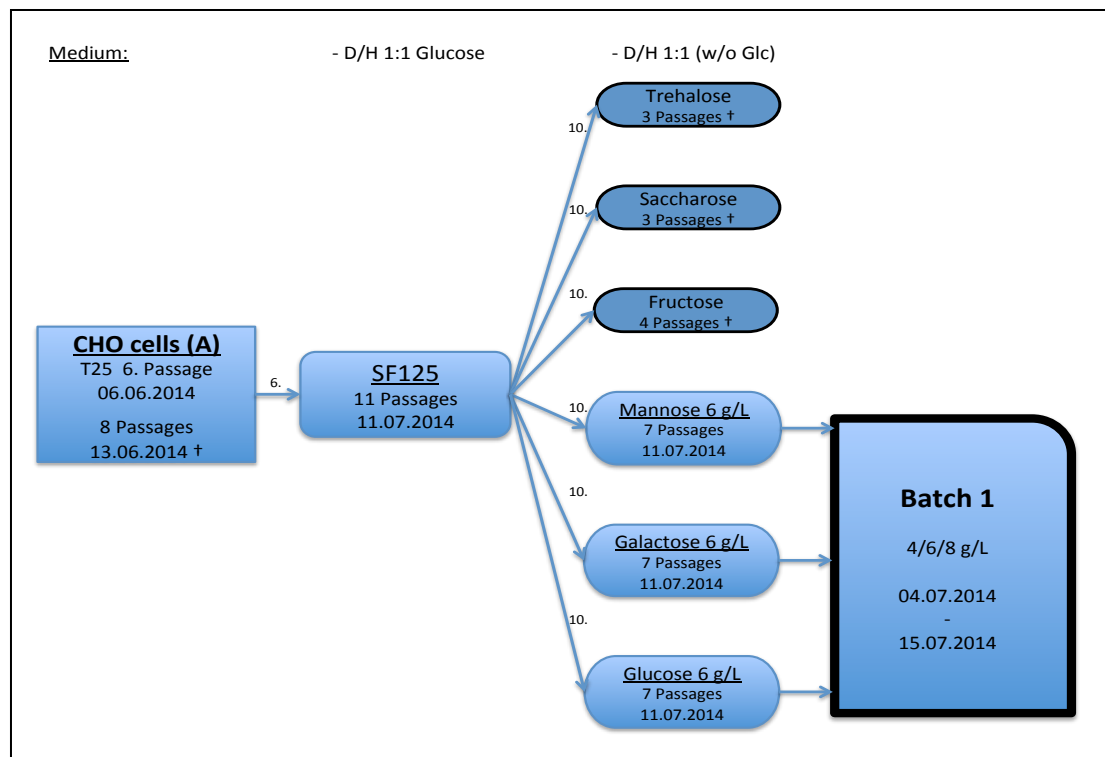


Figure 8: More detailed view about the phase, where the CHO cells A have first been thawed and worked with. T25 – 50 mL rous flask, SF125 – 125 mL shaking flask, † - describes the death of this culture.

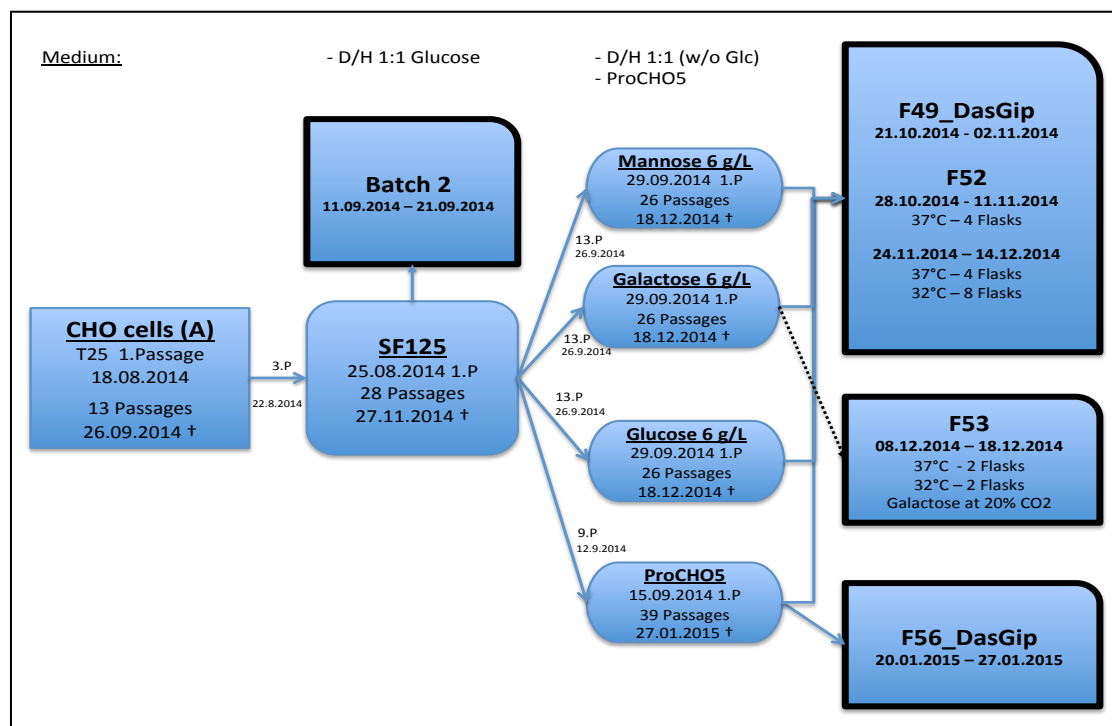


Figure 9: More detailed view about the second phase, where the CHO cells A have been newly thawed and additional experiments were performed. Flasks – shaking flasks

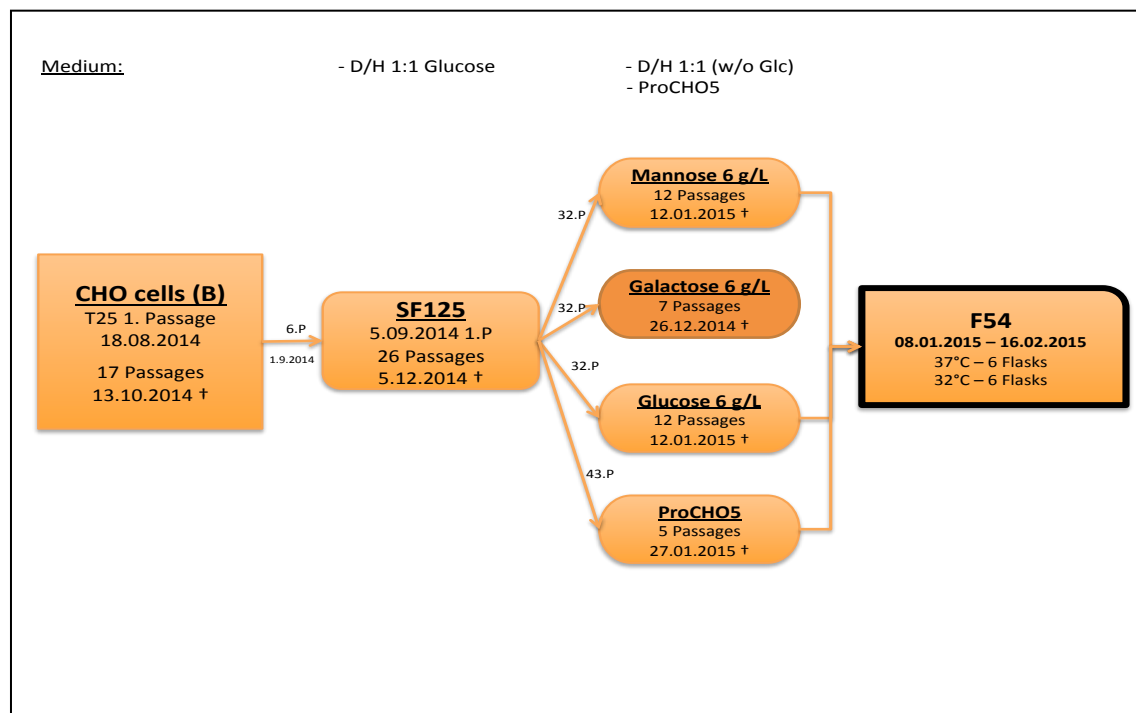


Figure 10: More detailed view about the CHO cells B that have been thawed along with the CHO cells A in the second phase.

All of the performed batch experiments were started with an inoculum concentration of 3×10^5 cells/mL and in the following table (Table 2) are the process conditions of each batch listed.

Table 2: The relevant process conditions of each batch experiment. The shaking flasks have all been incubated in the Kuhner Shaker at 90% humidity. In contrast to the shaking flasks, the DASGIP bioreactors were run with an integrated pH controlling system, thus the CO₂ concentration was not fixed at 7%, but always automatically adapted to the circumstances.

Batch	CHO cells	Vessel type	Duplicates	Medium	Sugars	Temp. [°C]	RPM [min ⁻¹]	Vol. [mL]	CO ₂ [%]
1	A	Shaking flasks	No	D/H 1:1 w/o Glc	Glucose 4,6,8 g/L Galactose 4,6,8 g/L Mannose 4,6,8 g/L	37	140	30	7
2	A	Shaking flasks	No	D/H 1:1 w Glc	Trehalose Sucrose (as supplements)	37	140	60	7
F49	A	DASGIP (4 parallel bioreactors) and shaking flasks	No	D/H 1:1 w/o Glc + ProCHO5*	Glucose 6 g/L Galactose 6 g/L Mannose 6 g/L	37	80 / (140)	570 / (30)	- / 7
F52	A	Shaking flasks	Yes	D/H 1:1 w/o Glc + ProCHO5*	Glucose 6 g/L Galactose 6 g/L Mannose 6 g/L	37 32	140	100	7
F53	A	Shaking flasks	Yes	D/H 1:1 w/o Glc	Galactose 6 g/L	37 32	140	100	20
F54	B	Shaking flasks	Yes	D/H 1:1 w/o Glc + ProCHO5*	Glucose 6 g/L Galactose 6 g/L Mannose 6 g/L	37 32	140	100	7
F56	A	DASGIP (4 parallel bioreactors)	No	ProCHO5	*Glucose ≥ 8 g/L	37	160, 80, 60	600	-

During a batch experiment, from each shaking flask or bioreactor daily samples of 2-3 or 10 mL, respectively, were drawn to determine specific process parameters (Table 3). 0.1 mL of this sample was used to determine the viability and an estimate about the cell concentration using a hemocytometer as described in 6.5. The rest of the sample was centrifuged and the supernatant subsequently separated from the cells. A part of the supernatant was immediately used to measure the metabolites concentrations at the Bioprofile 100plus (6.6) while the rest of it was stored at -20°C until further analysis such as ELISA (6.9) or Western Blot (6.10). The cell pellet was resolved in Coulter buffer and after an incubation period of one hour, the cell concentration was determined using the Z2 Coulter counter (6.4). The shaking flasks and reactors were run as long as the viability was higher than 60%. As soon as the viability dropped below 60% they were harvested. This harvesting day represented the last day of the experiment for the particular shaking flask or bioreactor, on which the cell broth was either discarded or centrifuged to separate the product from the cells.

Table 3: Sample plan for batch experiments. cs – culture supernatant, HPLC – high performance liquid chromatography, ELISA – enzyme-linked immunosorbent assay, WB – western blot, MS – mass spectrometry

Day	Viability	Cell concentration	Bioprofiler	HPLC	ELISA/WB	FACS	MS (Glycosylation analysis)
0 - 3	0.1 ml	2.9 ml (cell pellet)	0.9 ml (cs)	1 ml (cs)	1 ml (cs)	-	-
4	0.1 ml	2.9 ml (cell pellet)	0.9 ml (cs)	1 ml (cs)	1 ml (cs)	2×10^6 c/ml	-
5 - 6	0.1 ml	2.9 ml (cell pellet)	0.9 ml (cs)	1 ml (cs)	1 ml (cs)	-	-
7	0.1 ml	2.9 ml (cell pellet)	0.9 ml (cs)	1 ml (cs)	1 ml (cs)	2×10^6 c/ml	-
8 - ...	0.1 ml	2.9 ml (cell pellet)	0.9 ml (cs)	1 ml (cs)	1 ml (cs)	-	-
Last Day	0.1 ml	2.9 ml (cell pellet)	0.9 ml (cs)	1 ml (cs)	1 ml (cs)	2×10^6 c/ml	Culture supernatant (only F52)

6.9 Antibody quantification by ELISA

IgM was quantified by Enzyme linked immunosorbent assay (ELISA). Table 4 lists the reagents that were used for quantification.

Table 4: Reagents used for ELISA.

Step	Reagent	Applied concentration
Coating	Goat anti-human IgM μ -chain antiserum (Sigma I1636)	1 μ g/mL
Coating Buffer	0.1 M NaHCO ₃ (pH 9.6 – 9.8)	-
Standard	IgM from human serum (Sigma I8260)	200 ng/mL
Conjugation	Goat anti-human IgM κ light chains-peroxidase antibody (A7164)	1 μ g/mL
Washing	PBST (PBS + 0.1% Tween20) buffer	-
Dilution	Washing buffer + 1% BSA	-
Staining	Tetramethylbenzidine (TMB)	-
Stop reaction	2.5 M H ₂ SO ₄	-

In more detail, a maxisorp plate (Thermo Scientific, US) was first coated with the coating antibody, which was directed against the human IgM μ -chain, at a concentration of 1 μ g/mL in coating buffer and 100 μ L/well and either left for 2 hours on a shaking device at room temperature or overnight at 4°C. Next the plate was neatly washed with washing buffer, before 50 μ L of the samples or IgM-standard, respectively, were transferred from the dilution plates into the maxisorp plate. The dilution plate was prepared in such a way, that in the first row the IgM-standard and samples had a concentration of 200 ng/mL (ready to use) followed by seven subsequent 1:2 dilutions (Figure 11). Now the plate was incubated for 1 hour on a shaking device with 300 rpm. Then the plate was washed again, so that only the IgMs that are bound the coating antibody remained, followed by the addition of 100 μ L/well HRP-conjugated detection antibody, which was directed against the human κ -chain, at a concentration of 1 μ g/mL and another incubation period of 1 hour on a shaking device. Now the plate was washed

one more time, to only retain the bound detection antibodies, before the staining solution was applied (100 μ L/well). The peroxidases of the bound detection antibodies now started to oxidize the staining solution and thereby turned it from a colourless into a blue solution. When a bright blue colour was seen in the row with the highest dilution, the stop solution was added (100 μ L/well), which caused a colour shift from blue to yellow. The intensity of the resulting yellow coloured end product was proportional to the concentration of the applied sample or IgM-standard, respectively, and measured by the Infinite M100 plate reader (Tecan, Switzerland; excitation at 450 nm, extinction at 620 nm).

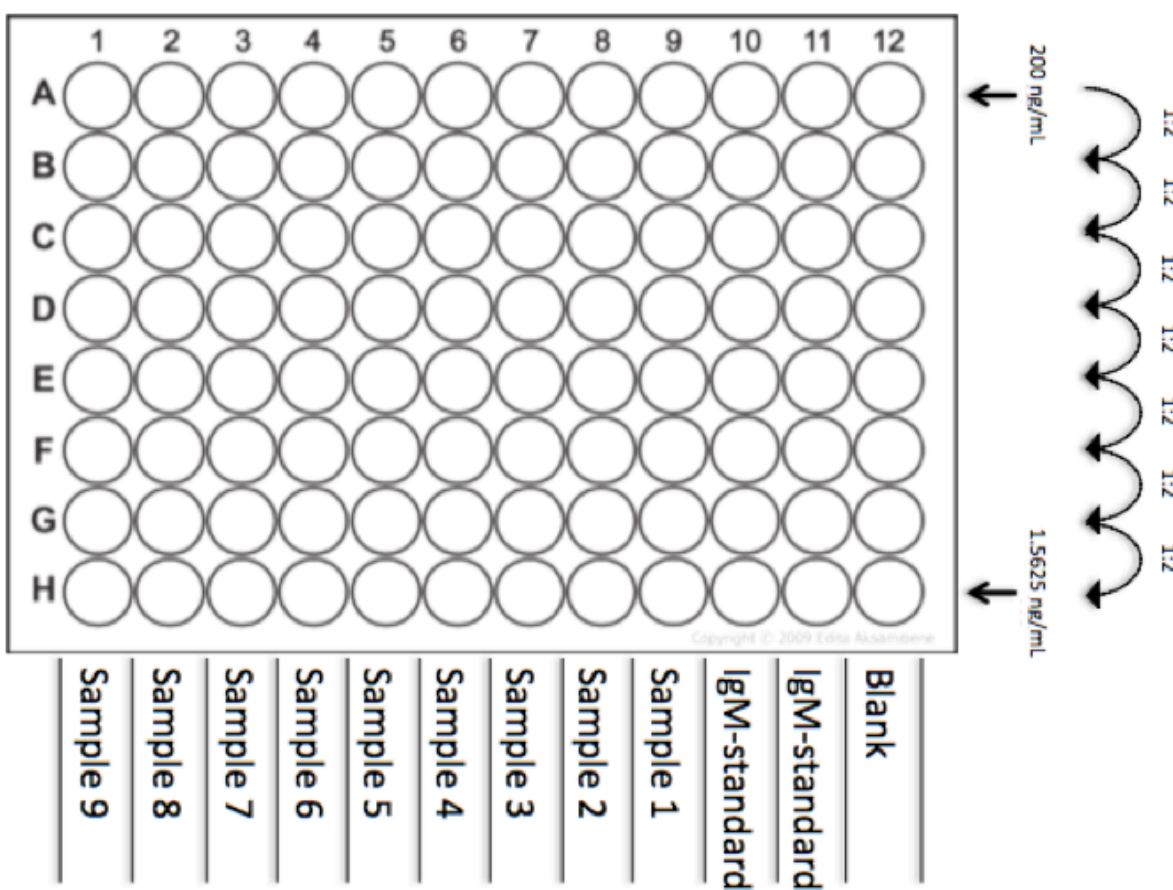


Figure 11: Setup of the dilution plate.

6.10 SDS-PAGE and Western Blot

SDS-PAGE (sodium dodecyl sulfate polyacrylamide gel electrophoresis) is a method to separate proteins in a sample based on their size. The SDS is an anionic detergent that linearizes proteins and makes them negatively charged in proportion to their size. When the samples were added to the gel, an electric field was applied, which made the negatively charged proteins to migrate away from the cathode towards the anode. Smaller proteins could easily migrate through the pores in the gel, while larger ones remained closer to the point of origin. The separated proteins were later visible as bands. In case of the IgMs monomers migrated much faster than the desired pentamer. The SDS-PAGE was run until the smallest proteins almost reached the end of the gel. Along with the samples a specific marker that contained proteins with known sizes was applied, enabling the correlation of the size of the protein bands in the samples according to the marker (Figure 12). Subsequently a Western Blot (WB) was performed. A WB is a blotting process, where all proteins are transferred from the gel into a polyvinylidene fluoride (PVDF) membrane. This was achieved by placing the membrane directly onto the gel and again applying an electrical field, which pulled the proteins from the gel into the membrane. Then the membrane was incubated in a solution containing an HRP-conjugated antibody directed against the human IgM μ -chain. In the last step the membrane was incubated with an enhanced chemiluminescent HRP substrate, before it was evaluated with the chemiluminescence imaging camera Fusion FX7 (Vilber Lourmat, Germany). See Table 5 for more details about the operating procedure.

Table 5: The operating procedure of the SDS-PAGE and Western Blot in more detail.

SDS-Page
1. Loading of the gel: 9 μ L sample + 3 μ L sample buffer; 9 μ L standard
2. Uncover the wells, rinse 2 times with buffer and remove the glue strip
3. Fix the gel in the chamber in the way that the writing is facing towards you
4. Fill the chamber with buffer until the wells are covered (no air bubbles in the wells)
5. Fill the wells with 10 μ L probe/marker/standard
6. Fill the rest of the chamber with buffer (up to ca. 1 cm underneath the edge)
7. Close the chamber with the lid, plug in the electrodes and start
8. Running Conditions: 200 V, 50 mA, 1 h
Blotting
1. Activate the membrane by immersing it with MetOH
2. Soak the membrane with transfer buffer (should be water-repellent)
3. Saturate the filters and pads in transfer buffer (no air bubbles)
4. Carefully untighten the gel by using the spatula and place a filter on the bottom side
5. Turn the gel and carefully place the membrane on it and another filter onto the membrane
6. Set up blotting-chamber: 2 pads, filter, gel, membrane, filter, 2 pads
7. Close the blotting-chamber and fill it with transfer buffer
8. Fill the surrounding of the blotting-chamber with RO-H ₂ O
9. Close the chamber with the lid, plug in the electrodes and start
10. Running conditions: 30 V, 170 mA, 1 h
Membrane processing
1. Put the membrane for 1 h in inactivation buffer on a shaking device (or overnight at 4°C)
2. Incubate 1 h in antibody solution on a shaking device (1:5000 dilution in inactivation buffer)
3. Rinse the membrane with PBST
4. Wash the membrane 2 times with PBST on a shaking device (~ 5 min)

5. Dry the membrane, tag the marker and place it on a plastic sheet
6. Cover it drop wise with the SuperSignal® West Pico substrates (mixed 1:1)
7. Close the plastic sheet (no air bubbles) and incubate for 5 min in the dark
8. Analyze the membrane under a chemiluminescence microscope

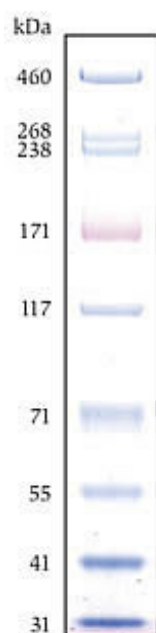


Figure 12: Protein bands of the HiMark Pre-Stained HMW Protein Standard. Source: <https://www.lifetechnologies.com/order/catalog/product/LC5699> [07/13/2015]

6.11 Silver Staining

Silver staining was another method used to investigate the isoform distribution. It was performed by the bachelor student Sarah Basas².

6.12 Intracellular Protein Content by Flow Cytometry

Flow cytometry is a laser-based technology that allows analysing up to thousands of particles per second. In our case we used this method to detect the amount of intracellular heavy and light antibody chains by labelling each with a different fluorescent marker. As the result, by comparing the outcomes with a non-producing negative control (CHO K1 host cell line), the amount of non-producing cells, which have lost the ability to produce IgMs, can be identified. Therefore a specific amount of cells was first fixed with ethanol to denature and preserve the cells while stored between 20 minutes up to several weeks at 4°C. Then the cells are treated with lysis buffer, to destroy the compactness and integrity of the lipid membrane and reveal all intracellular proteins. In the following steps the antibodies, either directed against the human μ -chain (heavy chain) or the human κ -chain (light chain), were applied. The anti-human heavy

² See the appendix for details about the silver staining

chain antibody was directly labelled with the fluorescent dye fluorescein isothiocyanate (FITC), while the anti-human light chain antibody was biotinylated to specifically bind a fluorescent dye (Alexa Flour-647). These two fluorescent dyes are recognized by the laser detector of the Gallios flow cytometer (Beckmann Coulter, US) and can be separated from each other based on their excitation at different wavelengths (Table 6). The evaluation was performed with the Kaluza Flow Cytometry Software (v 1.2).

Table 6: The detailed operating procedure of the sample preparation for Flow cytometry.

Ethanol fixation
1. Centrifuge 1×10^6 cells (10 min, 1000 rpm)
2. Wash cell pellet with 8 ml Dulbecco's PBS
3. Centrifuge (10 min, 1000 rpm)
4. Re-suspend pellet (shake, till the pellet spreads)
5. Add 1 ml 70% ice cold EtOH (vortex and add slowly drop wise to prevent formation of clumps)
6. Incubate at 4°C for at least 20 minutes
Staining
1. Centrifuge (10 min, 1000 rpm)
2. Wash in 1 ml Tris buffer. Add buffer slowly and drop-wise as when you fix with EtOH
3. Centrifuge (10 min, 1000 rpm)
4. Wash in 100 μ l Tris/20% FCS
5. Incubate 30 min at 37°C
6. Re-suspend in 100 μ l Tris/20% FCS with 1 st antibody (1:50 dilution → total dilution 1:100)
7. Incubate 30 min at 37°C
8. Centrifuge (10 min, 1000 rpm)
9. Wash in 1 ml Tris buffer
10. Centrifuge (10 min, 1000 rpm)
11. Re-suspend in 200 μ l Tris/20% FCS with 2 nd antibody (1:100) in
12. Incubate 30 min at 37°C
13. Centrifuge (10 min, 1000 rpm)
14. Wash in 1 ml Tris buffer
15. Centrifuge (10 min, 1000 rpm)
16. Re-suspend in 1 ml Tris buffer + DAPI (1:100)
1 st antibody: Anti human κ light chain antibody (Biotin)
2 nd antibody: Anti human μ heavy chain antibody (FITC) + Alexa Flour-647 (Strep)
Excitation wavelengths
Anti human κ light chain antibody: Alexa Flour-647 (Strep) 650/668 nm
Anti human μ heavy chain antibody (FITC): Alexa Flour-647 (Strep) 491/519 nm

6.13 Glycosylation analysis by Mass Spectrometry (MS)

This analysis was performed by Dipl.-Ing. Clemens Gruber from the Department of Biochemistry (Division of Biochemistry) under the direction of Ao.Univ.Prof. Dipl.-Ing. Dr.nat.techn. Friedrich Altmann.

A liquid chromatography electron spray ionization mass spectrometry (LC-ESI-MS) of tryptic and endoproteinase GluC (*Staphylococcus aureus* protease V8) digested IgMs with data mining using GPM and manual searches was conducted with the following procedure:

“Peptide analysis

The relevant protein bands were cut out and digested in gel. The proteins were S-alkylated with iodoacetamide (in gel) and digested with modified trypsin (Promega) or GluC (Roche) and trypsin.

About 1 µg of each digest was loaded on a BioBasic C18 column (BioBasic-18, 150 x 0.32 mm, 5 µm, Thermo Scientific) using 0.1% formic acid as the aqueous solvent. A gradient from 95% solvent A and 5% solvent B (Solvent A: 65 mM ammonium formate buffer pH 3, B: 100% acetonitrile) to 32% B in 35 min was applied, followed by a 15min gradient from 32% B to 75% B that facilitates elution of large peptides, at a flow rate of 6 µL/min. Detection was performed with a QTOF MS (Bruker maxis 4G ETD) equipped with the standard ESI source in positive ion, DDA mode (= switching to MSMS mode for eluting peaks). MS-scans were recorded (range: 150-2200 Da) and the 6 highest peaks were selected for fragmentation. Instrument calibration was performed using ESI calibration mixture (Agilent).

The analysis files were converted (using Data Analysis, Bruker) to mgf files, which are suitable for performing a MS/MS ion search with GPM. GPM is a web-based, open source user interface for analyzing and displaying protein identification data. The interface creates a series of web browser page views of tandem mass spectrometry data that has been assigned to protein sequences.”

(Extracted from: Gruber, Altmann (01/2015): Analysis report: Analysis of recombinantly produced IgM grown on different carbon sources.)³

³ See appendix for full Analysis report

6.14 List of Equipment and Reagents

Table 7: All the equipment and reagents that were used and its purpose.

Equipment	Purpose
DASGIP® Parallel Bioreactor Systems (Eppendorf, Germany)	Fully automated bioreactor with the possibility to run up to four fermentations in parallel at different conditions.
Bioprofile 100Plus Analyzer (Nova Biomedical, US)	A device which analyzes the concentration of metabolites such as glucose, glutamate, glutamine, lactate and ammonium as well as the pH, sodium/potassium concentration and the osmolality on an enzymatically based technique. It was used to monitor the progress of fermentations by analyzing the consumption and production of key metabolites. Thus it was able to identify growth-limiting nutrients along with growth-inhibiting secondary metabolites.
Scale (Sartorius, Germany)	Used to weigh equipment
Vortex Genie 2 (Scientific Industries, US)	Mixing device
Laminair (Thermo Scientific, US)	Clean Bench enabling working in a sterile environment.
Wave Biotech STF-IRc Sterile Tube Fuser (GE Healthcare Life Sciences, US)	Allowed the sterile connection of medium and inoculum to the DASGIP Bioreactors by fusing sterile thermoplastic tubes without in a non-sterile environment.
Heraeus Oven (Thermo Scientific, US)	Used for drying and depyrogenation of tubes and other equipment.
ISF1-X Climo Shaker (Kuhner, Switzerland)	Fully automated shaking device enabling the setup of temperature [°C], shaking speed [rpm], CO ₂ [%] and humidity [%].
Inverted Laboratory Microscope with LED Illumination Leica DM IL LED (Leica, Germany)	Magnification device which was used for qualitative and quantitative analysis of the CHO cells. Usually a 10x magnification was applied.
Hemocytometer Neubauer Improved (Marienfeld, Germany)	A device with prepared squares of defined volume for quantification of cells.
Trypan Blue Solution 0.4% (Sigma Life Sciences, US)	Vital stain enabling the identification of dead cells.
Sample vessels (Corning, US)	Safe-Lock Tubes 1.5 mL (Eppendorf, Germany), Falcon® Centrifuge Tubes 15/50 mL
Shaking Flasks (Corning, US)	Erlenmeyer Flasks, 125/250/500/1000 mL, sterile, nonpyrogenic, polycarbonate
Roux Flasks (Thermo Scientific Nunclon Sphera, US)	T25 and T250
Centrifuge (Thermo Scientific, US)	Megafuge 16 Heraeus Centrifuge
Heracell™ 150i CO ₂ Incubator (Thermo Scientific, US)	Static incubation device enabling the setup of temperature [°C] and CO ₂ [%].
Varioklav (Thermo Scientific, US)	Used for sterilization of process equipment at predefined conditions

Rotilabo®-syringe filters, PES, sterile, 0.22 µm (Carl Roth, Germany)	Sterile filtration of liquids.
Z2 Coulter® Particle Count and Size Analyzer (Beckmann Coulter, US)	Used to determine cell concentrations based on the electrical sensing zone method.
Coulter buffer (G0012)	0.1 M Citric acid and 2% w/w Triton® X-100 in RO water.
Coulter solution	Physiological (0.9%) sodium chloride solution (0.22 µm filtered)
F96 Maxisorp Nunc-Immuno Plates (Thermo Scientific, US)	Surface treated high protein-binding capacity polystyrene 96 well ELISA plates.
F96 Without Lid SH Microwell Plates (Thermo Scientific, US)	Used as dilution plates.
Incubating Microplate Shaker (VWR, US)	Shaking device for ELISA plates.
ELISA Plate Washer (Tecan, Switzerland)	Washing device for ELISA plates.
Infinite M100 Reader (Tecan, Switzerland)	ELISA plate reader.
8.4 g NaHCO ₃ , 4.2 g Na ₂ CO ₃ filled up to 1000 mL with RO water (pH 9.5-9.8).	Coating buffer
PBST (1.15 g Na ₂ HPO ₄ · 2H ₂ O, 0.2 g KH ₂ PO ₄ , 0.2 g KCl, 8.0 g NaCl, 1.0 mL Tween filled up to 1000 mL with RO water (pH 7.2-7.4))	Washing buffer
Washing buffer + 1% BSA	Dilution buffer
Anti human IgM (µ-chain) antibody dev. in goat (1 mg/mL, Sigma I 1636)	Coating antibody
Anti human κ light chain antibody - HRP dev. in goat (1 mg/mL, Sigma A 7164)	Detection antibody
IgM standard from human serum (1 mg/mL, Sigma I 8260)	IgM standard for ELISA and WB
Tetramethylbenzidine (TMB)	Staining solution for ELISA
2.5 M H ₂ SO ₄	Stop solution for ELISA
NativePage 3-12% Bis-Tris Gel (Life Technologies, Thermo Fisher Scientific, US)	Gel used for protein separation in WB
HiMark Pre-stained Protein Standard (Life Technologies, Thermo Fisher Scientific, US)	High molecular weight (30 to 460 kDa) protein standard
NuPage-LDS Running Buffer (Life Technologies, Thermo Fisher Scientific, US)	Sample buffer
0.25 M TRIS, 1.92 M Glycine, 1% SDS, pH 8.4-8.9 filled up to 1000 mL with RO water	10x running buffer for SDS-Page after Laemmli
NuPage Transfer Buffer 20x (Life Technologies, Thermo Fisher Scientific, US)	Blotting transfer buffer
PBST washing buffer + 3% milk powder	Inactivation buffer
PVDF Transfer Membrane (Life Technologies, Thermo Fisher Scientific, US)	Membrane used for blotting
SuperSignal® West Pico Chemiluminescent Substrate (Thermo Scientific, US)	Luminol/Enhancer and Stable Peroxide solution used for identification of specific proteins (enhanced chemiluminescent HRP substrate)
Xcell SureLock Mini-Cell Electrophoresis System	Electrophoresis and blotting chamber

(Life Technologies, Thermo Fisher Scientific, US)	
PowerEase®500 Power Supply ((Life Technologies, Thermo Fisher Scientific, US)	A programmable power supply for electrophoresis and blotting
Fusion FX7 (Vilber Lourmat, Germany)	Chemiluminescence imaging camera
Anti human μ heavy chain antibody dev. In goat (FITC, 1 mg/mL)	Fluorescent labeling of IgM heavy chains
Anti human κ light chain antibody dev. in goat (Biotin, 1 mg/mL) + Alexa Flour-647 (Strep, 1 mg/mL)	Indirect fluorescent labeling of IgM light chains
Gallios flow cytometer (Beckman Coulter, US)	Used for investigation intracellular protein content

6.15 Calculations

The cell concentration (CC) was calculated as shown above in 0.

Viable cell concentration (VCC): to quantify the living cell concentration

$$\text{Eq. 4} \quad VCC = \frac{x * \text{viability}}{100} \quad x - \text{cell concentration [c/mL]}$$

Specific growth rate: Displays the growth rate relative to the size of a cell population

$$\text{Eq. 5} \quad \mu = \frac{\ln x_2 - \ln x_1}{t_2 - t_1} \quad t - \text{time [d]}$$

Viable cell specific growth rate: Indicates the proliferation rate regarding the living cells

$$\text{Eq. 6} \quad \mu_v = \frac{\ln VCC_{i+1} - \ln VCC_i}{t_2 - t_1}$$

Viable cell day (VCD): Calculates the amount of viable cells that newly arise from one day to the next.

$$\text{Eq. 7} \quad VCD = \frac{VCC_{i+1} - VCC_i}{\mu_v}$$

Viable cumulative cell days (VCCD): The integral of viable cells at a constant specific growth rate. Equation 8 shows the solution for VCCD within the time interval from t_1 to t_n at distinct time points t_i .

$$\text{Eq. 8} \quad VCCD = \sum_{i=1}^n \frac{x_{i+1} - x_i}{\mu_v}$$

The cell specific productivity (qP) and other cell-specific metabolic rates (qM) for glucose ($qGlc$), lactate ($qLac$), glutamine ($qGln$), glutamate ($qGlu$) and ammonium (qNH_4^+) were calculated according to equation 9. A negative value represents consumption, whereas positive values indicate production. The cell-specific rates represent the produced or consumed concentration of a product per one cell per day.

$$\text{Eq. 9} \quad qP \text{ or } qM = \frac{c_{m,n} - c_{m,1}}{VCCD}$$

$c_{m,n}$ and $c_{m,1}$ indicate the product or metabolite concentrations at time points t_n and t_1 .

Space-time-yield (STY) or volumetric productivity: Illustrates the accumulated product concentration produced in a volume of one liter relating to the process time. In equation # c_p is the product concentration at the time point t and c_p^0 is the initial product concentration at the beginning of the batch process t_0 .

$$\text{Eq. 11} \quad STY = \frac{c_p - c_p^0}{t - t_0}$$

7 Results

7.1 Adaption of cell line A to alternative sugar sources

After passaging the cells into new shaking flasks with the D/H medium containing the alternative sugar substrate, the cells were successfully adapted to glucose, mannose and galactose showing stable cell concentrations (Figure 13) and viabilities (Figure 14) within 4 passages. In the case of fructose, sucrose or trehalose, the cells rapidly declined both in cell concentrations (Figure 13) and viability (Figure 14) within 3 to 4 passages. The following graphs (Figure 13, Figure 14) show the behavior of the cells from passage to passage before and after the adaption to the alternative sugar sources.

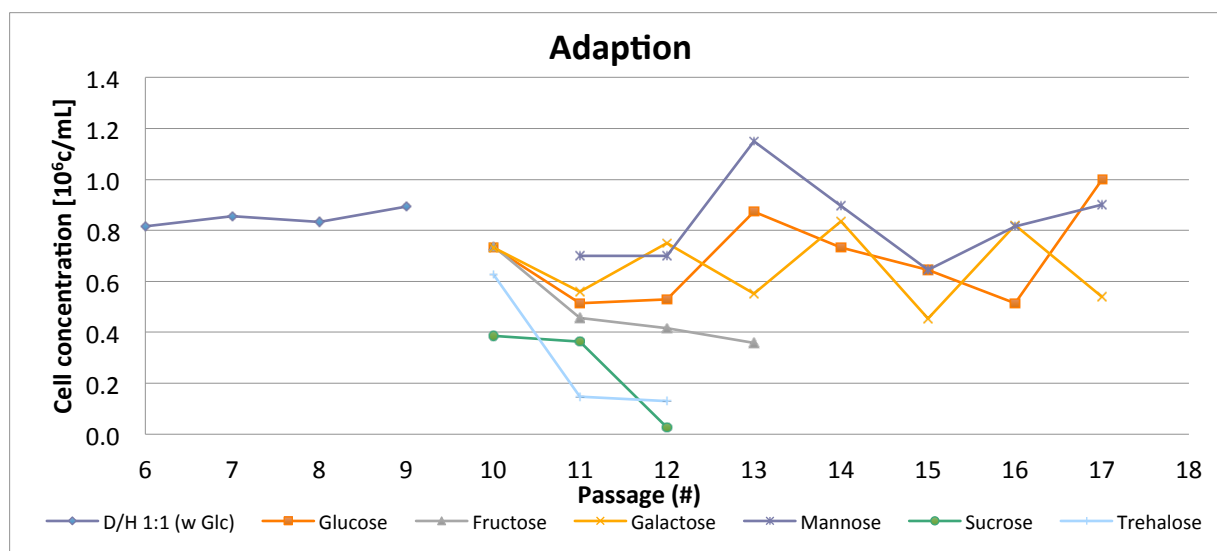


Figure 13: The cell concentrations at the end of each passage before and after the cells have been passaged into new medium containing the alternative sugar substrates. The adaption was performed between passage 9 and 10.

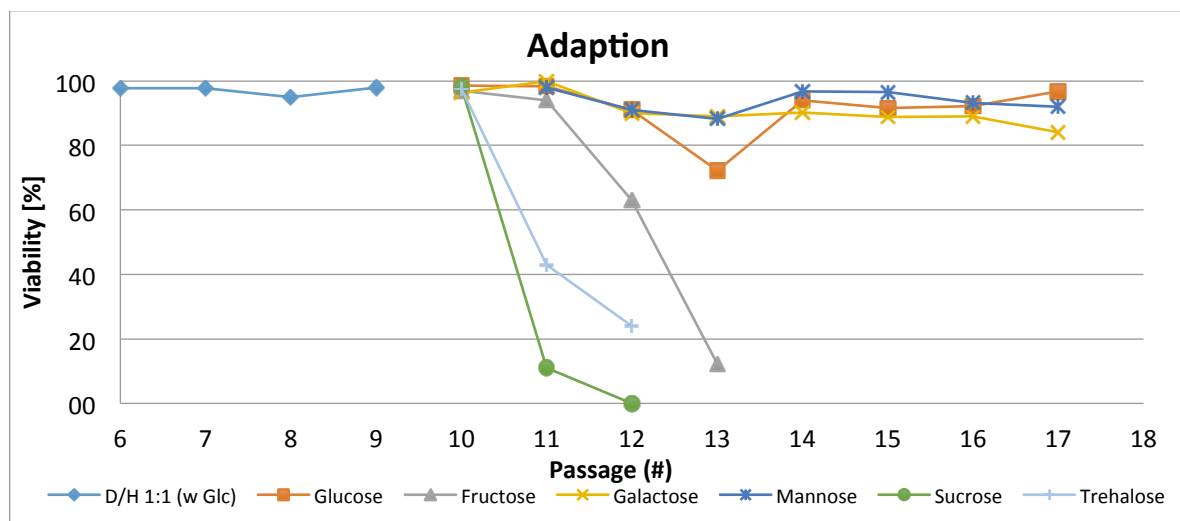


Figure 14: The viabilities at the end of each passage before and after the cells have been passaged into new medium containing the alternative sugar substrates. The adaption was performed between passage 9 and 10.

7.2 Batch 1 – determination of the optimal sugar concentration (cell line A)

Following the adaption of the cells to the new sugar source a batch experiment in shaking flasks was performed to determine the optimal sugar concentrations. This means, that for each of the three sugars three separate shaking flasks at concentrations of 4, 6 and 8 g/L of the carbon source were operated. In total nine 125 mL shaking flasks have been set up and for every one 9.0×10^6 cells from the corresponding routine passages were centrifuged and resuspended in 30 mL D/H medium working volume to reach a starting concentration of 3.0×10^5 cells/mL.

For each sugar the cells displayed the typical growth curve (Figure 6). In the shaking flasks containing glucose the cell concentrations peaked at 1.8×10^6 c/mL for 4 g/L, at 1.4×10^6 c/mL for 6 g/L and at 1.1×10^6 c/mL for 8 g/L (Figure 15). This relatively high peak concentration for 4 g/L glucose may be due to an outlier, since it shows an abnormal steeply rising from day 5 to day 6 (Figure 15) and the estimated cell concentration determined with the hemocytometer was 1.24×10^6 c/mL. But the viable cumulative cell concentrations also indicated that the 4 g/L glucose concentration may lead to higher growth, since it peaks at 8.31×10^6 c/mL compared to 6.74×10^6 for 6 g/L (Figure 16). In contrast to the cell concentrations, the viabilities for the different glucose concentrations show not much of a difference (Figure 15). For both galactose and mannose the growth and viabilities between the different concentrations were very similar (Figure 18, Figure 19, Figure 21, Figure 22). Interestingly the cell concentrations and viabilities of glucose and mannose were rather similar, while the cells in the flasks containing galactose showed about 50% lower cell concentrations and faster declining viabilities. Accordingly the consumption of the sugars glucose and mannose were almost exactly the same and both the 4 g/L concentrations were depleted before the viabilities dropped below 60%, while galactose was used much slower and never came close to being depleted (Figure 24). The titers also showed corresponding results. Not only did all three sugars illustrate high similarity in the titers if the concentrations of each sugar were compared, but also between glucose and mannose only minor differences could be demonstrated (Figure 17, Figure 20, Figure 23). Only the titers of the galactose flasks were much lower (ca. 120 μ g/mL compared to 150 μ g/mL for glucose on day 9), analogous to the lower cell concentrations and viabilities. Because the titers are strongly related on the different cell concentrations, the specific productivities (qP) were also calculated to display the product generating performance normalized per cell and day. The results for the specific productivities (Figure 25) indicated that the productivity for galactose was rather equally (~ 25 pg/c/d) or for 4 and 8 g/L even higher (~ 30 pg/c/d) compared to glucose and mannose. For glucose the qP was slightly lower for the 4 and 6 g/L concentrations (~ 20 pg/c/d), while a 8 g/L mannose concentration demonstrated a higher qP (~ 30 pg/c/d). The product quality regarding the isoform distribution showed that for all sugars and concentrations the vast majority of produced IgMs were pentamers, with only little additional bands seen at the monomer region (Figure 26).

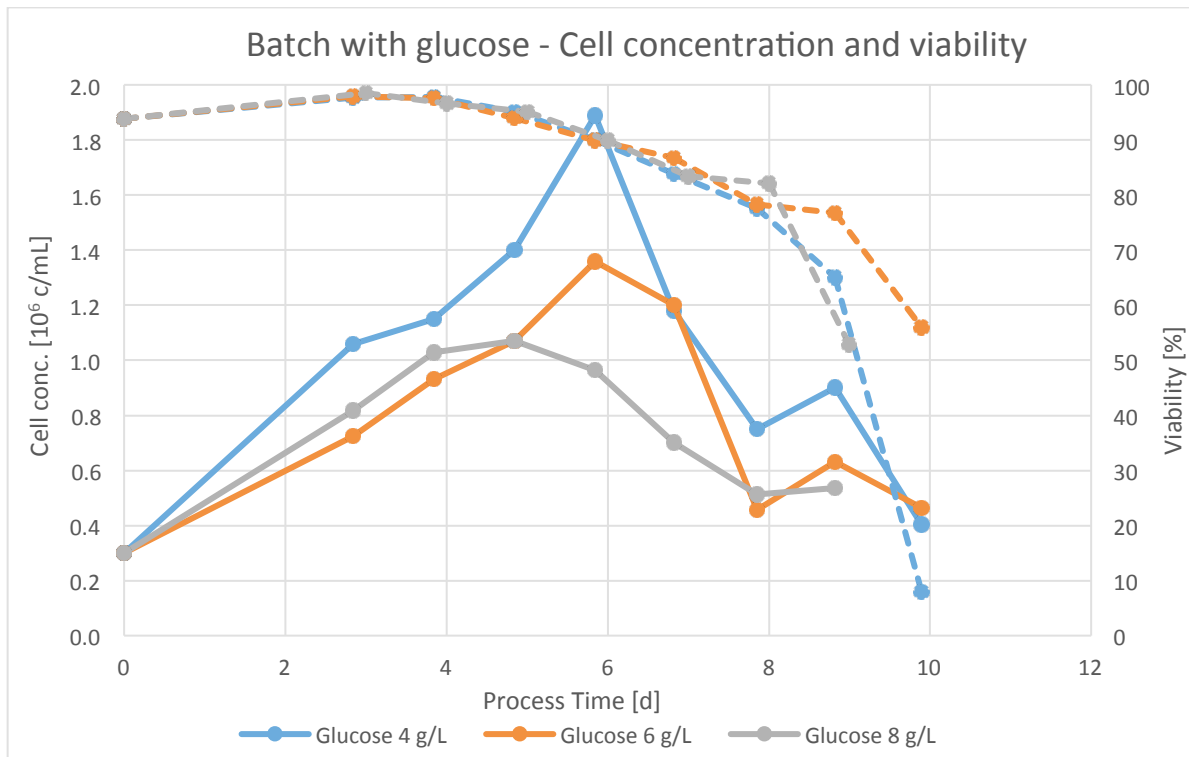


Figure 15: The cell concentrations as well as the viabilities over the time of the batch experiment as a comparison between the three different glucose concentrations.

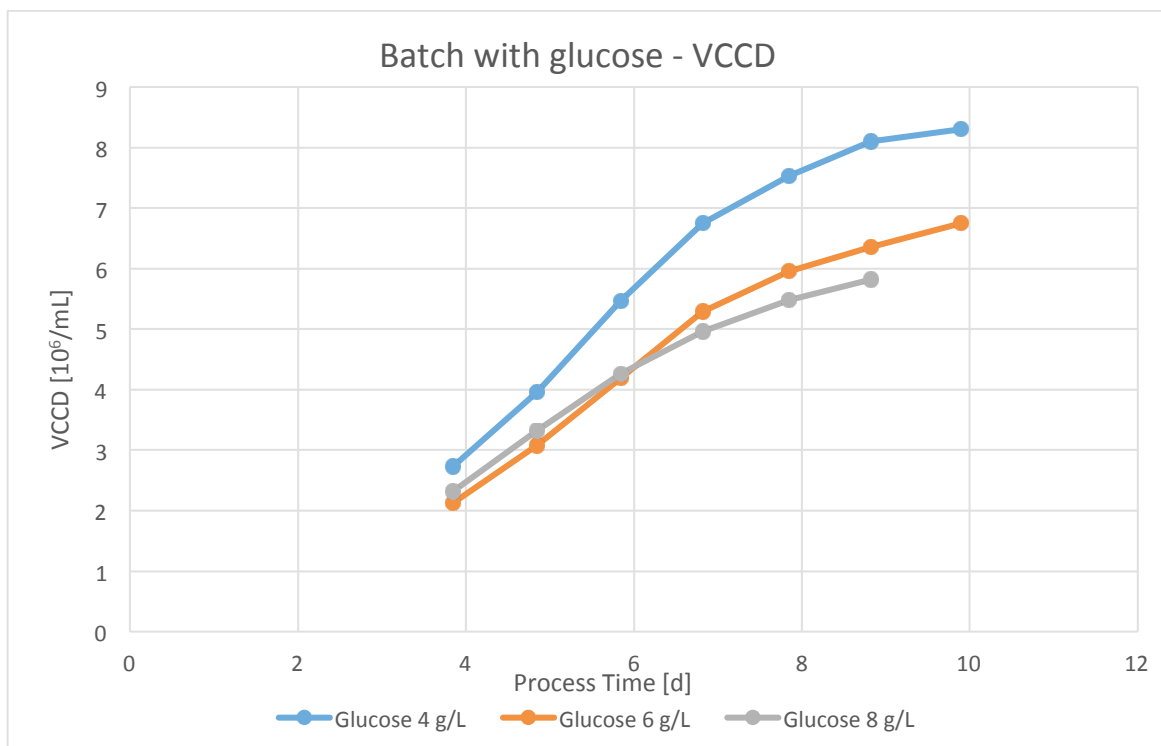


Figure 16: The viable cumulative cell days (VCCD) over the time of the batch experiment.

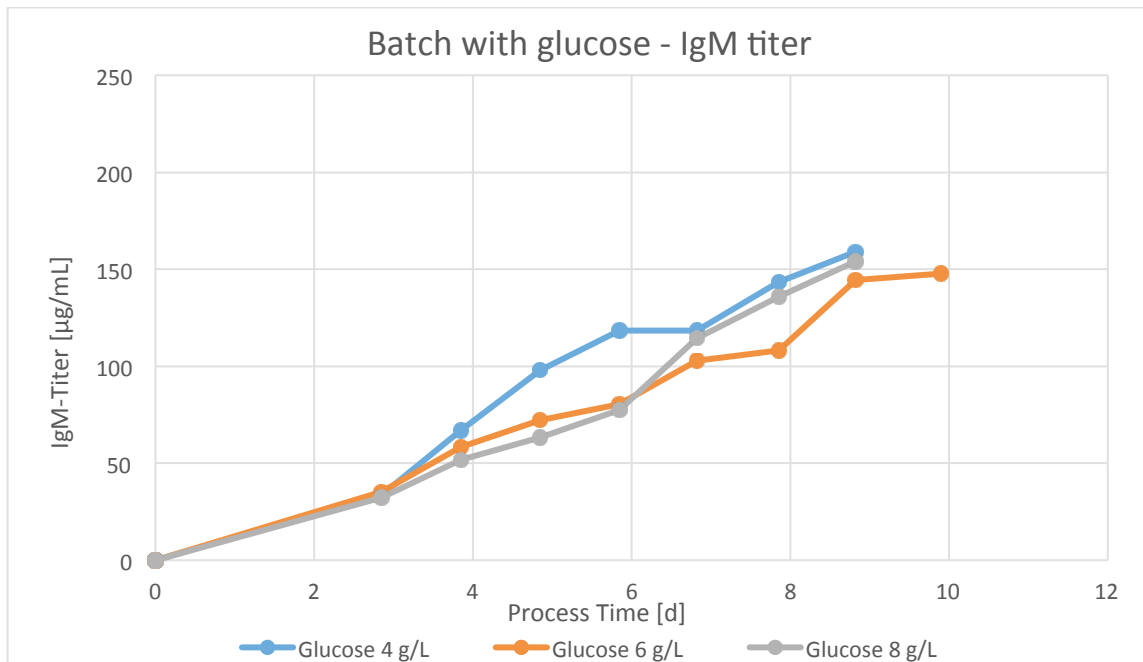


Figure 17: The product titers over the time of the batch experiment as a comparison between the three different glucose concentrations.

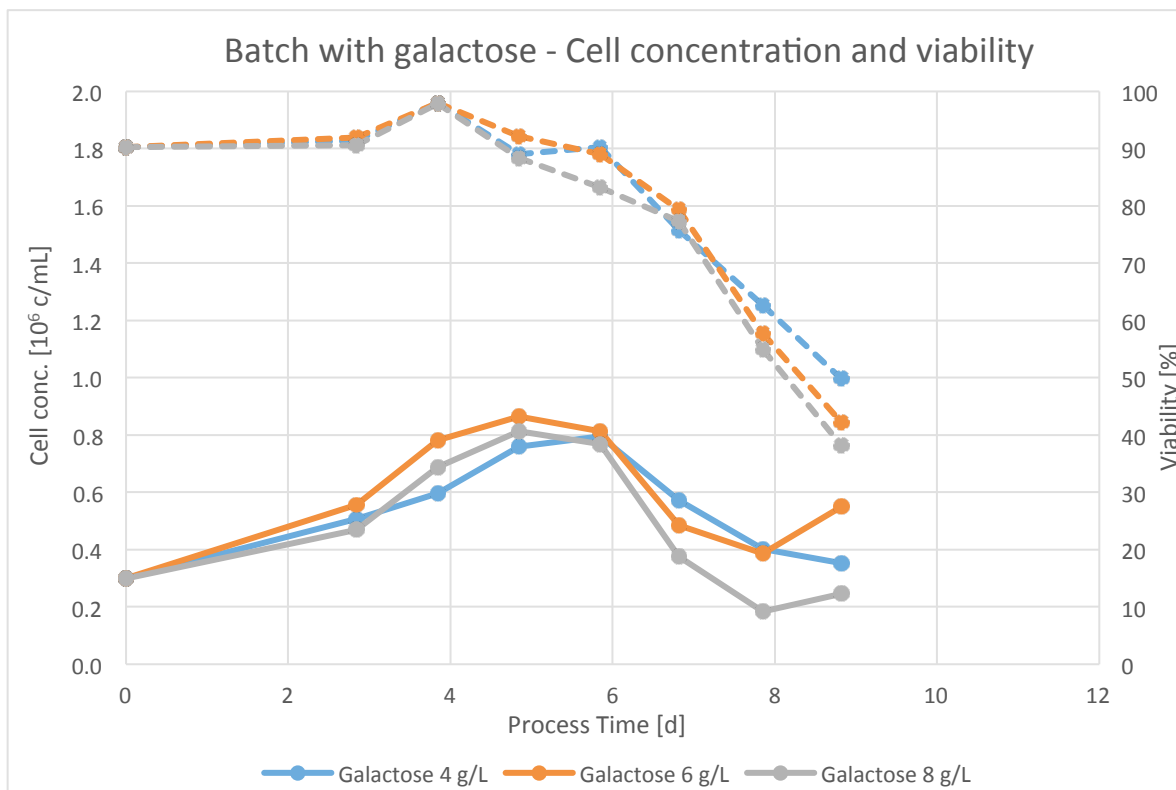


Figure 18: The cell concentrations as well as the viabilities over the time of the batch experiment as a comparison between the three different galactose concentrations.

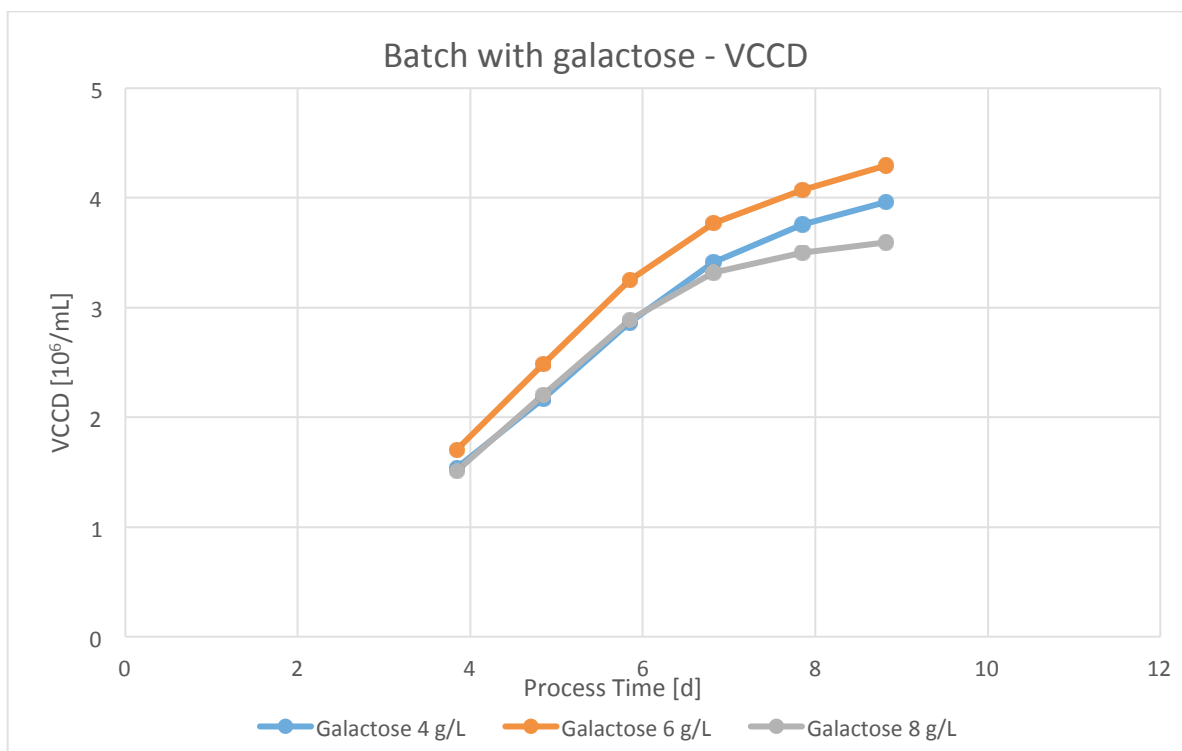


Figure 19: The viable cumulative cell days (VCCD) over the time of the batch experiment.

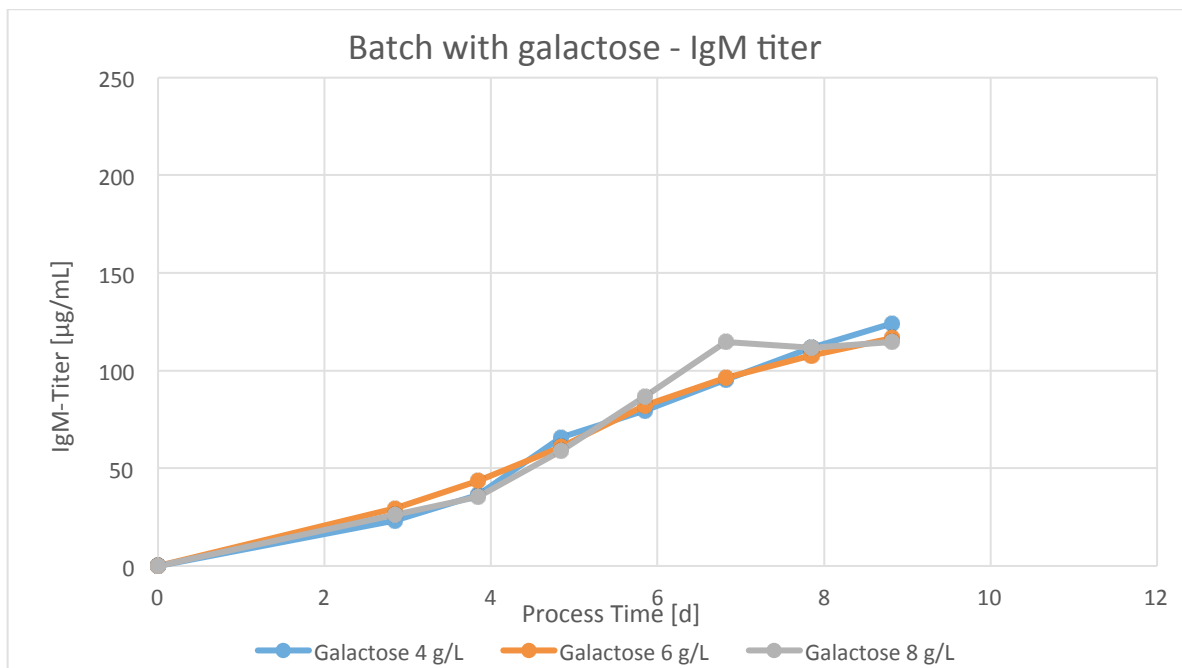


Figure 20: The product titers over the time of the batch experiment as a comparison between the three different galactose concentrations.

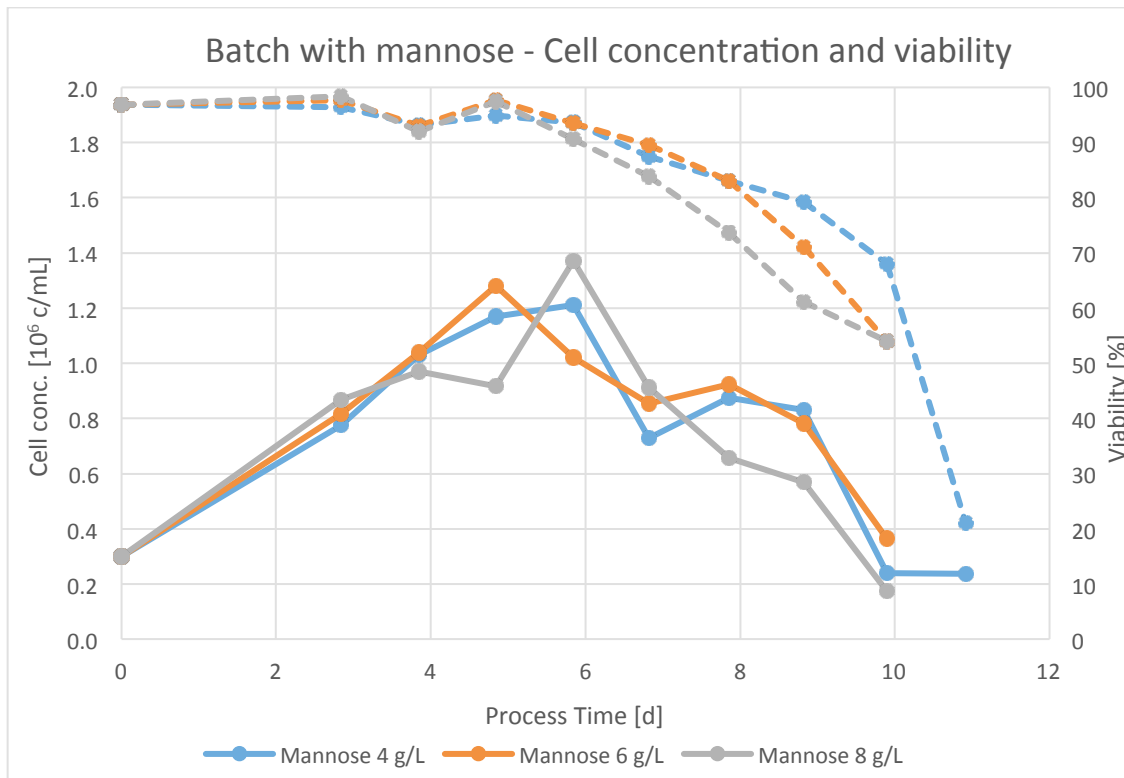


Figure 21: The cell concentrations as well as the viabilities over the time of the batch experiment as a comparison between the three different mannose concentrations.

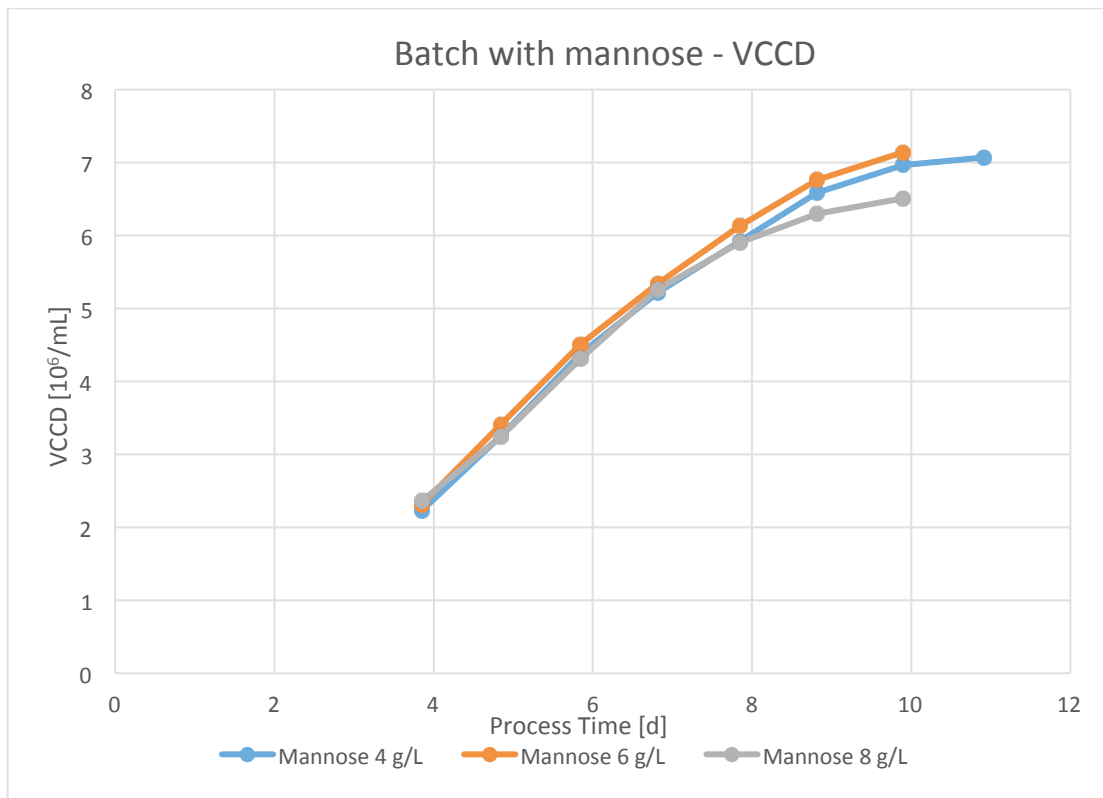


Figure 22: The viable cumulative cell days (VCCD) over the time of the batch experiment.

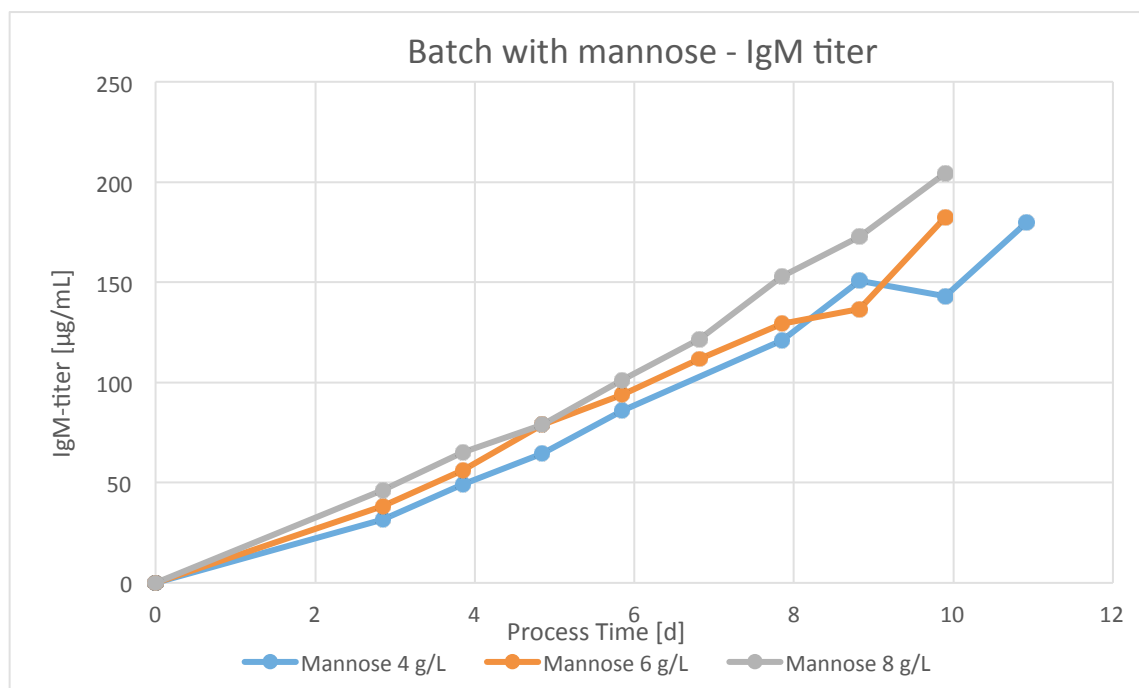


Figure 23: The product titers over the time of the batch experiment as a comparison between the three different mannose concentrations.

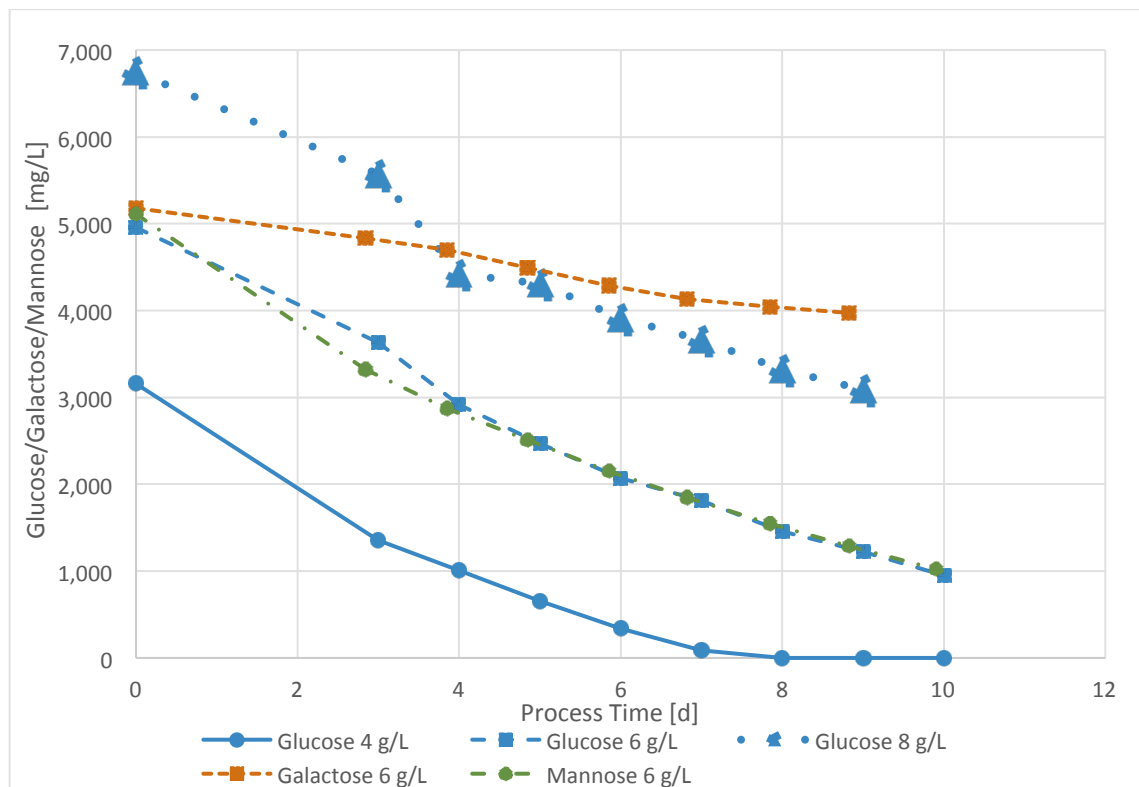


Figure 24: Consumption of glucose, galactose and mannose. Note: The glucose concentrations were measured with the help of the bioprofiler. Since we observed that glucose at 4 g/L was depleted in the course of the batch experiment and the curves for the consumption of 6 and 8 g/L were following the same gradient, we only sent the samples of 6 g/L galactose and mannose to be analyzed by HPLC.

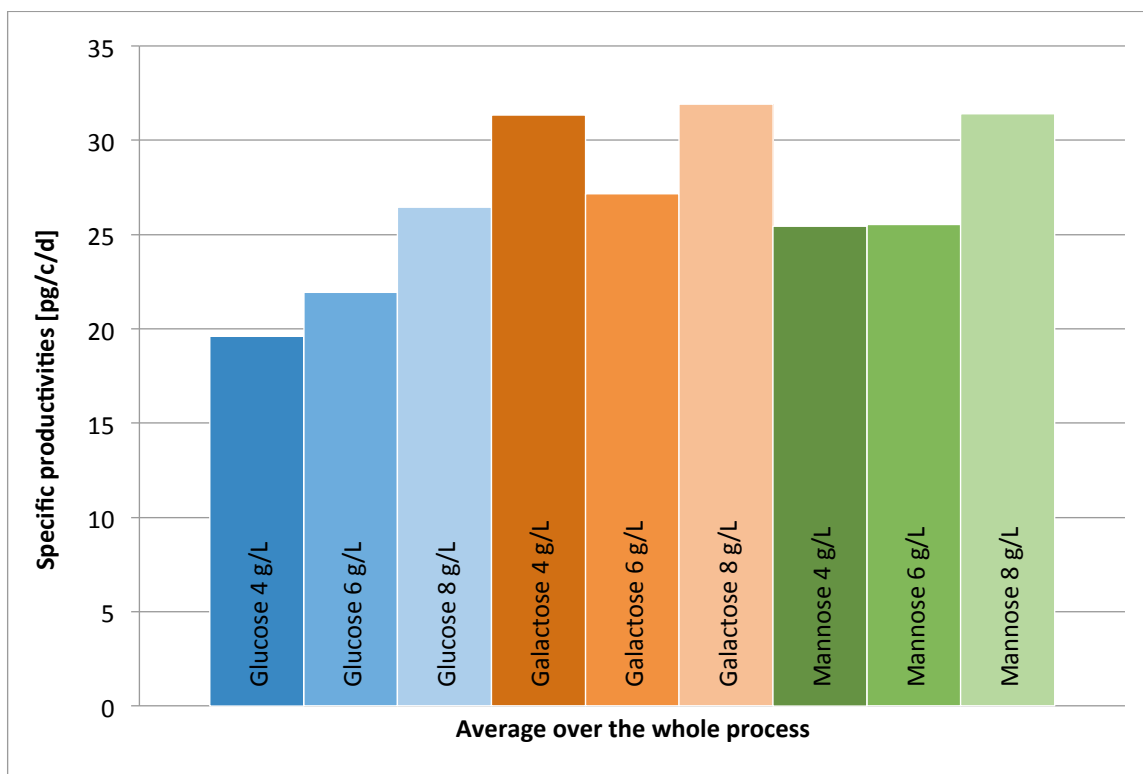


Figure 25: Specific productivities as the average over the whole process. Calculation: IgM titer of the last day divided by the VCCD of the last day.

Table 8: Summary of Batch 1. The specific growth rate μ is given for the exponential growth phase from the starting day until day 4.

	Glucose			Galactose			Mannose		
Parameter	4 g/L	6 g/L	8 g/L	4 g/L	6 g/L	8 g/L	4 g/L	6 g/L	8 g/L
Peak cell concentration [10^6 c/mL]	1.89	1.36	1.07	0.76	0.86	0.81	1.2	1.28	1.37
μ [1/d]	0.26	0.28	0.29	0.17	0.28	0.27	0.31	0.30	0.24
Titer [μ g/mL]	158.83	153.84	147.89	124.27	116.72	114.74	179.87	182.44	204.43
VCCD [10^6 c/mL]	8.31	6.74	5.81	3.96	4.29	3.60	7.07	7.14	6.51
qP [pg/cell/day]	19.61	21.93	26.46	31.35	27.18	31.90	25.44	25.55	31.40
qGlc/qGal/qMan [pg/c/d]	419	594	630	222	281	-	-	573	-
Batch duration [d]	10	10	9	9	9	9	11	10	10

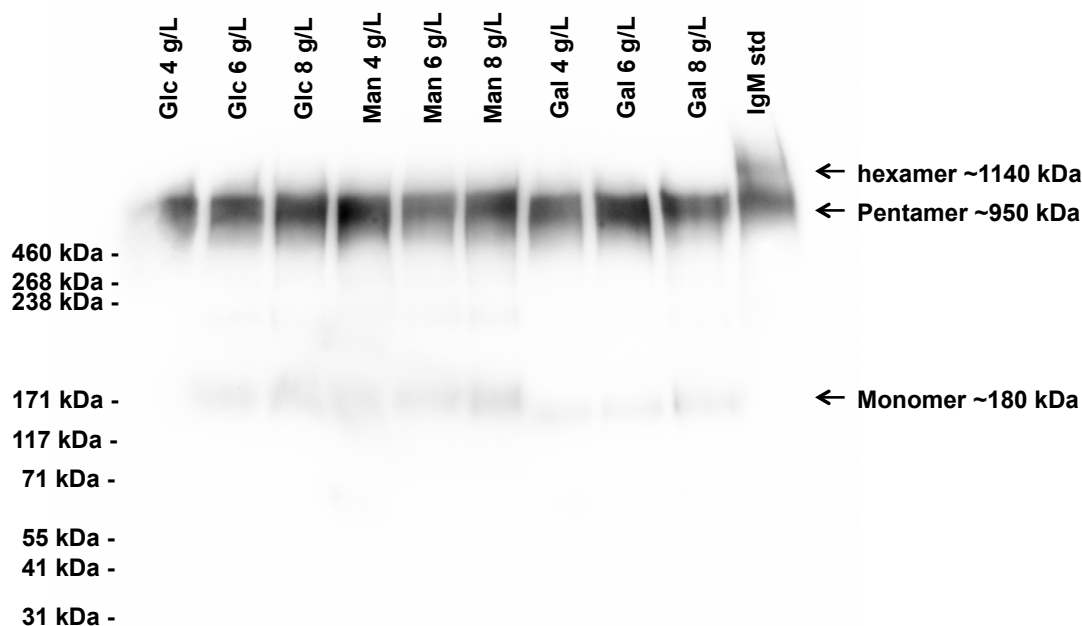


Figure 26: The western blot. The marker used was the *HiMark™ Pre-Stained HMW Protein Standard*. Exposure time was 3 seconds.

Since neither the growth nor the viability, product titer or isoform distribution showed a significant advantage between the sugar concentrations and because glucose and mannose, respectively, ran out at 4 g/L, for all subsequent passages and experiments a sugar concentration of 6 g/L was applied.

7.3 Batch 2 – investigating a potentially beneficial effect of sucrose or trehalose as supplement (cell line A)

As another pre-experiment it was investigated whether the addition of sucrose or trehalose as supplements have a beneficial impact regarding the product titer and/or isoform distribution because of their known protein stabilizing effect (Jeffrey L. Cleland 2001). For this purpose several shaking flasks with D/H medium containing glucose were set up and sucrose or trehalose, respectively, was added at concentrations of 0.1, 0.5, 1 and 2 g/L as well as one shaking flask without sucrose or trehalose as a negative control.

The results for the cell concentrations (Figure 27, Figure 28, Figure 31, Figure 32), viabilities (Figure 27, Figure 31) and product titers (Figure 29, Figure 33) revealed, that all shaking flasks

independent from the added disaccharides and concentrations performed similar to a very high degree. Only the shaking flask supplemented with trehalose at a concentration of 0.1 g/L illustrated a higher peaked cell concentration of 1.8×10^6 c/mL compared to the other shaking flasks, which peaked around 1.4×10^6 and 1.5×10^6 c/mL. Moreover that shaking flasks also showed a lower specific productivity of about 13 pg/c/d compared to the others, which all lay between 15 and 18 pg/c/d (Figure 30, Figure 34). On the contrary, the shaking flasks supplemented with the disaccharides at the highest concentration of 2 g/L both indicated the lowest cell concentrations (Figure 28, Figure 32), but the highest specific productivities (Figure 30, Figure 34). In this batch fermentation all shaking flasks almost exclusively produced pentameric IgMs next to very few monomers (Figure 35, Table 10). But since the product quality regarding the isoform distribution could already be proven as being very high in the previous experiment, these IgM producing cells are inappropriate to investigate a potentially beneficial impact on this product characteristic.

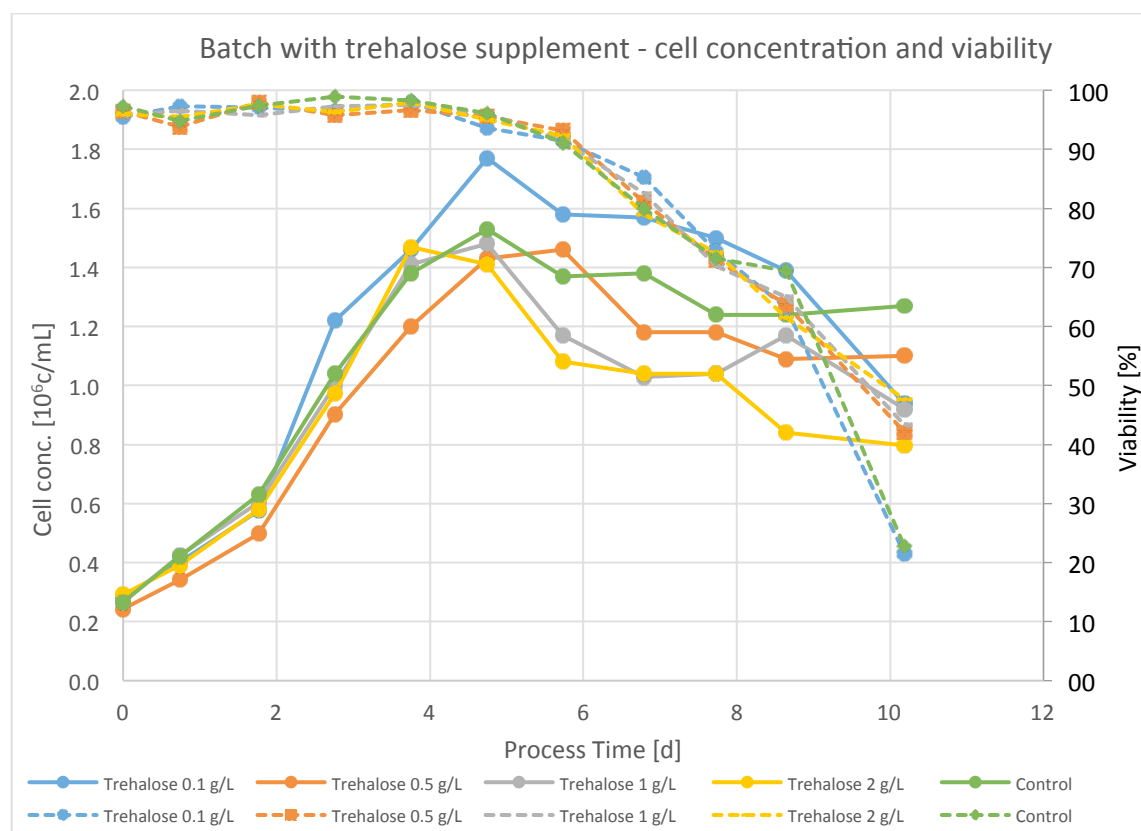


Figure 27: Daily cell concentrations and viabilities of the shaking flasks supplemented with trehalose at different concentrations along with the control (*CHO cells A*).

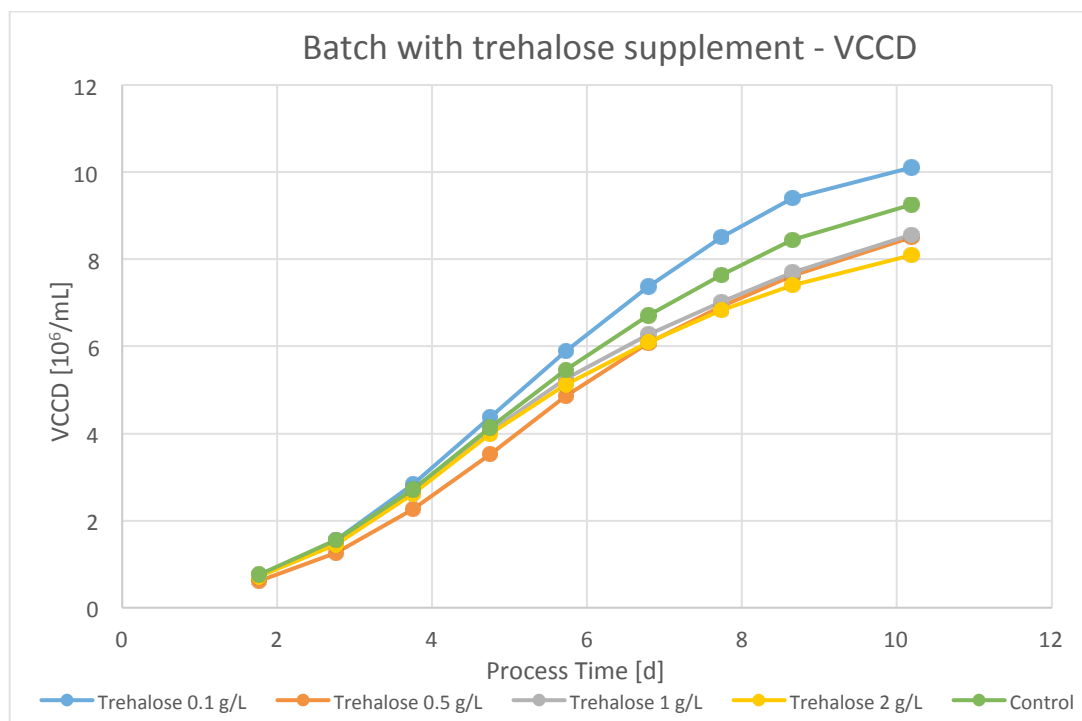


Figure 28: The viable cumulative cell days (VCCD) over the time of the batch experiment.

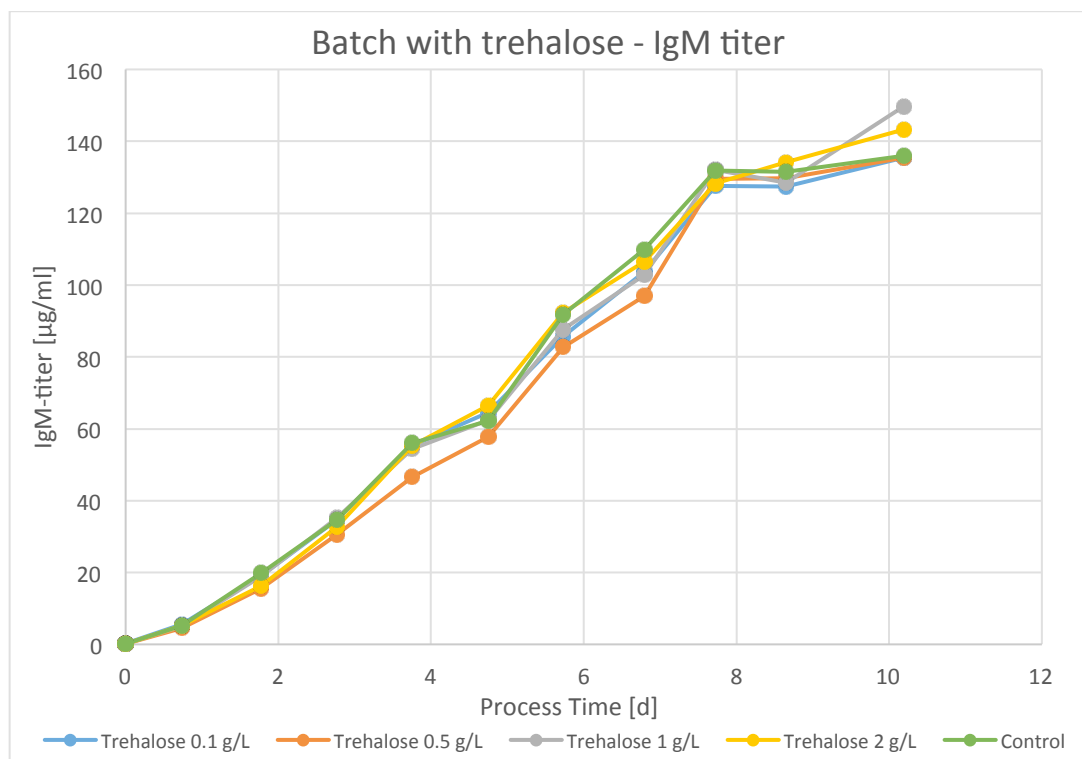


Figure 29: Daily product titers of the shaking flasks supplemented with trehalose at different concentrations along with the control (*CHO cells A*).

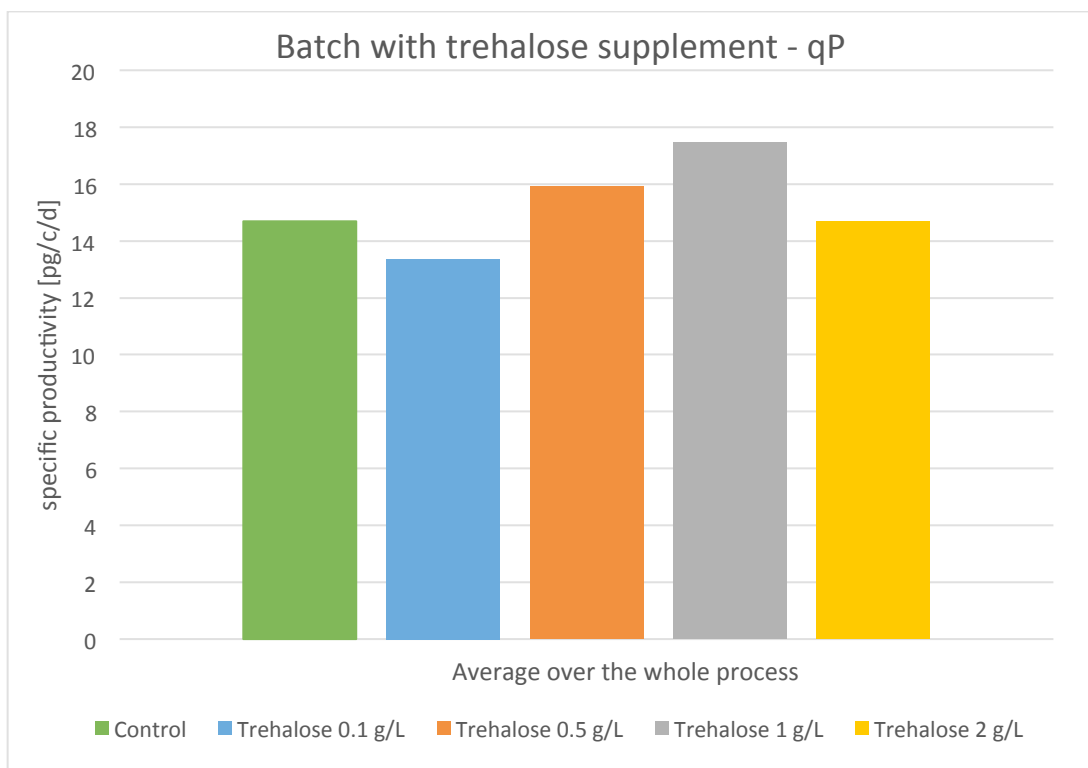


Figure 30: Average specific productivities over the whole batch experiment of the shaking flasks supplemented with trehalose at different concentrations as well as the control (*CHO cells A*). Calculation: IgM titer of the last day divided by the VCCD of the last day.

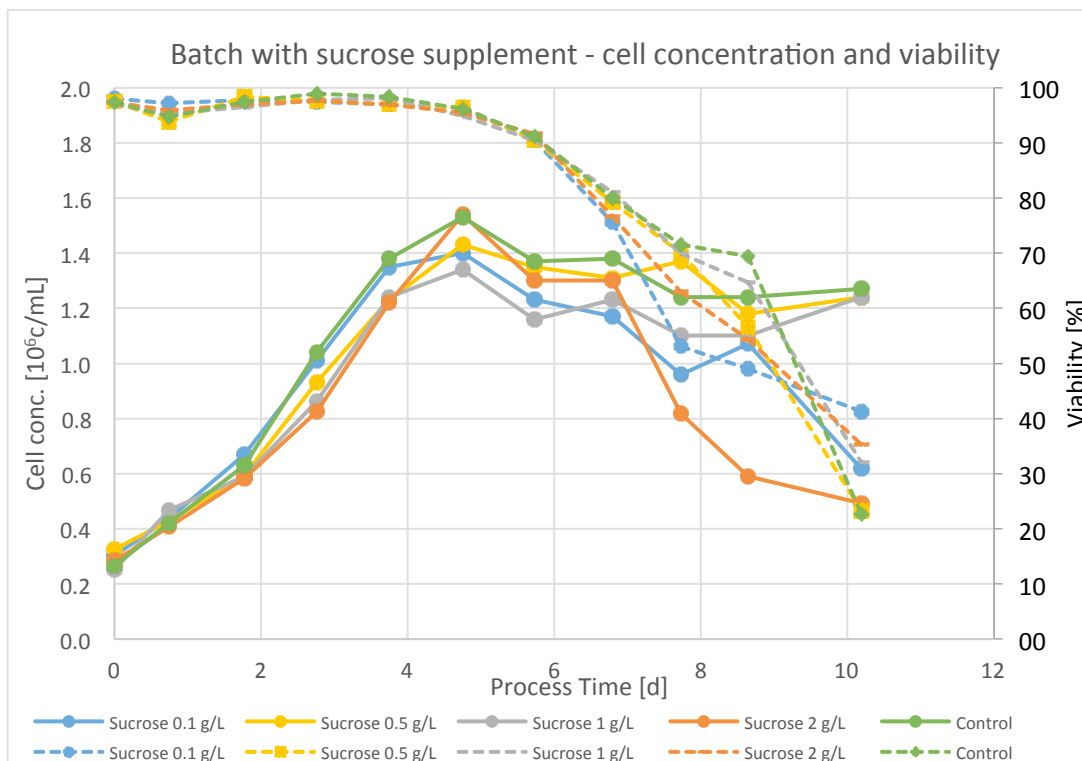


Figure 31: Daily cell concentrations and viabilities of the shaking flasks supplemented with sucrose at different concentrations along with the control (*CHO cells A*).

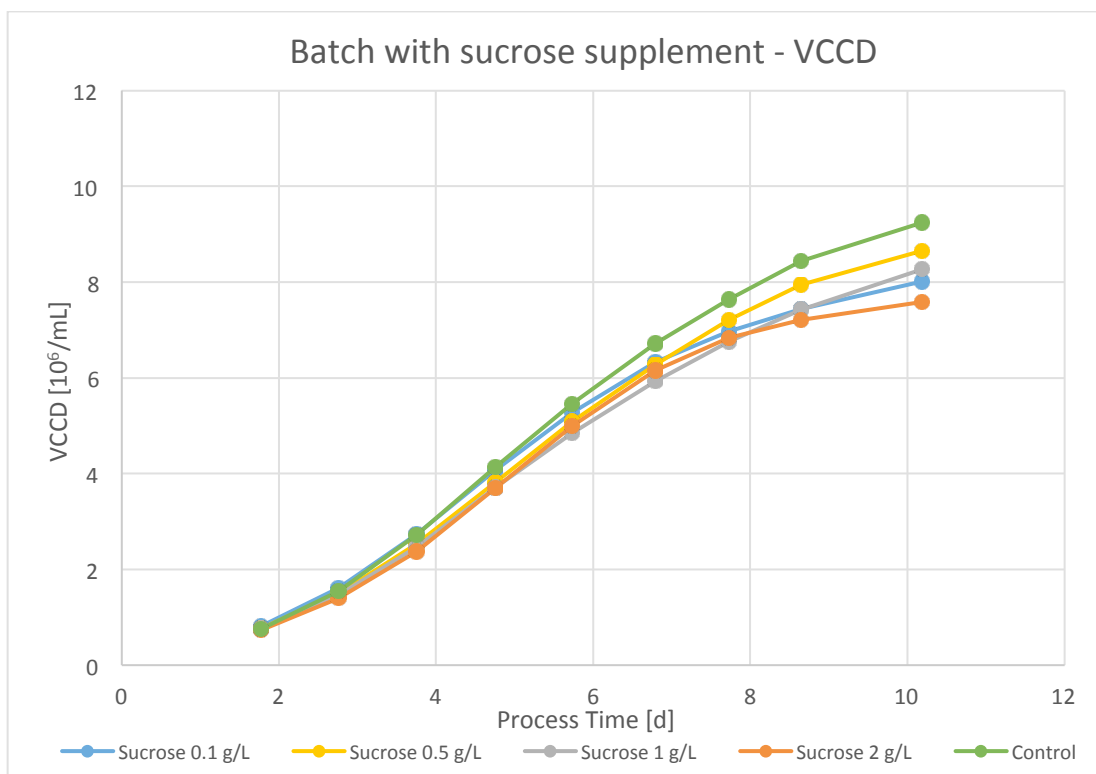


Figure 32: The viable cumulative cell days (VCCD) over the time of the batch experiment.

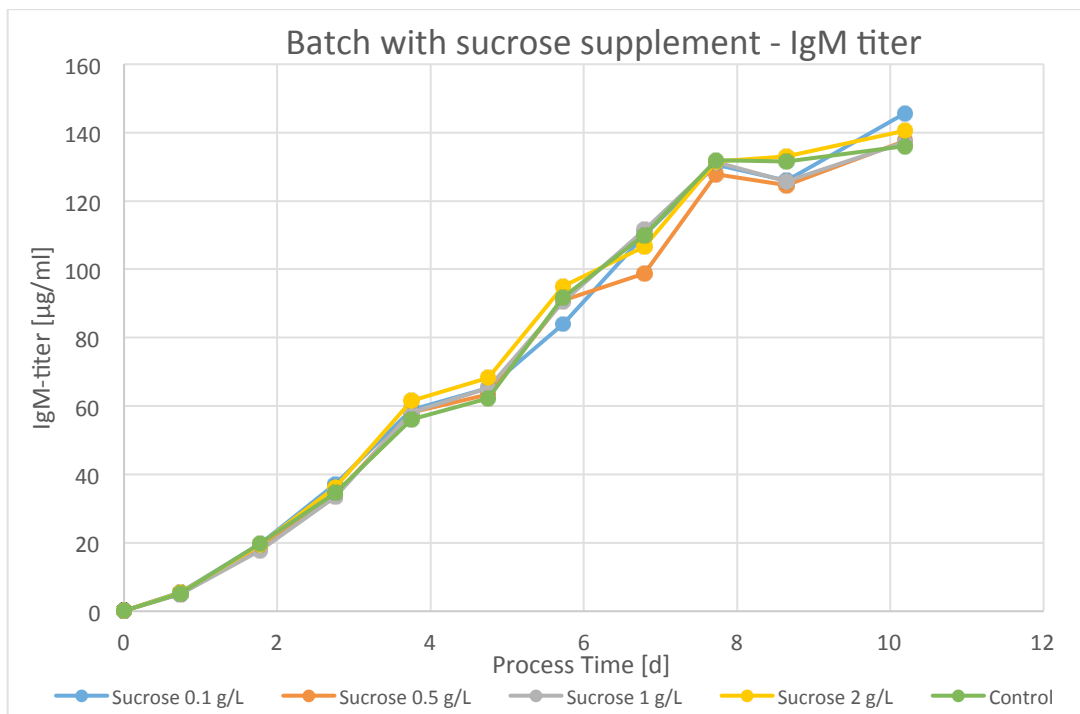


Figure 33: Daily product titers of the shaking flasks supplemented with sucrose at different concentrations along with the control (*CHO cells A*).

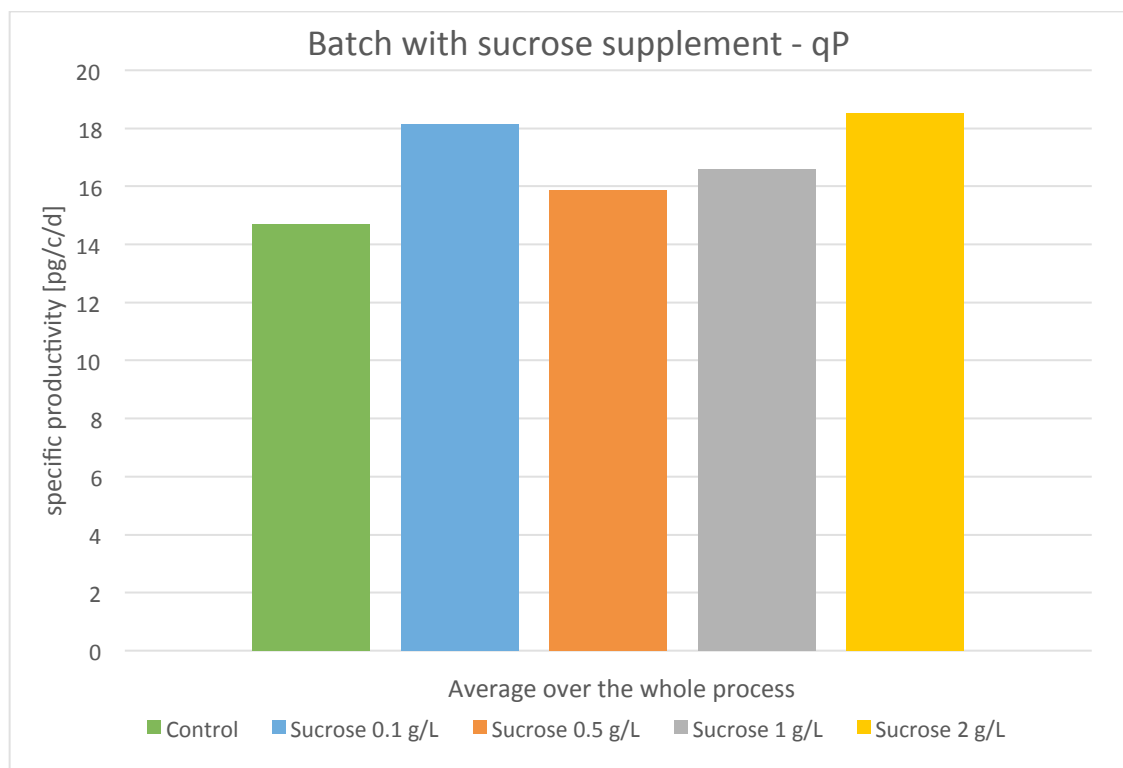


Figure 34: Average specific productivities over the whole batch experiment of the shaking flasks supplemented with sucrose at different concentrations as well as the control (*CHO cells A*). Calculation: IgM titer of the last day divided by the VCCD of the last day.

Table 9: Summary of Batch 2. The specific growth rate μ is given for the exponential growth phase from the starting day until day 4.

	Control	Trehalose [g/L]				Sucrose [g/L]			
Parameter		0.1	0.5	1	2	0.1	0.5	1	2
Peak cell concentration [10^6 c/mL]	1.53	1.77	1.46	1.48	1.47	1.40	1.43	1.34	1.54
μ [1/d]	0.45	0.44	0.43	0.46	0.43	0.41	0.36	0.45	0.40
Titer [μ g/mL]	136.02	135.40	135.47	149.63	143.29	145.49	137.48	137.16	140.60
VCCD [10^6 c/mL]	9.25	10.10	8.50	8.56	8.09	8.02	8.65	8.26	7.58
qP [pg/cell/day]	14.69	13.37	15.92	17.47	17.69	18.15	15.88	16.59	18.53
qGlc [pg/c/d]	492.41	404.27	501.94	500.19	504.85	399.14	496.84	504.38	476.28
Batch duration [d]	10	10	10	10	10	10	10	10	10

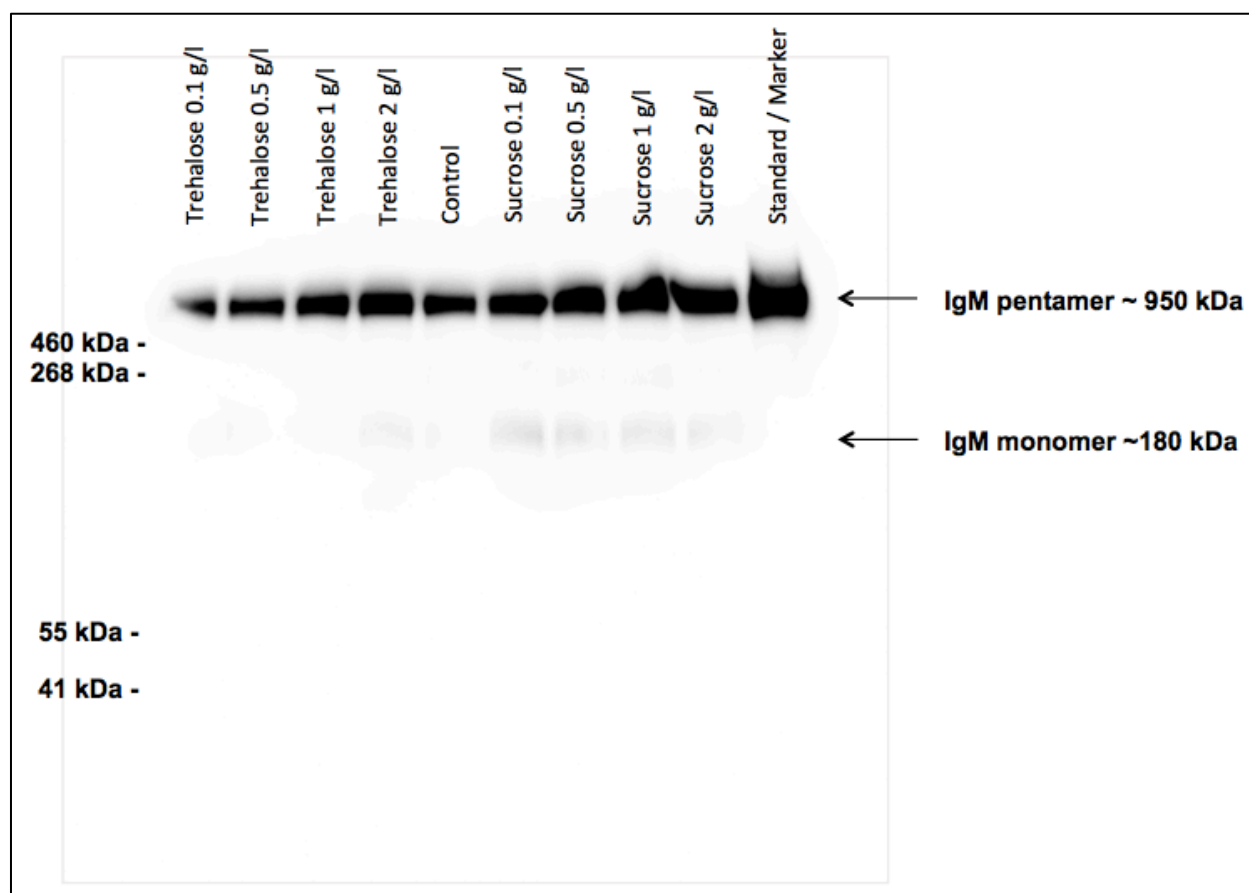


Figure 35: Results of the western blot. The marker used was the *HiMark™ Pre-Stained HMW Protein Standard*. The standard applied was the IgM standard from human serum (I 8260). Exposure time was 40 seconds.

Table 10: Isoform distribution of the sucrose and trehalose supplemented approaches, the control and the standard (IgM standard from human serum, I 8260).

	Control	Trehalose [g/L]				Sucrose [g/L]				Standard
Parameter		0.1	0.5	1	2	0.1	0.5	1	2	
Pentamers [%]	98.69	100	99.56	100	95.61	92.11	94.70	91.33	93.29	100
Monomers [%]	1.31	0.00	0.44	0.00	4.39	7.89	5.30	8.67	6.71	0.00

The results of this batch experiments indicated that neither sucrose nor trehalose as supplements had a beneficial effect on the titer of cell line A.

7.4 Batch F49 – Comparison of different sugars in D/H medium with ProCHO5 in the DASGIP module and in shaker flasks (cell line A)

This batch experiment was focused on study the behavior of the cells in the DASGIP Bioreactor by operating 4 reactors in parallel with three of them containing D/H medium with a different sugar source and the fourth containing ProCHO5 medium.

Key parameters:

Temperature [°C]:	37.0
Stirrer-speed [rpm]:	80
pH:	7.00
Dissolved oxygen [% sat.]:	30
Gas-flow [L/h]:	1
Volume [mL]:	600
Starting cell concentration:	3×10^5 c/mL
Media:	D/H (w/o Glc) + Glucose 6 g/L D/H (w/o Glc) + Galactose 6 g/L D/H (w/o Glc) + Mannose 6 g/L ProCHO5 (w Glc)

The following figures clearly show that the DASGIP bioreactors were heavily inferior to the shaking flasks for every medium and sugar. The cells reached three times higher cell concentrations in the shaking flasks with glucose, mannose and ProCHO5 and 2 times higher cell concentration in the case of galactose (Figure 36, Figure 38). Furthermore all shaking flasks showed a much better viability with a survival time of 12 days for ProCHO5, glucose and mannose and 9 days for galactose, respectively, compared to 8 (glucose), 6 (mannose and ProCHO5) and 4 days (galactose) (Figure 36, Figure 38). Because of the lower performance in the bioreactors the titers, metabolites and product qualities were not analyzed. Specific adjustments such as stirrer speed and type of aeration as possible reasons for the low performance were later on investigated in the batch F56 (7.8).

As the consequence all subsequent batch fermentations were performed in shaking flasks.

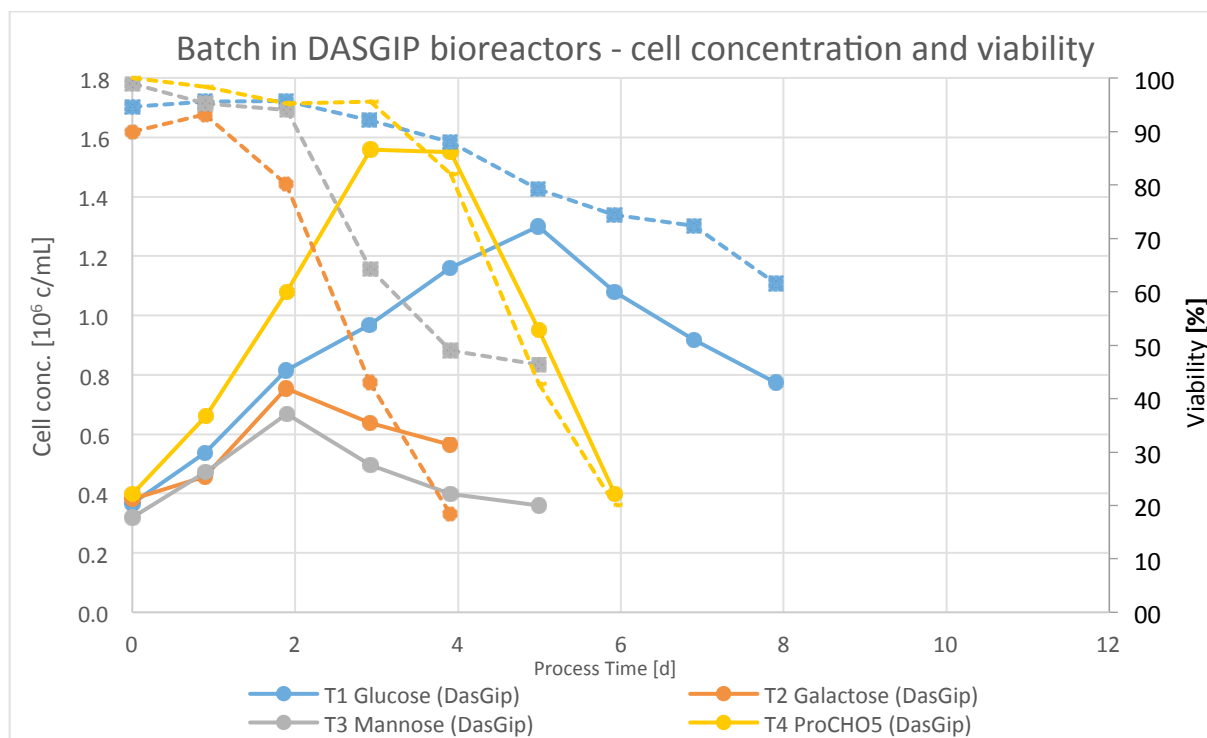


Figure 36: Daily cell concentrations and viabilities of the DASGIP bioreactors.

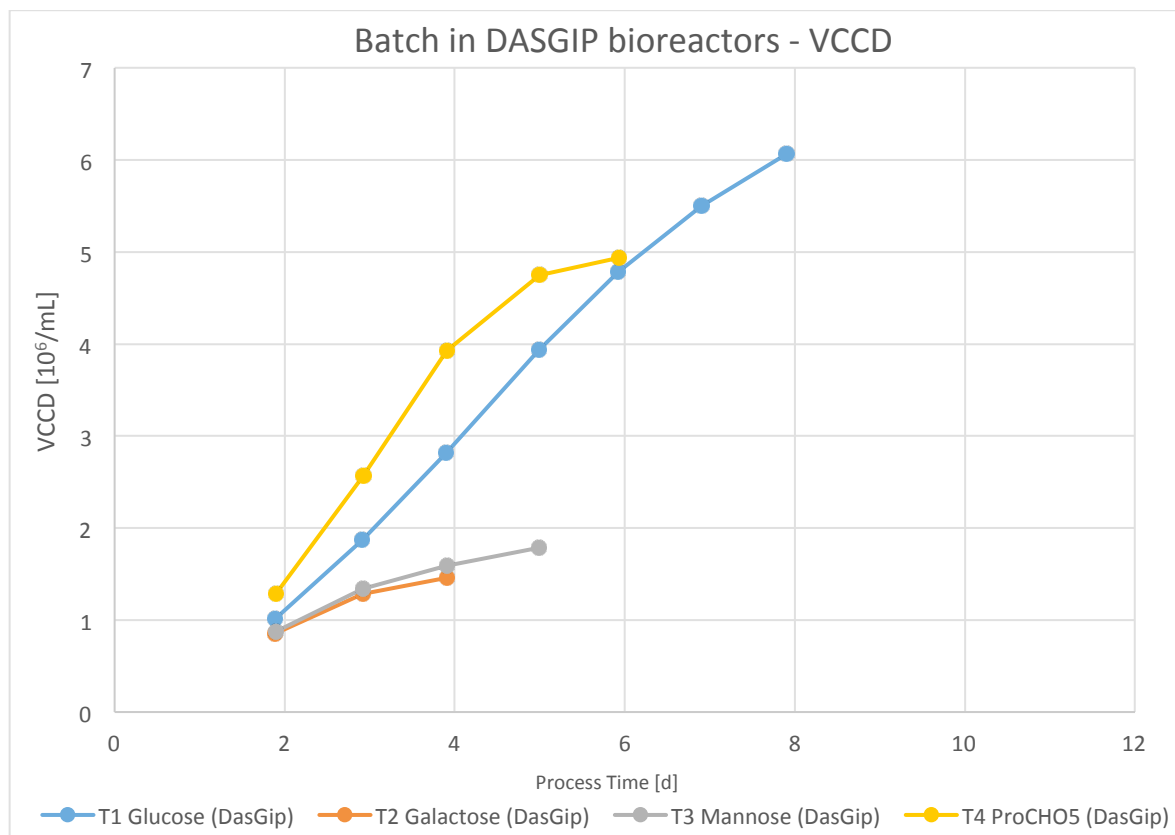


Figure 37: The viable cumulative cell days (VCCD) over the time of the batch experiment.

To get a better impression on the performance of the cells in the DASGIP bioreactors it was decided to compare them with corresponding 125 mL shaking flasks. Therefore a 30 mL equivalent was drawn from each reactor on day 0 and transferred into shaking flasks.

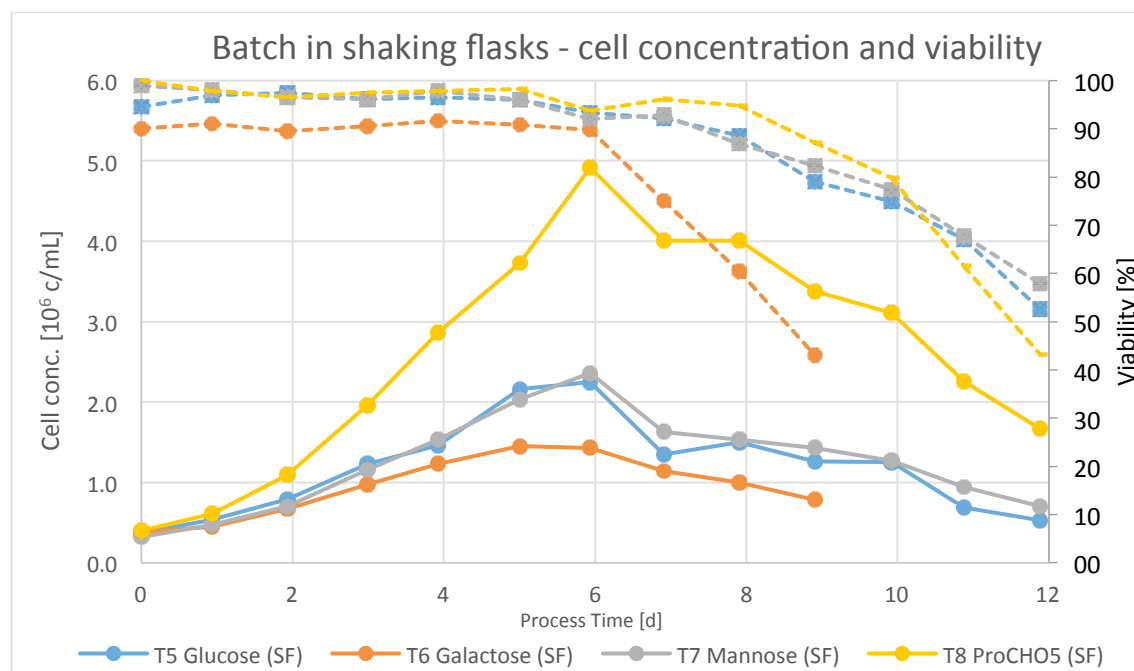


Figure 38: Daily cell concentrations and viabilities of the shaking flasks. Note: The data for the starting day (day 0) were derived from the corresponding bioreactors. Monitoring of the shaking flasks started on day 1.

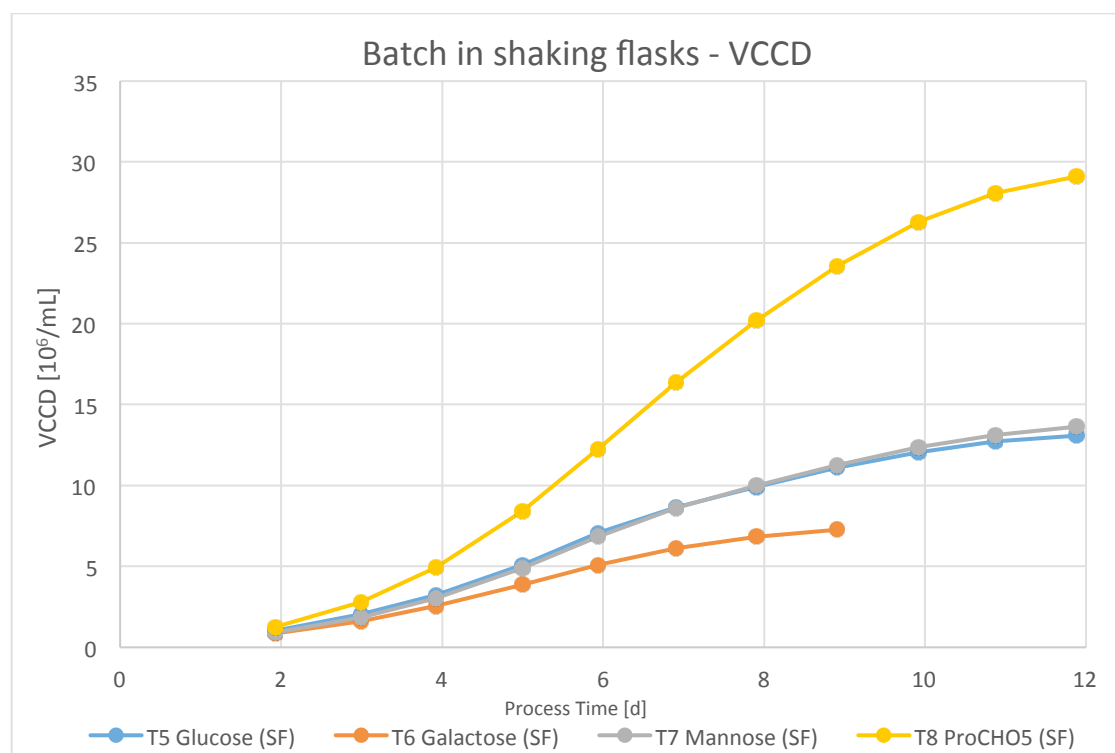


Figure 39: The viable cumulative cell days (VCCD) over the time of the batch experiment.

Table 11: Summary of Batch F49. The specific growth rate μ is given for the exponential growth phase from the starting day until day 4. Because of the bad performance of the cells, the titers were not analyzed.

	Glucose		Galactose		Mannose		ProCHO5	
Parameter	DASGIP	Flask	DASGIP	Flask	DASGIP	Flask	DASGIP	Flask
Peak cell concentration [10^6 c/mL]	1.3	2.25	0.76	1.45	0.67	2.36	1.56	4.92
μ [1/d]	0.30	0.35	0.10	0.30	0.06	0.40	0.35	0.50
VCCD [10^6 c/mL]	6.06	13.10	1.45	7.28	1.80	13.60	4.94	29.10
qGlc [pg/c/d]	1053	336	-	-	-	-	1134	250
Batch duration [d]	8	12	4	9	5	12	6	12

The results of this experiment revealed that the cell line A showed inferior performance in the DASGIP bioreactors compared to shaking flasks. Furthermore did the cells in this experiment also demonstrate better specific growth when compared to the corresponding shaking flasks in batch 1 (0.35 d^{-1} compared to 0.28 d^{-1} for glucose, 0.30 d^{-1} compared to 0.28 d^{-1} for galactose, 0.40 d^{-1} compared to 0.30 d^{-1} for mannose).

7.5 Batch F52 – Shaker batch experiments with temperature reduction to 32°C (cell line A)

Since the DASGIP bioreactor was shown to be inferior to shaking flasks the next batch experiment was operated in 250 mL shaking flasks with the same media and sugar setup that was used in the batch F49 (7.4), investigating the performance at 37°C and 32°C in duplicates.

The results for the shaking flasks at 37°C show that there was almost no difference between the D/H medium supplemented with glucose or mannose regarding the growth (Figure 40, Figure 41), viability (Figure 40), productivity (Figure 44, Table 12) and metabolism (Table 13) of the cells. The D/H medium supplemented with galactose also showed the same specific productivity (Table 12), but on the contrary lead to a decreased growth and viability (Figure 40, Figure 41) of the cells. Moreover the cells showed with 171 pg galactose per cell and day a half as much specific sugar consumption ($q_{\text{Glc}} = 333 \text{ pg/c/d}$), while accordingly they demonstrated a non-detectable or very low specific lactate production ($67 \text{ pg lactate/c/d}$ compared to around $300 \text{ pg lactate/c/d}$ for glucose, mannose and ProCHO5). This was accompanied by a ca. 1.8 fold increased specific glutamine consumption rate and a 2.6 fold increased specific ammonium production rate when supplemented with galactose (Table 13). Because of the lower cell concentrations, the shakers supplemented with galactose also showed slightly lower titers ($92 \mu\text{g/mL}$ compared to $104 \mu\text{g/mL}$ for glucose and mannose on day 9) and are thus also characterized by a lower space-time-yield (Table 12). In the ProCHO5 medium the cells peaked into a 2.5 times higher cell concentration when compared to the D/H medium supplemented with glucose (4.7×10^6 cells/mL to 1.8×10^6 cells/mL), while the viability dropped below 60% two days earlier (Figure 40,

Figure 41). Although the shaking flasks with ProCHO5 reached much higher cell concentrations, they showed a lower titer (68 $\mu\text{g/mL}$ on day 9) and thus an about 30% decreased specific productivity and space-time-yield (**Table 12**). Regarding the metabolism, the cells in the ProCHO5 medium revealed with around 230 pg glucose per cell and day a decreased specific glucose consumption rate, but interestingly the same specific lactate production as the cells in the D/H medium with glucose. They also illustrated with around 129 pg glutamine per cell and day a decreased glutamine consumption rate as well as a decreased specific ammonium production rate (7 pg/c/d compared to 10 pg/c/d for glucose), but a higher specific glutamate production (18 pg/c/d compared to 9 pg/c/d for glucose) (**Table 13**).

All the results about this batch so far described the shaking flasks stored at 37°C. The results for the shaking flasks incubated at 32°C reveal some major differences when compared to the corresponding shaking flasks at 37°C. First, the cells showed a 75% decreased specific growth rate during the exponential growth phase in both media (Glucose: 0.09 d^{-1} compared to 0.40 d^{-1} , Mannose: 0.07 d^{-1} compared to 0.41 d^{-1} , ProCHO5: 0.16 d^{-1} compared to 0.56 d^{-1}) (**Figure 42**, **Figure 43**). For the galactose supplemented medium the specific growth rate even turned from 0.30 d^{-1} to a negative value (-0.02 d^{-1}) due to a steadily decreasing cell concentration after inoculation (**Table 14**). It was also the ProCHO5 medium showing the best growth, but here the cells merely peaked at 1.0×10^6 cells/mL and at 6×10^5 and 5×10^5 cells/mL for the D/H medium supplemented with glucose and mannose, respectively. The biggest impact was observed on the shaking flasks with D/H medium and galactose, where the cells did not grow at all (**Figure 42**, **Figure 43**). Second, except for the galactose flasks (6 compared to 9 days) the cells showed an increased viability and stayed for about 50% longer above a viability of 60% (**Figure 42**). Third, the titers were 6 times lower for glucose and mannose on day 14 (day of culture termination for glucose and mannose at 37°C) and 6 times lower for galactose on day 6 (day of culture termination for galactose at 37°C) (**Figure 44**, **Figure 45**), the specific productivities 30 to 50% lower and the space-time-yields even 75% lower for the D/H medium independent from the sugar (**Table 12**). The same applied for the ProCHO5 medium with the only difference that here the lower temperature lead to an increase of the specific productivity of about 25%. Fourth, the metabolism of the cells showed some alterations. For all four media the specific glutamine consumption decreased between 30 and 50%, whereas at the same time the specific glutamate production increased (50% for glucose, 150% for galactose, 400% for mannose, 20% for ProCHO5) as well as the ammonium production (ca. 50% for each sugar). In the galactose supplemented D/H medium additionally the specific sugar consumption decreased by 50% and the production of lactate could not even be measured, while the ProCHO5 medium only showed a 50 % lower specific lactate production, but the same specific sugar consumption compared to 37°C. In case of the D/H medium supplemented with glucose or mannose, respectively, the specific sugar consumption and specific lactate production also did not differ much compared to 37°C.

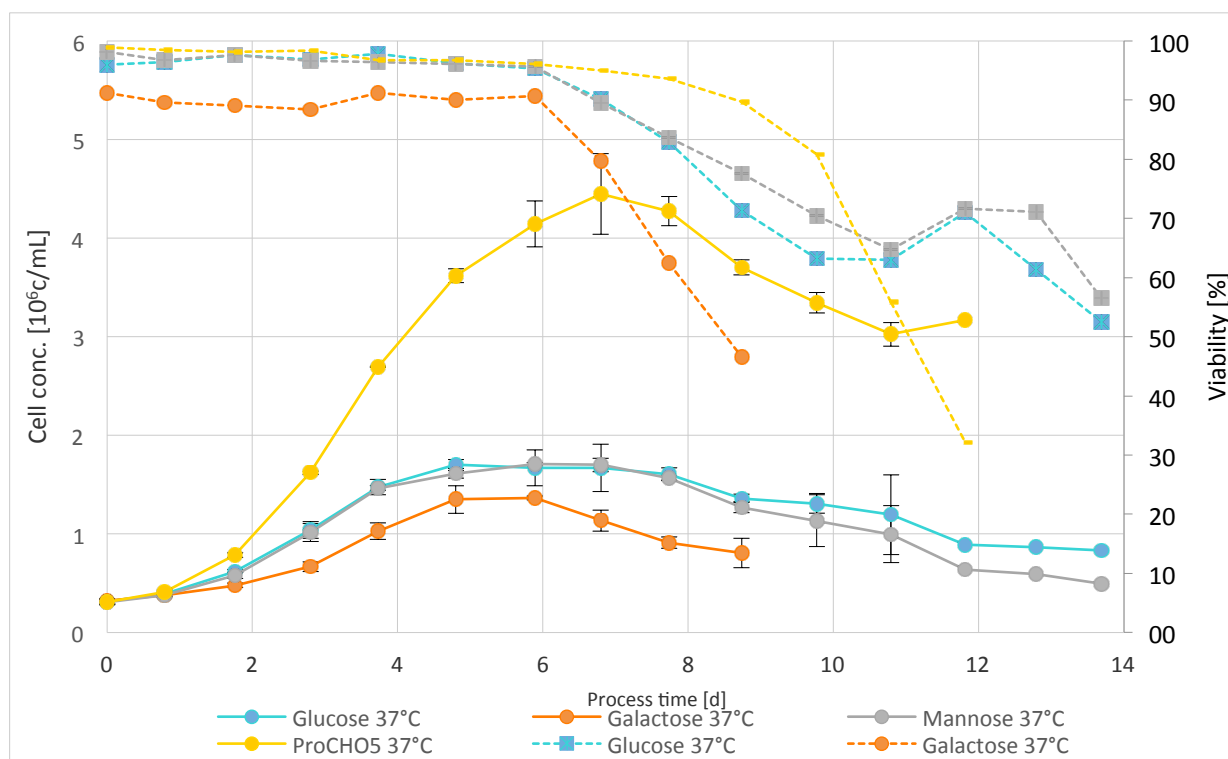


Figure 40: Daily cell concentrations and viabilities of the shaking flasks stored at 37°C as the average of the duplicates.

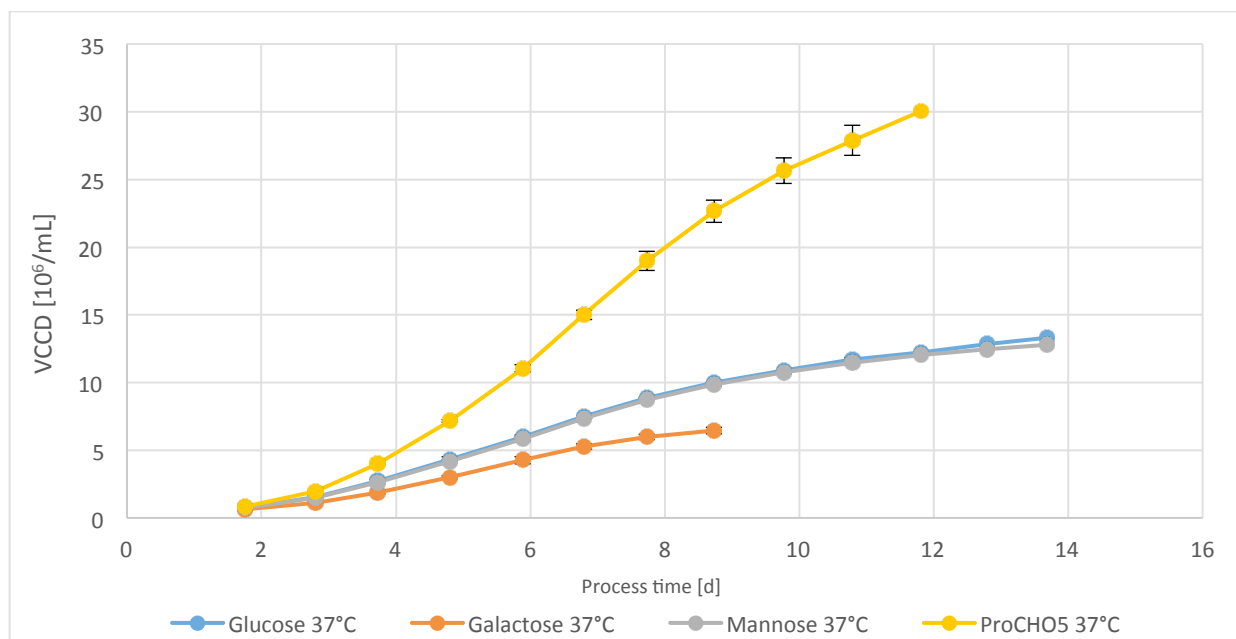


Figure 41: The viable cumulative cell days (VCCD) over the time of the batch experiment.

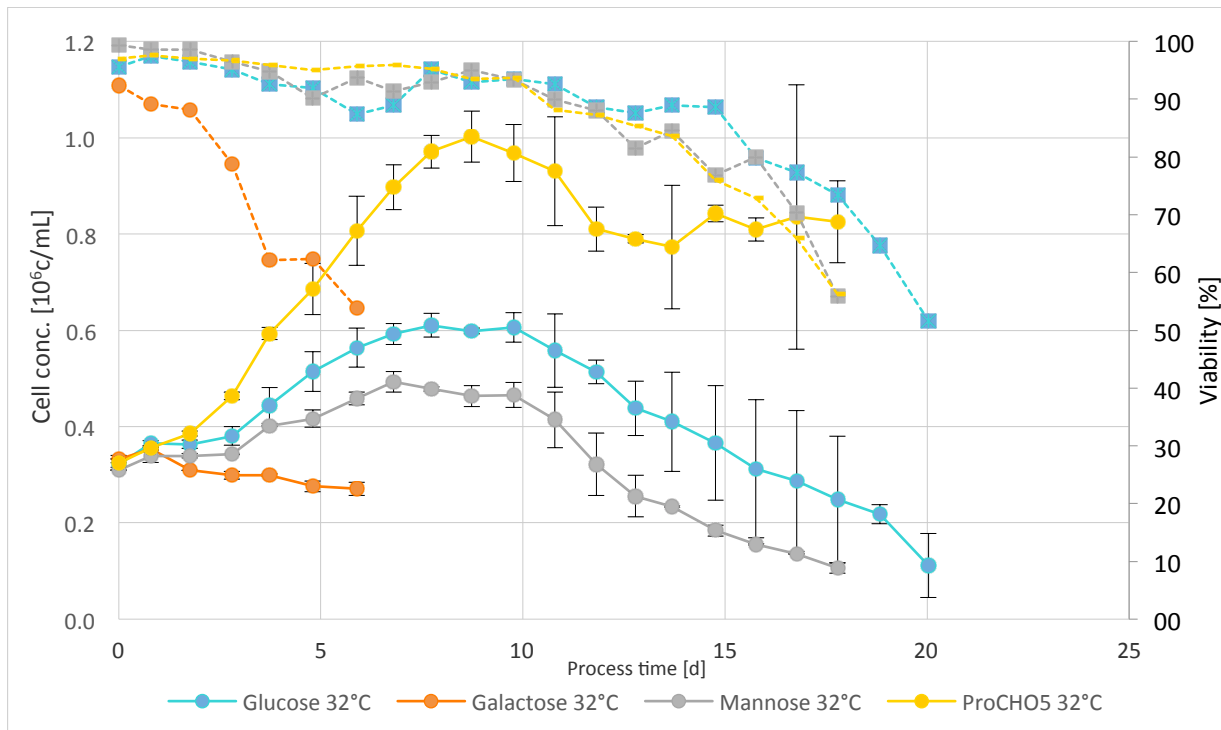


Figure 42: Daily cell concentrations and viabilities of the shaking flasks stored at 32°C as the average of the duplicates.

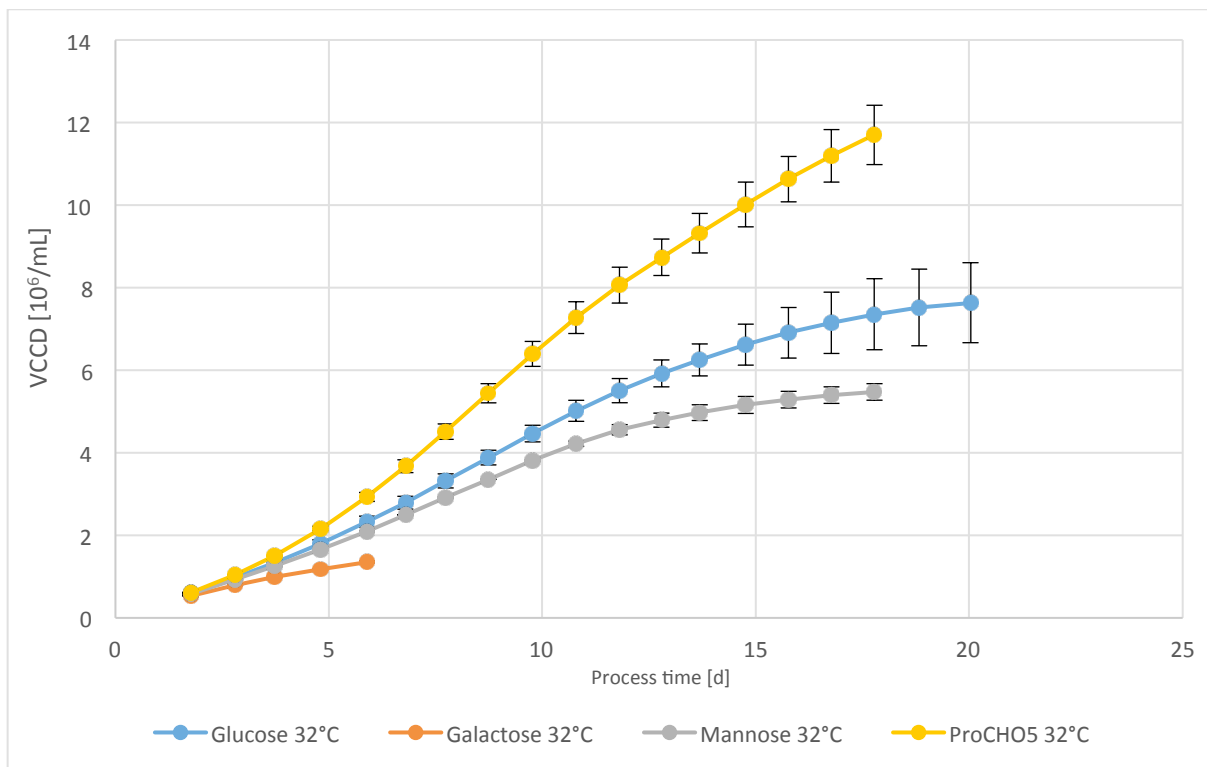


Figure 43: The viable cumulative cell days (VCCD) over the time of the batch experiment.

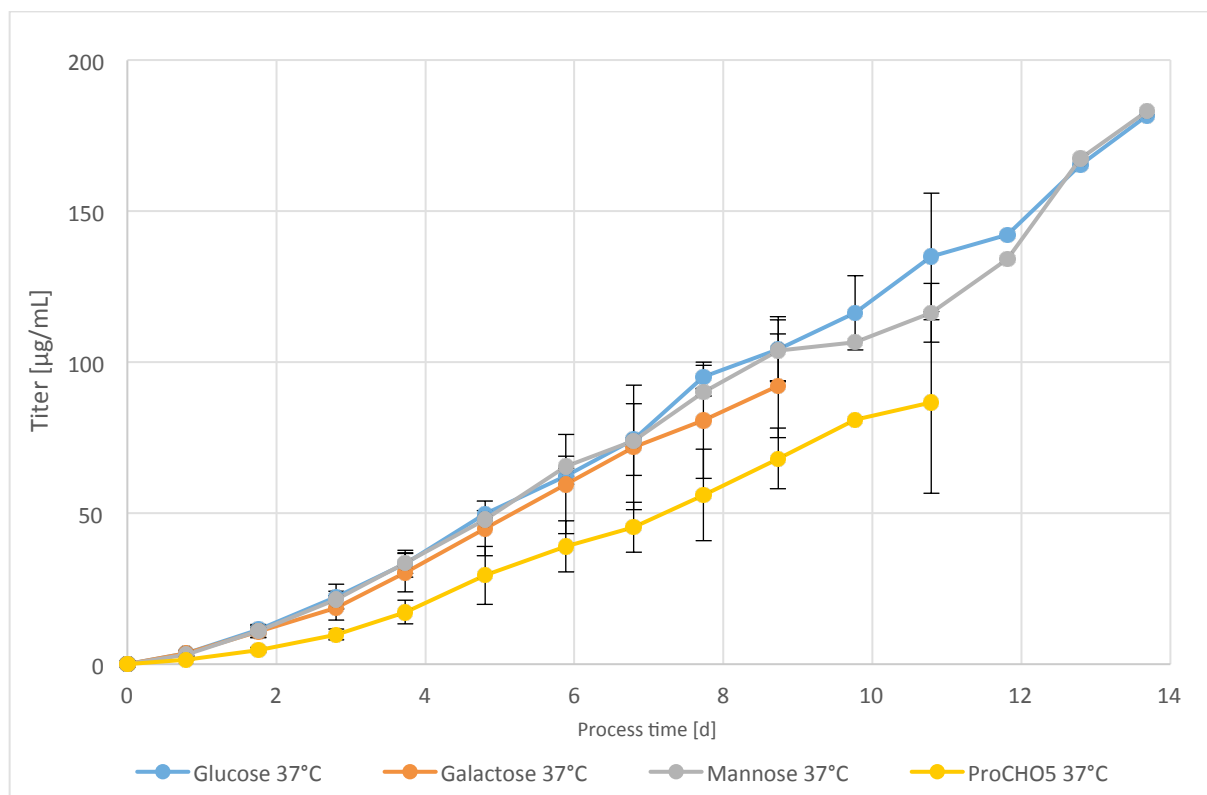


Figure 44: Daily titers of the shaking flasks stored at 37°C as the average of the duplicates.

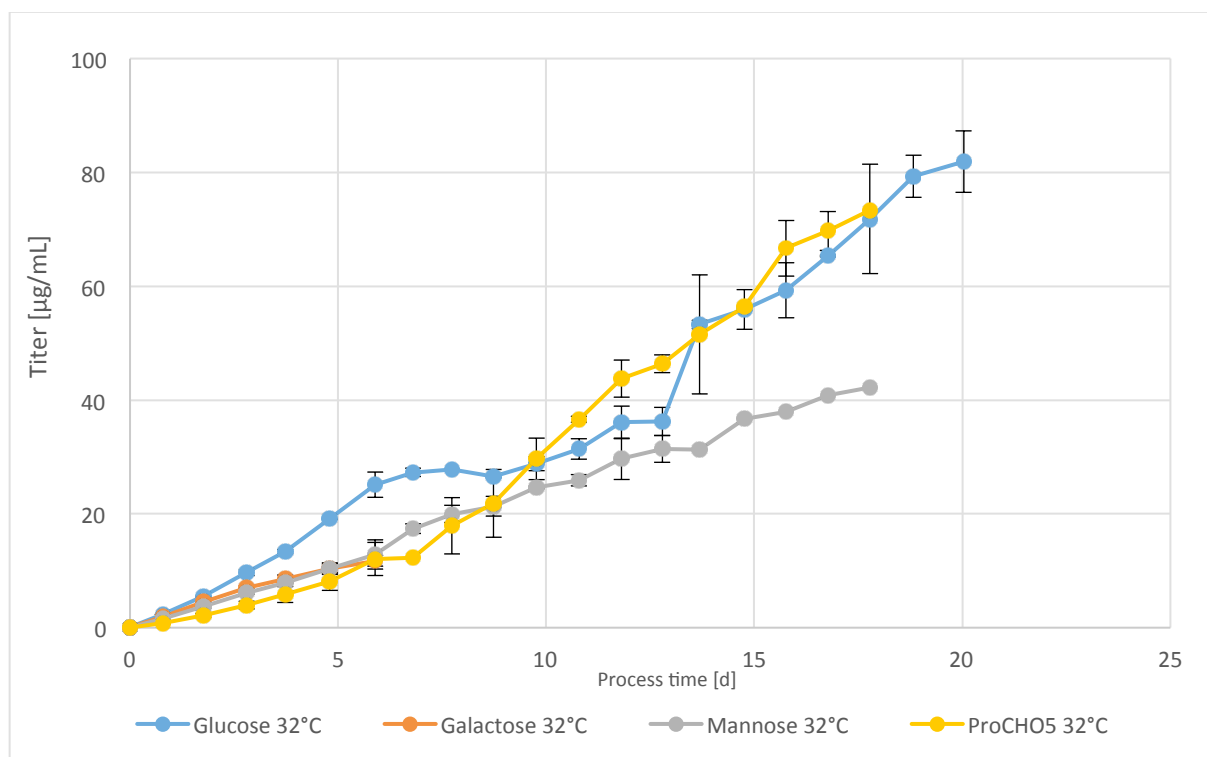


Figure 45: Daily titers of the shaking flasks stored 32°C as the average of the duplicates.

Table 12: All product related parameters as the average of the duplicates. D0 – Inoculation day, DX – Day of culture termination

Approach	Temp. [°C]	Flasks	qp day-to-day [pg/c/d]	qp DX - D0 [pg/c/d]	QP day-to-day [mg/d]	QP DX - D0 [mg/d]	STY day-to-day [mg/(L*d)]	STY DX - D0 [mg/(L*d)]
Glucose	37	2	15,18 ± 1,69	13,18 ± 0,49	0,75 ± 0,15	0,75 ± 0,15	9,84 ± 1,55	13,50 ± 0,40
	32	2	9,78 ± 0,65	8,54 ± 0,29	0,20 ± 0,01	0,13 ± 0,01	2,72 ± 0,01	4,08 ± 0,20
Galactose	37	2	15,43 ± 1,79	14,36 ± 2,27	0,66 ± 0,03	0,67 ± 0,03	8,02 ± 0,39	10,48 ± 1,32
	32	2	8,57 ± 0,52	8,68 ± 0,39	0,16 ± 0,01	0,15 ± 0,01	1,70 ± 0,11	1,98 ± 0,12
Mannose	37	2	15,49 ± 5,64	11,93 ± 2,37	0,67 ± 0,04	0,63 ± 0,02	8,61 ± 1,03	11,68 ± 1,52
	32	2	6,74 ± 0,42	6,60 ± 0,48	0,13 ± 0,02	0,11 ± 0,02	1,59 ± 0,22	2,47 ± 0,11
ProCHO5	37	2	4,02 ± 0,49	3,22 ± 0,76	0,54 ± 0,11	0,50 ± 0,15	6,90 ± 1,27	8,11 ± 1,91
	32	2	5,23 ± 0,81	5,55 ± 0,64	0,18 ± 0,02	0,17 ± 0,01	2,53 ± 0,26	4,21 ± 0,09

Table 13: All metabolism related parameters as the average of the duplicates. In case of qSugar and qGlutamine a positive value equals consumption. For qLactate, qGlutamate and qAmmonium a positive value means production.⁴

Approach	Temp. [°C]	Flasks	qSugar Bioprofiler [pg/c/d]	qSugar HPLC [pg/c/d]	qLactate Bioprofiler [pg/c/d]	qGlutamate Bioprofiler [pg/c/d]	qGlutamine Bioprofiler [pg/c/d]	qAmmonium Bioprofiler [pg/c/d]
Glucose	37	2	372 ± 11	333 ± 27	310 ± 128	9 ± 3	172 ± 8	10 ± 1
	32	2	373 ± 17	304*	338 ± 45	13 ± 0	79 ± 10	15 ± 1
Galactose	37	2	-	171 ± 18	67 ± 4	7 ± 8	288 ± 26	26 ± 1
	32	2	-	79*	0	19 ± 14	219 ± 9	38 ± 0
Mannose	37	2	-	342 ± 22	321 ± 108	4 ± 0	159 ± 9	10 ± 1
	32	2	-	407*	353 ± 10	21 ± 9	99 ± 6	17 ± 1
ProCHO5	37	2	246 ± 10	230 ± 3	334 ± 118	18 ± 6	129 ± 20	7 ± 0
	32	2	239 ± 2	241*	166 ± 15	22 ± 0	56 ± 2	13 ± 0
*No standard deviation since not both 32°C shaking flasks were analyzed, but only one								

⁴ See appendix 11.2 for detailed figures about the metabolic data for the batch F52.

Analysis of product size by silver staining revealed that for almost all approaches the vast majority of IgMs produced were pentamers (Figure 46). Only the flask with mannose at 32°C displayed additional small bands at the tetramer and monomer region. Moreover it was galactose at 32°C where a much lower amount of IgM antibodies seemed to be applied, because it was only showing a very small band at the pentamer and another small one at the tetramer region.

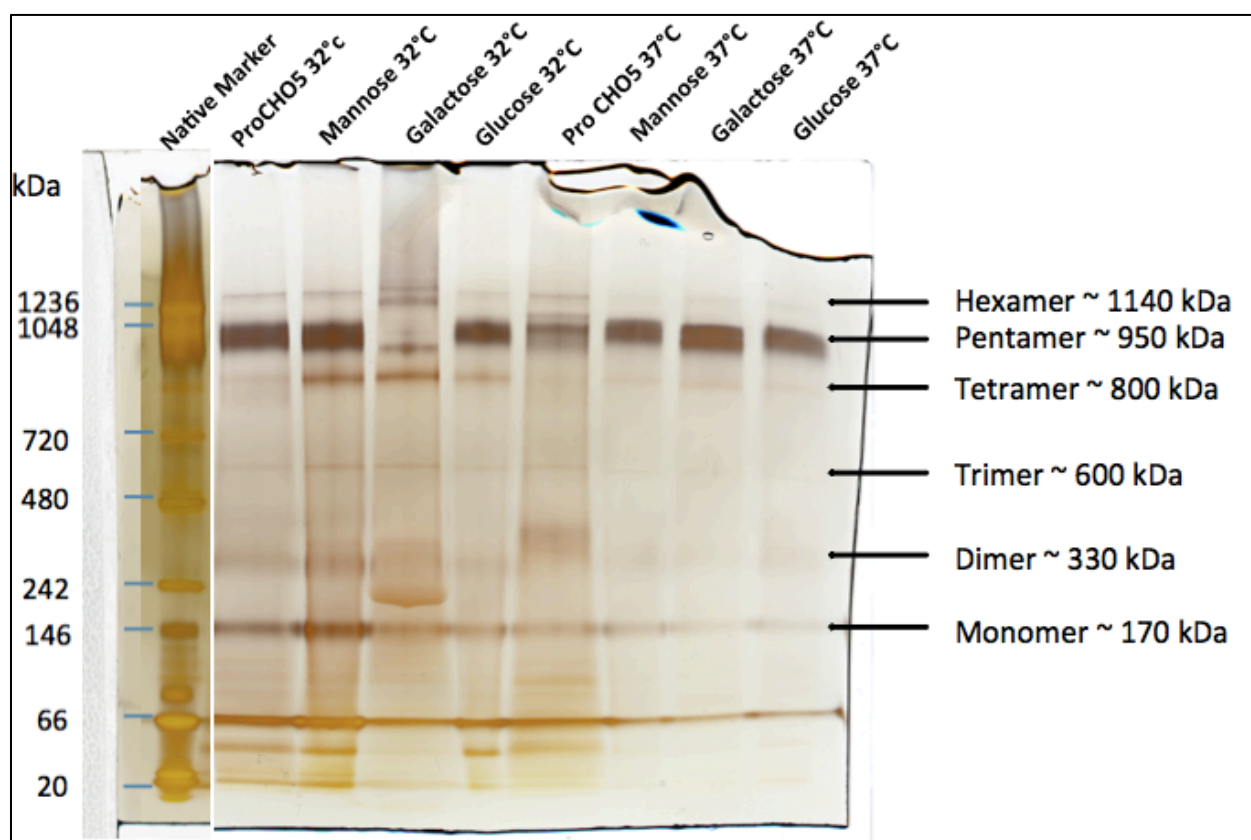


Figure 46: Result of the silver staining. For each sample 400 ng in 10 μ l were applied.

Table 14: Summary of Batch F52. The specific growth rate μ is give for the exponential growth phase from the starting day until day 4.

Parameter	Glucose		Galactose		Mannose		ProCHO5	
	37°C	32°C	37°C	32°C	37°C	32°C	37°C	32°C
Peak cell concentration [10 ⁶ c/mL]	1.70 \pm 0.06	0.61 \pm 0.02	1.37 \pm 0.02	0.35 \pm 0.00	1.71 \pm 0.01	0.49 \pm 0.02	4.45 \pm 0.41	1.00 \pm 0.05
μ [1/d]	0.40 \pm 0.06	0.09 \pm 0.03	0.30 \pm 0.07	-0.02 \pm 0.02	0.41 \pm 0.10	0.07 \pm 0.03	0.56 \pm 0.06	0.16 \pm 0.02
Titer [μ g/mL]	182 \pm 15	82 \pm 5	92 \pm 17	12 \pm 1	183 \pm 10	42 \pm 3	87 \pm 30	73 \pm 4
VCCD [10 ⁶ c/mL]	13.3 \pm 0.15	7.64 \pm 0.97	6.45 \pm 0.25	1.35 \pm 0.03	12.8 \pm 0.13	5.48 \pm 0.20	30.1 \pm 1.10	11.7 \pm 0.72
Batch duration [d]	14	20	9	6	14	18	12	18

The samples that were investigated for the glycosylation were taken from the last day of the shaking flasks at 37°C. The mass spectrometry revealed, that for glucose and mannose as carbon sources the glycosylation pattern of the glycopeptide 3 of the IgMs was almost identical. They both showed the same glycoforms (Figure 48) and almost the exact same relative appearance of these glycoforms, with N-acetylneuraminic acid, galactose and fucose (NaAF) attached to the common pentasaccharide core at around 36% being the most frequent glycoform. In case of galactose, however, the IgMs demonstrated a different set of glycoforms (N-acetylglucosamine+N-acetylglucosamine+fucose (GnGnF) and N-acetylneuraminic acid+N-acetylneuraminic acid+fucose (NaNaF) instead of N-acetylneuraminic acid+N-acetylneuraminic acid+galactose+fucose (NaNAAF) and N-acetylneuraminic acid+ N-acetylneuraminic acid+ N-acetylneuraminic acid+fucose (NaNaNaF)) with galactose+galactose+fucose (AAF) at around 60% being the prevalent glycoform. Interestingly, the glycosylation of the IgMs produced by the cells cultivated in ProCHO5 medium, represented the same glycoforms as with galactose in D/H medium, but to a different extent. Although AAF was also the most prominent glycoform, its relative abundance was only about 47%.

“Glycosylation

In the following tables the glycan distribution of glycopeptide 3 (THTNISE) is shown.”

GLC	RT [min]	Area	Intens.	%
NaNaNaF	6.3	40873	2780	0.32
NaNaAF	6.3	1002591	32993	7.84
NaNaF	6.4	3761291	152589	29.43
NaAF	6.4	4592649	187345	35.93
AAF	6.4	2869409	119447	22.45
AGnF	6.4	515701	22986	4.03

MAN	RT [min]	Area	Intens.	%
NaNaNaF	6.5	26204	1576	0.18
NaNaAF	6.5	1168370	29350	8.01
NaNaF	6.6	4658595	198109	31.92
NaAF	6.6	5263830	222045	36.07
AAF	6.6	2874174	128616	21.10
AGnF	6.7	398075	14913	2.73

PRO	RT [min]	Area	Intens.	%
NaNaF	6.8	69698	3860	1.18
NaAF	6.8	939240	34155	15.91
AAF	6.9	2598076	107281	46.82
AGnF	6.9	1258730	39548	21.33
GnGnF	7	870994	29957	14.76

GAL	RT [min]	Area	Intens.	%
NaNaF	7	194001.3	6853	3.26
NaAF	7	698202.4	20974	11.74
AAF	7	3388660	115089	60.26
AGnF	7.1	1051752	32416	17.68
GnGnF	7.2	420332.2	13913	7.07

Gn - N-acetylglucosamine; F – fucose; A – galactose, Na – N-acetylneuraminic acid

(Extracted from: Gruber, Altmann (01/2015): Analysis report: Analysis of recombinantly produced IgM grown on different carbon sources.)

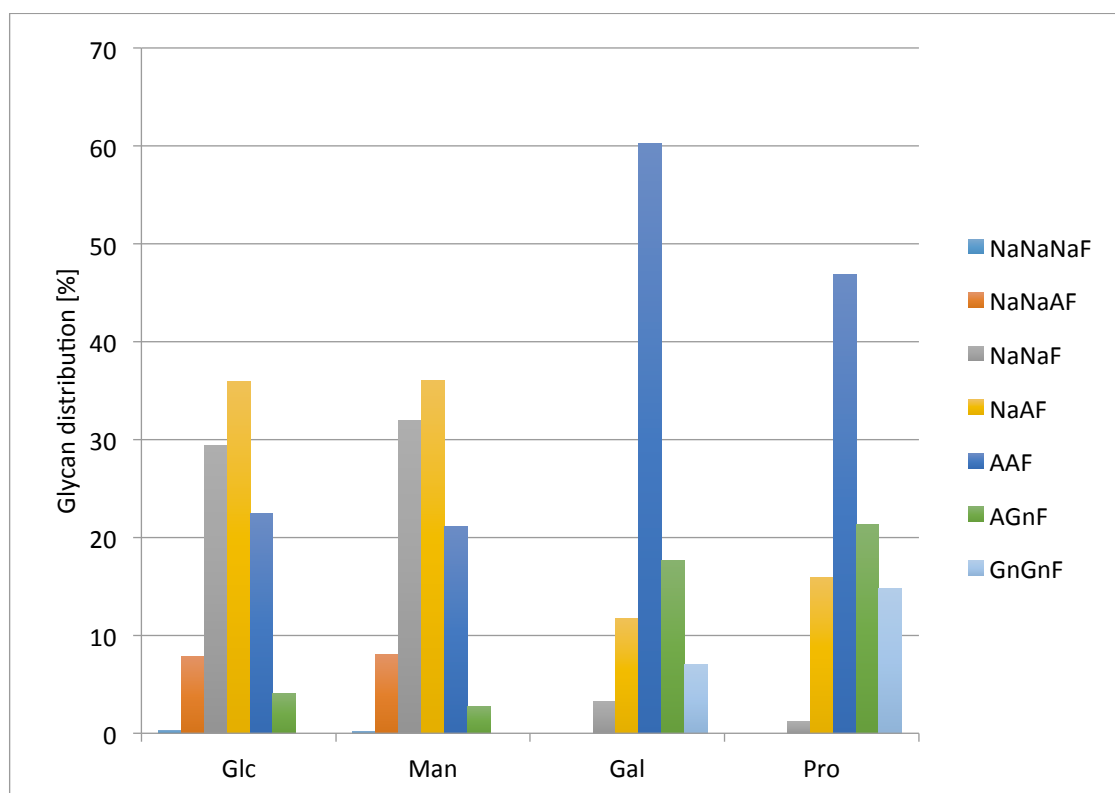


Figure 47: Glycan distribution. Glc – Glucose, Man – Mannose, Gal – Galactose, Pro – ProCHO5; Gn - N-acetylglucosamine; F – fucose; A – galactose, Na – N-acetylneuraminic acid.

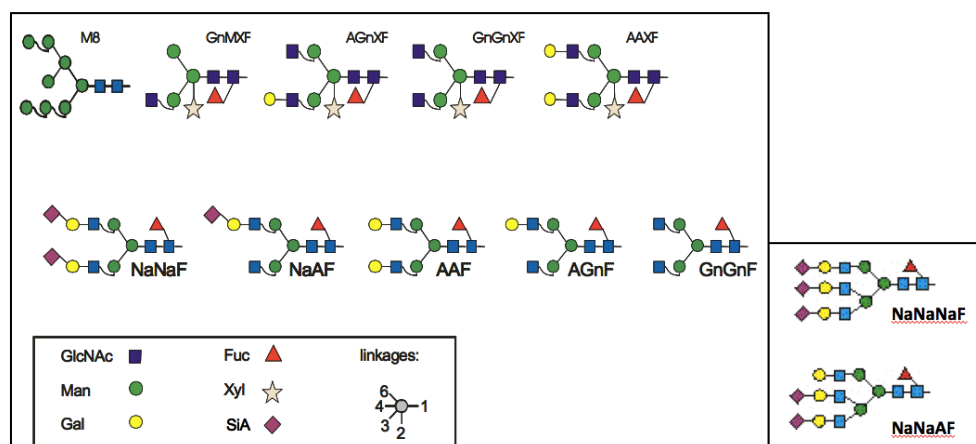


Figure 48: Illustration of different glycoforms described in this thesis. M – mannose; Gn - N-acetylglucosamine; X – xylose; F – fucose; A – galactose, Na – N-acetylneuraminic acid. Source: Prof. Altmann personal communication and www.proglycan.com [2015/06/01]

This batch experiment revealed that the cells in the ProCHO5 medium showed superior growth, but inferior productivity when compared to the D/H medium. Moreover it was shown that the cells demonstrated very similar performance when the D/H medium was supplemented with glucose or mannose, respectively. The supplementation with galactose led to inferior growth and viability, but similar productivity when compared to glucose/mannose.

The results for the glycosylation analysis showed that the IgMs produced by cells growing on glucose and mannose exhibited almost the exact same glycoforms and distribution of these. In comparison the IgMs generated by the cells grown on galactose and ProCHO5 showed some additional glycoforms while leaving others out and represented a different distribution of the glycoforms.

7.6 Batch F53 – Investigation of the bad performance of medium supplemented with galactose (cell line A)

As a consequence of the bad performance of the cells in the D/H medium supplemented with galactose, particularly at 32°C, this batch experiment was set up to investigate a potentially enhanced outcome if these shaking flasks are incubated with 20% CO₂ to compensate the missing pH influence by lactate. Therefore new 250 mL shaking flasks with a working volume of 100 mL, inoculum concentration of 3×10^5 cells/mL, 140 rpm and 20% CO₂ have been incubated at 37 and 32°C in duplicates.

The results of this batch are compared with the data about the galactose flasks compiled from the previous batch.

The comparison shows that the amount of 20% CO₂ in the headspace of the shaking flasks had no substantial effect. The pH values for the flasks at 32°C nevertheless increased when compared to the pH values of the glucose, mannose and ProCHO5 flasks at 32°C from the batch F52 (Figure 52). The major noteworthy difference were first, that the shaking flasks incubated at 32°C with 20% CO₂ showed a better viability and stayed above 60% four days longer (Figure 49). Secondly the shaking flask stored at 37°C and 20% CO₂ showed slightly better growth, which was primarily indicated by the higher VCCD (8.23×10^6 c/mL versus 6.45×10^6 c/mL on day 9) (Figure 50). All the other process parameters such as titers, productivity (Figure 51, Table 15) and metabolites (Table 16) showed not much of a difference.

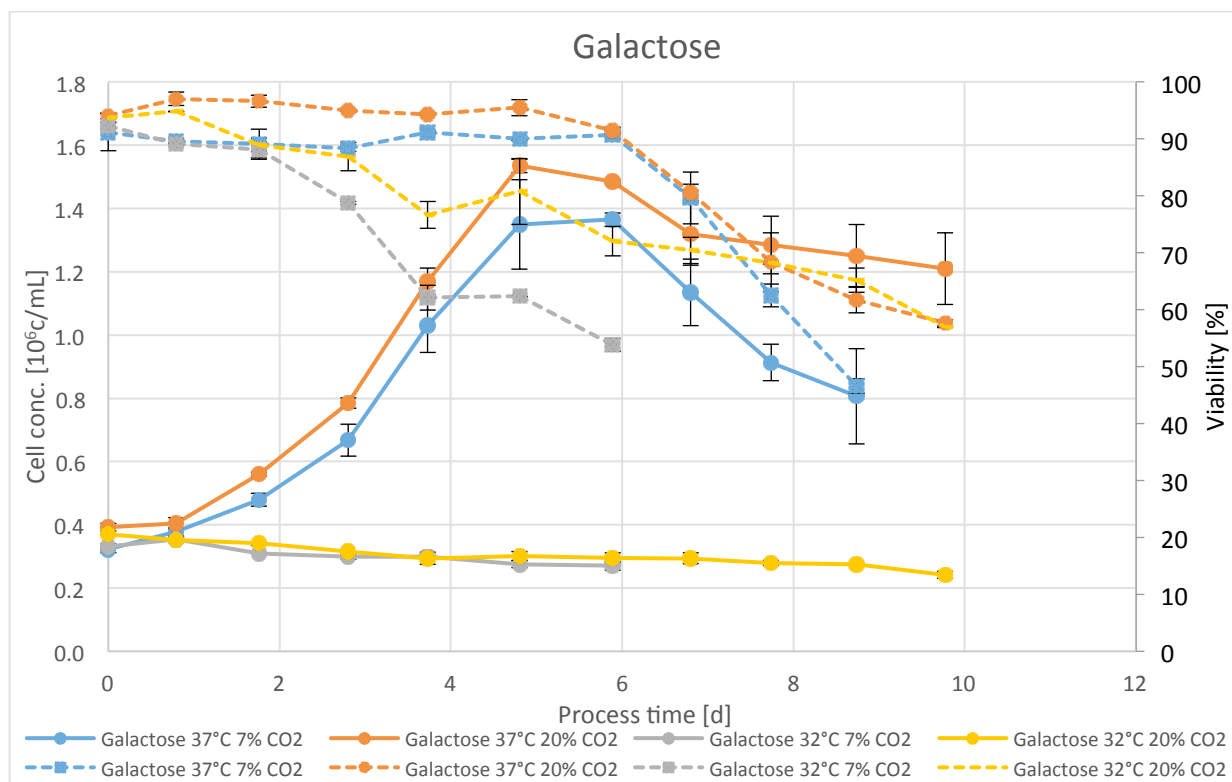


Figure 49: Daily cell concentrations and viabilities as the average of the duplicates.

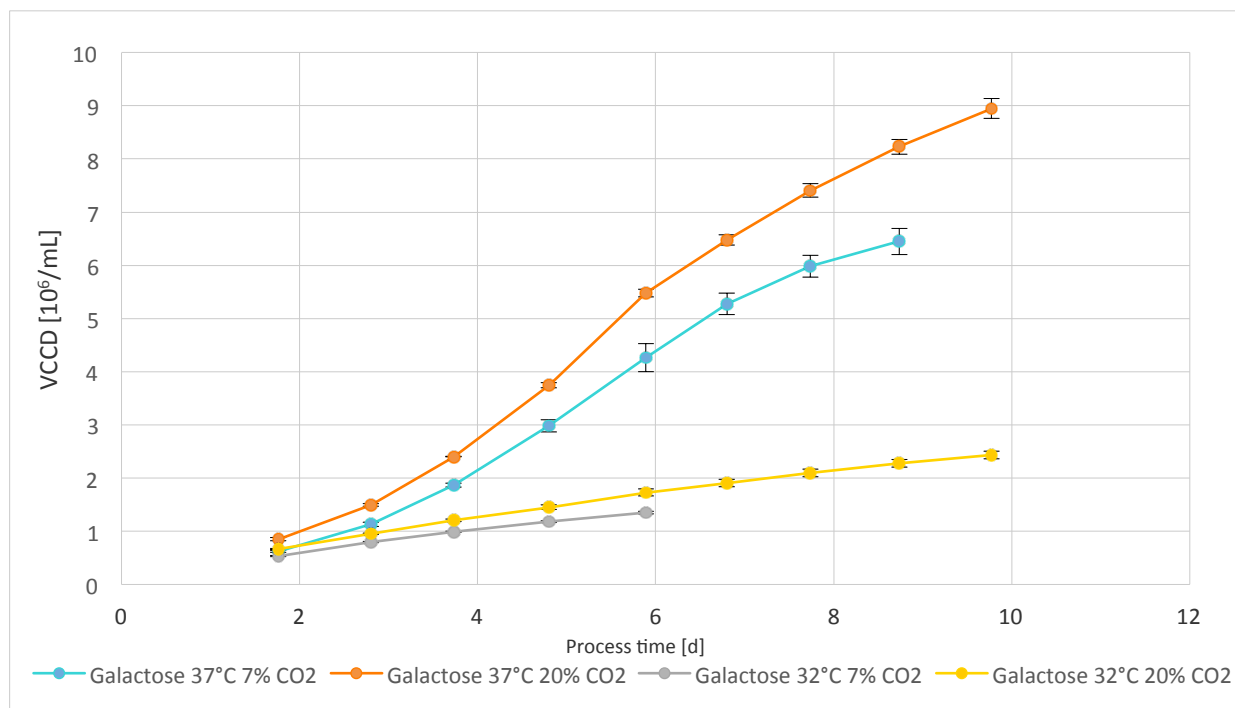


Figure 50: The viable cumulative cell days (VCCD) over the time of the batch experiment.

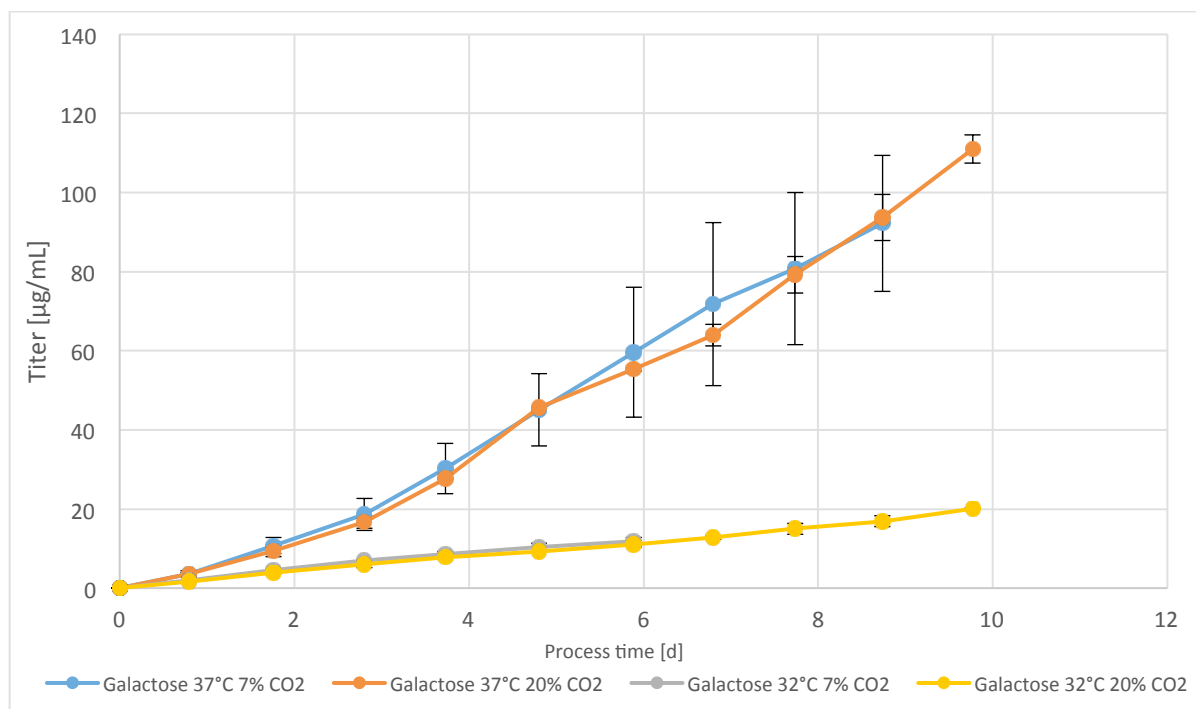


Figure 51: Daily titers as the average of the duplicates.

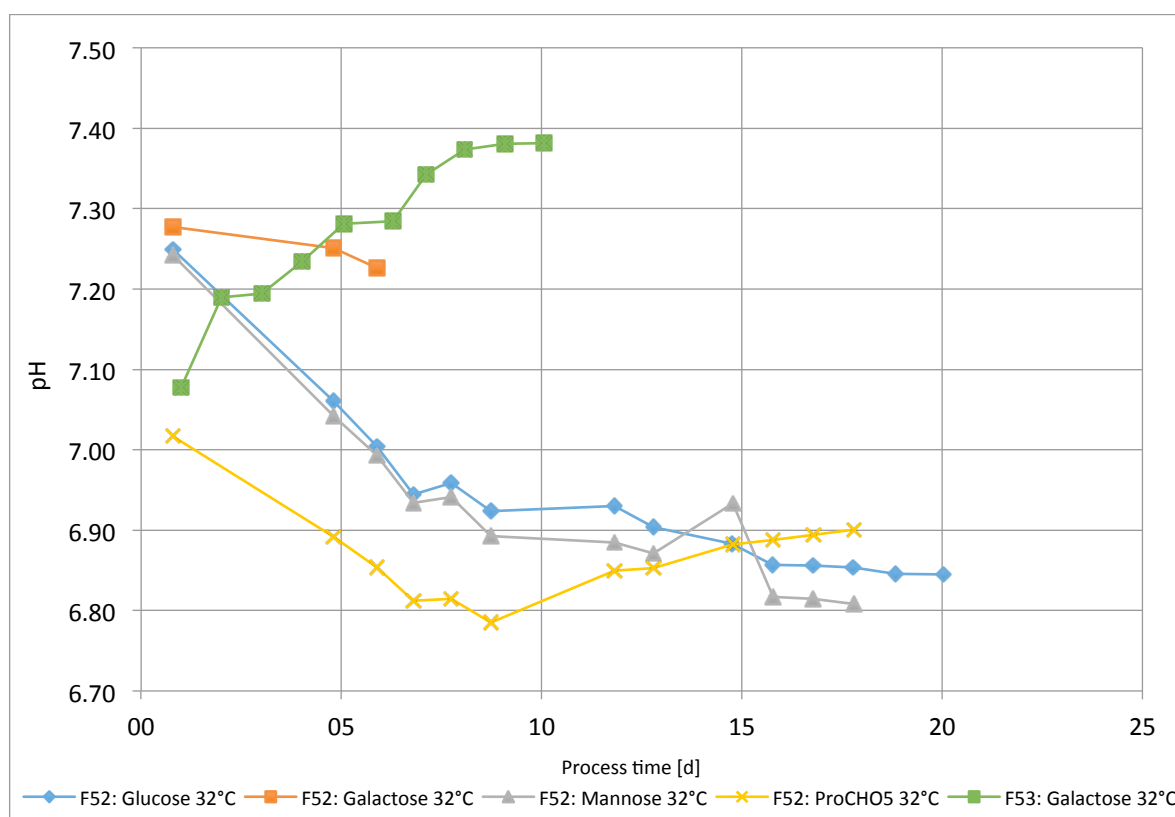


Figure 52: pH values for shaking flasks incubated at 7% CO₂ and 32°C (F52) and 20% CO₂ and 32°C (F53) over the time of the batch experiments.

Table 15: All product related parameters as the average of the duplicates. D0 – Inoculation day, DX – Day of culture termination

Temp. [°C]	CO ₂ in HS [%]	Flasks	qp day-to-day [pg/c/d]	qp DX - D0 [pg/c/d]	QP day-to-day [mg/d]	QP DX - D0 [mg/d]	STY day-to-day [mg/(L*d)]	STY DX - D0 [mg/(L*d)]
37	7	2	15.43 ± 1.79	14.36 ± 2.27	0.66 ± 0.03	0.67 ± 0.03	8.02 ± 0.39	10.48 ± 1.32
37	20	2	13.07 ± 0.18	12.40 ± 0.10	0.73 ± 0.02	0.73 ± 0.02	9.20 ± 0.29	11.03 ± 0.25
32	7	2	8.57 ± 0.52	8.68 ± 0.39	0.16 ± 0.01	0.15 ± 0.01	1.70 ± 0.11	1.98 ± 0.12
32	20	2	9.08 ± 0.33	8.24 ± 0.13	0.11 ± 0	0.11 ± 0	1.37 ± 0.02	1.99 ± 0.01

Table 16: All metabolism related parameters as the average of the duplicates. In case of qSugar and qGlutamine a positive value equals consumption. For qLactate, qGlutamate and qAmmonium a positive value means production.

Temp. [°C]	CO ₂ in HS [%]	Flasks	qSugar HPLC [pg/c/d]	qLactate Bioprofiler [pg/c/d]	qGlutamate Bioprofiler [pg/c/d]	qGlutamine Bioprofiler [pg/c/d]	qAmmonium Bioprofiler [pg/c/d]
37	7	2	171 ± 18	67 ± 4	7 ± 8	288 ± 26	26 ± 1
37	20	2	177*	0	4 ± 2	250 ± 1	23 ± 1
32	7	2	79*	0	19 ± 14	219 ± 9	38 ± 0
32	20	2	126*	0	18 ± 6	154 ± 7	39 ± 0
*No standard deviation since not both shaking flasks were analyzed, but only one							

Table 17: Summary of Batch F53. The specific growth rate μ is give for the exponential growth phase from the starting day until day 4.

Parameter	Galactose 20% CO ₂		Galactose 7% CO ₂	
	37°C	32°C	37°C	32°C
Peak cell concentration [10 ⁶ c/mL]	1.54 ± 0.02	0.37 ± 0.01	1.37 ± 0.02	0.35 ± 0.00
μ [1/d]	0.27 ± 0.07	-0.06 ± 0.03	0.30 ± 0.07	-0.02 ± 0.02
Titer [µg/mL]	111 ± 4	20 ± 1	92 ± 17	12 ± 1
VCCD [10 ⁶ c/mL]	8.95 ± 0.18	2.43 ± 0.07	6.45 ± 0.25	1.35 ± 0.03
Batch duration [d]	10	10	9	6

During this run, cell samples were taken and subsequently fixed for later flow cytometry analysis to determine the intracellular light chain and heavy chain polypeptide content. The flow cytometry outcomes indicated that for each shaking flask the amount of producing cells was above 95% for both the heavy chain (Figure 53) and light chain (Figure 54). The results were the same for all other batch experiments regarding the proportion of producing and non-producing cells and are not shown.

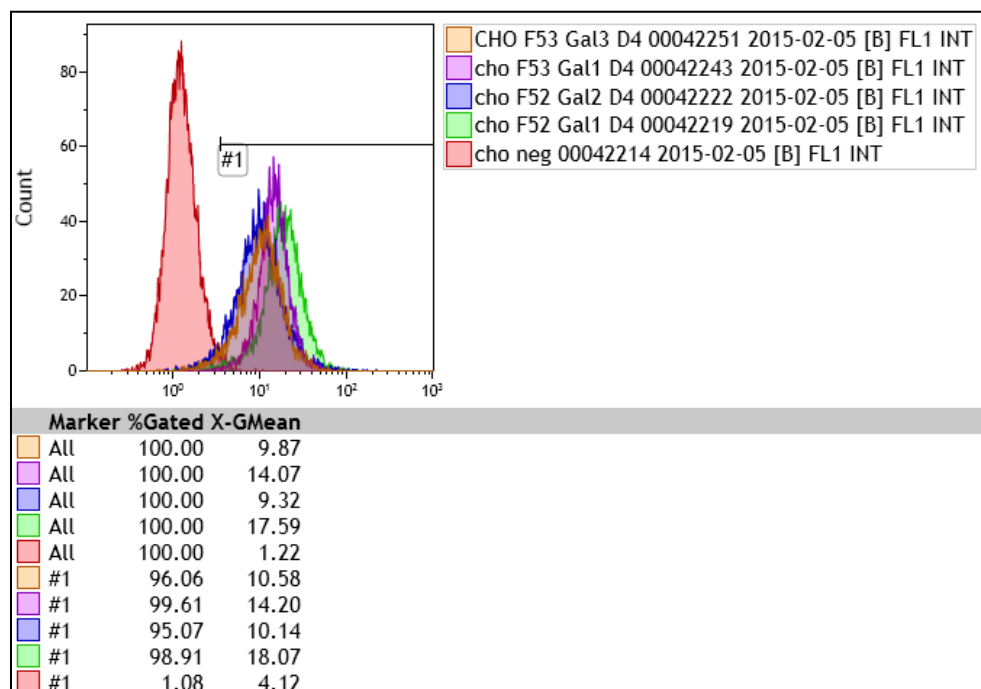


Figure 53: Flow cytometry results of CHO cells A from Batch F53 for intracellular heavy chains. The numbers in percent at the bottom indicate the amount of heavy chain producing cells relative to the negative control (non-producing CHO host cell line).

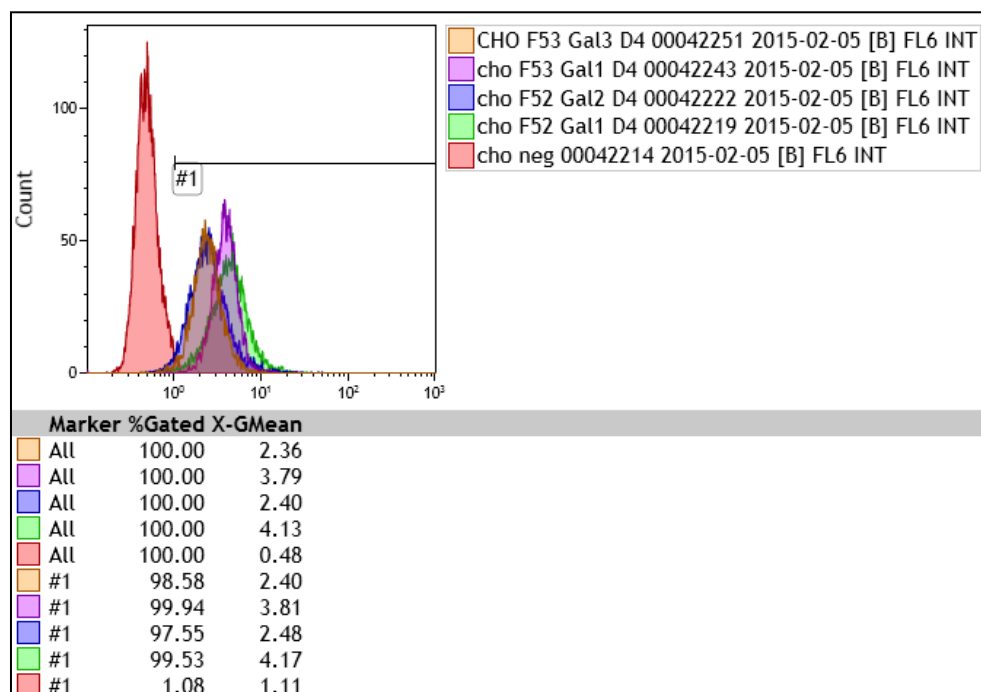


Figure 54: Flow cytometry results of CHO cells A from Batch F53 for intracellular light chains. The numbers in percent at the bottom indicate the amount of light chain producing cells relative to the negative control (non-producing CHO host cell line).

This batch experiment revealed that the application of 20% CO₂ in the headspace of shaking flasks did not lead to important improvements of the performance of cell line A when grown on galactose.

7.7 Batch F54 – Fermentation with temperature reduction to 32°C (cell line B)

This batch experiment was performed with a different recombinant IgM-producing CHO cell population. Since the CHO cell population we have investigated so far mainly produced pentamers, we investigated a different CHO cell population that was likely more suitable to study the impact of alternative sugar substrates on the isoform distribution. From other pre-experiments it was known that the IgM-producing cells used for this batch experiment have a rather imperfect pentamer production ratio. Thus the aim of this batch was to investigate the impact of alternative sugar substrates on the isoform distribution.

The adaption was performed as described under 6.7⁵. Unfortunately this cell population could only be successfully adapted to D/H medium supplemented with mannose and glucose as well as the ProCHO5 medium, but not to galactose as alternative sugar source in D/H medium.

A comparison of the cells in the D/H medium with glucose and the cells in the D/H medium with mannose almost exactly show the same performance regarding the growth (Figure 55, Figure 56, Figure 57, Figure 58), viability (Figure 55, Figure 57), productivity (Figure 59, Figure 60, Table 18) and metabolism (Table 19) at 37 and 32°C, respectively. This is in accordance with the results seen in batch F52. For example did the cells similarly peak in the highest cell concentrations in the shaking flasks containing the ProCHO5 medium (3×10^6 c/mL compared to 1.65×10^6 and 1.58×10^6 c/mL for glucose and mannose, respectively, at 37°C). Interestingly in this experiment the cells in the ProCHO5 medium additionally also showed a significantly longer survival time of 17 days at 37°C and 28 days at 32°C compared to 8 and 22/18 days for glucose/mannose. Moreover 3 times higher product titers were observed at 37 and 32°C on day 8 and day 18, respectively. But because of the higher cell concentrations the specific productivity with around 1.5 pg per cell and day was just as high as for the D/H medium (Table 18). In the end the space-time-yield was about 66% higher compared to glucose in D/H medium, since a much higher product titer was achieved based on the longer survival time (Table 18).

⁵ See appendix for detailed information about this adaption.

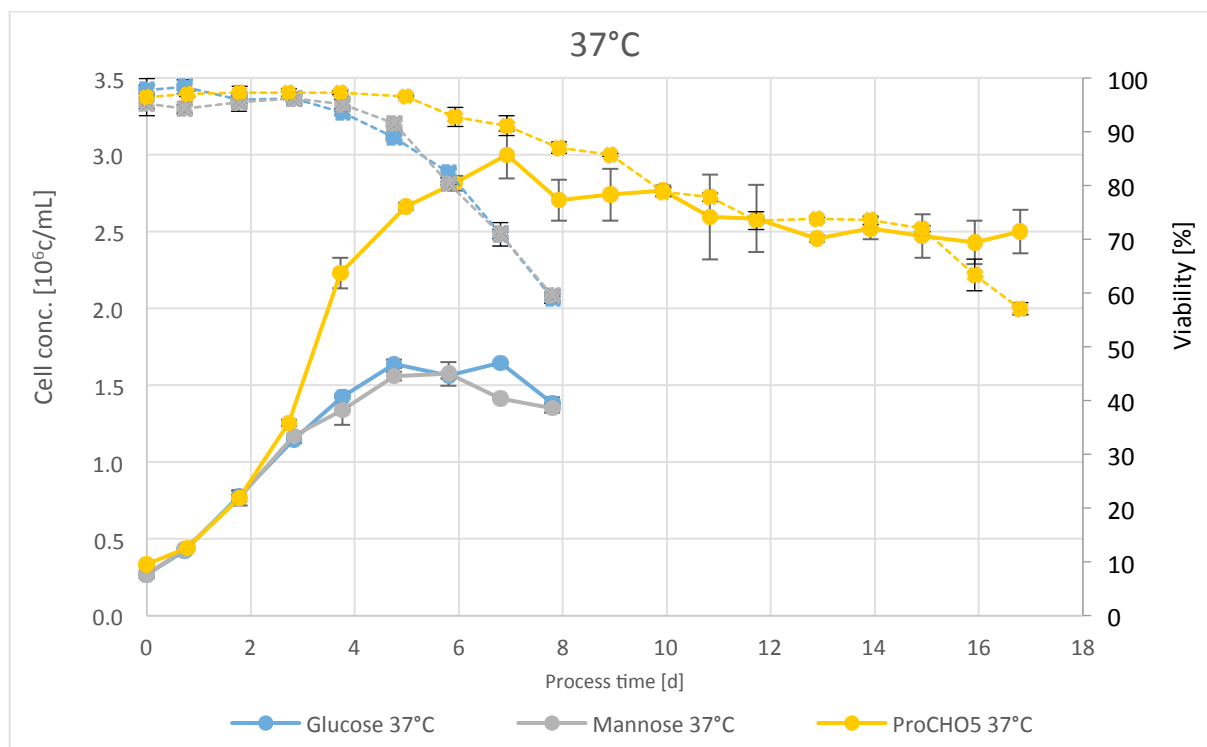


Figure 55: Daily cell concentrations and viabilities of the shaking flasks incubated at 37°C as the average of the duplicates.

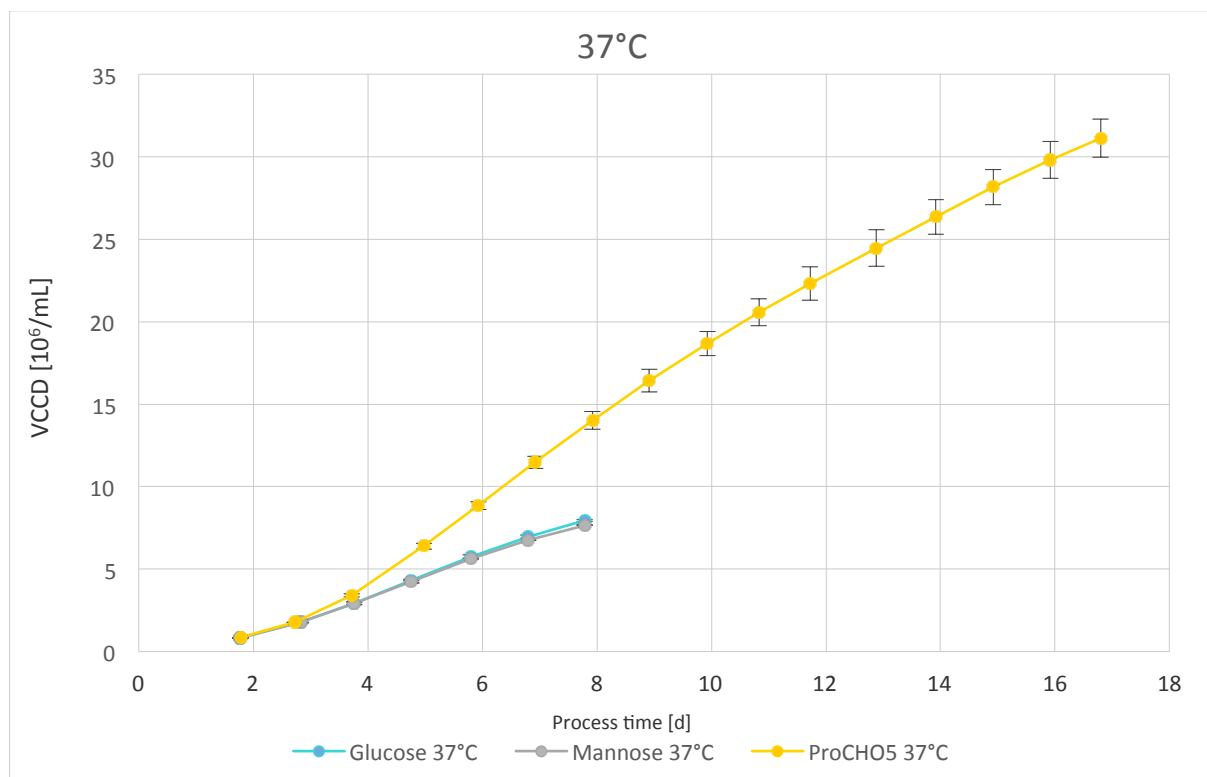


Figure 56: The viable cumulative cell days (VCCD) over the time of the batch experiment.

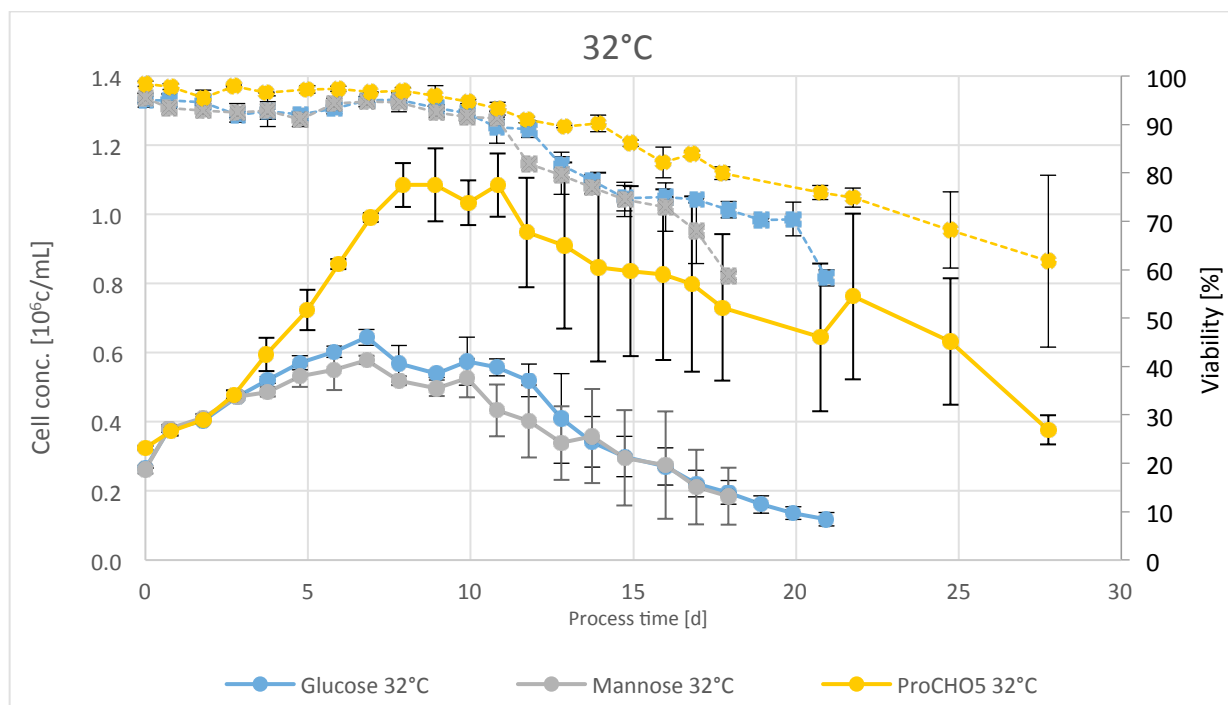


Figure 57: Daily cell concentrations and viabilities of the shaking flasks incubated at 32°C as the average of the duplicates.

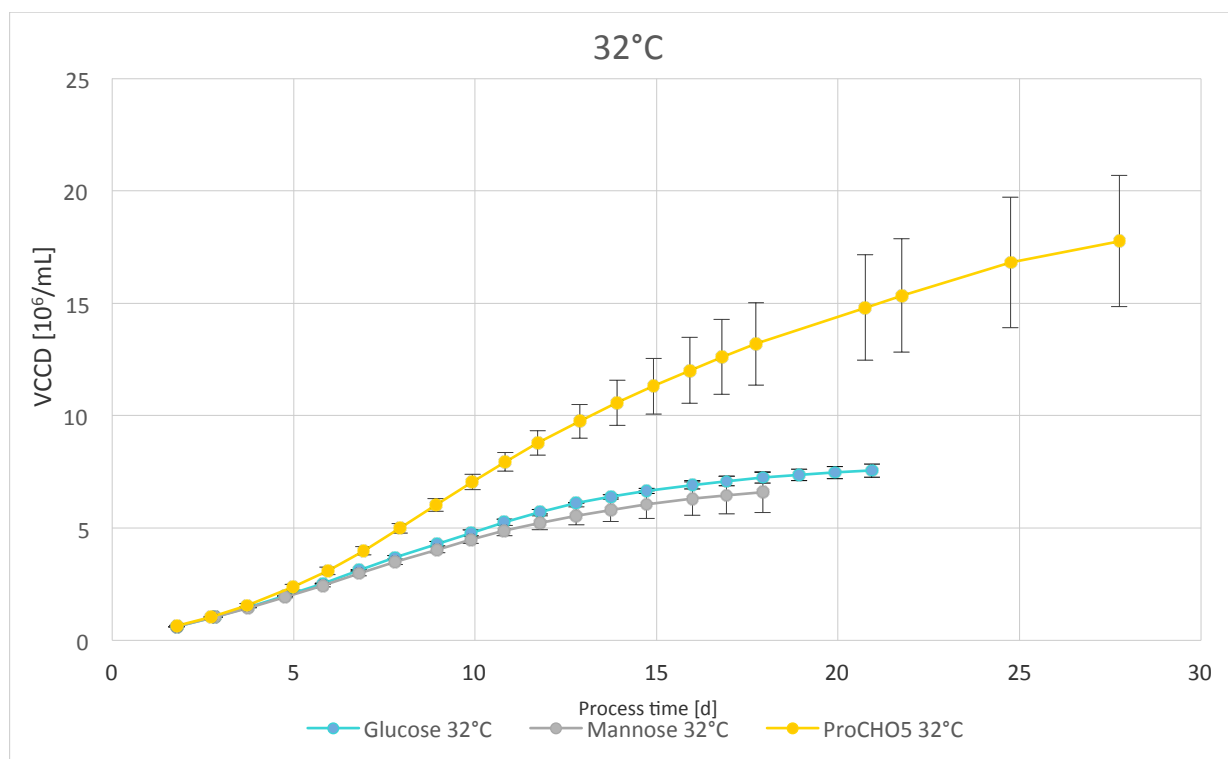


Figure 58: The viable cumulative cell days (VCCD) over the time of the batch experiment.

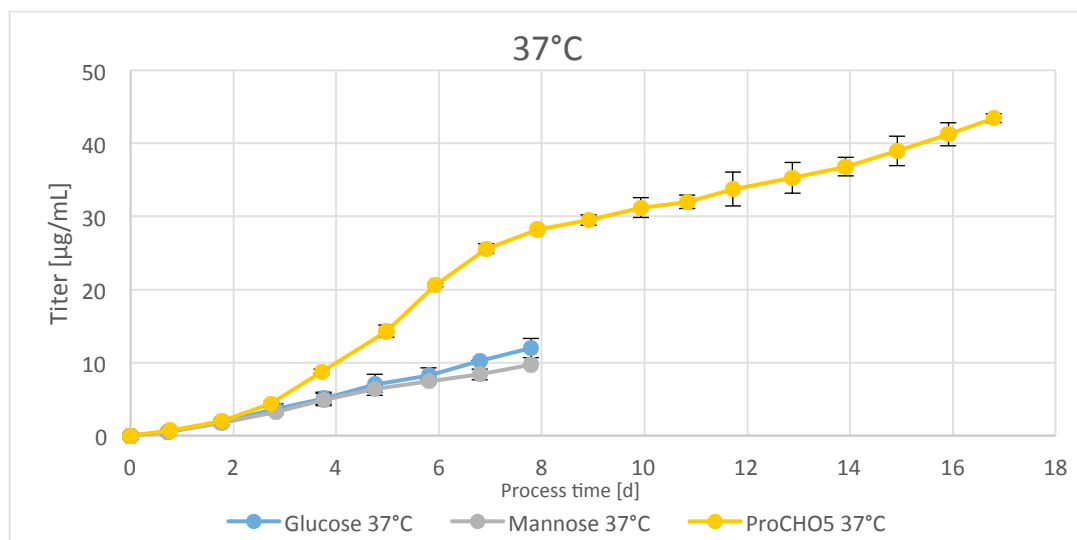


Figure 59: Daily titers of the shaking flasks incubated at 37°C as the average of the duplicates.

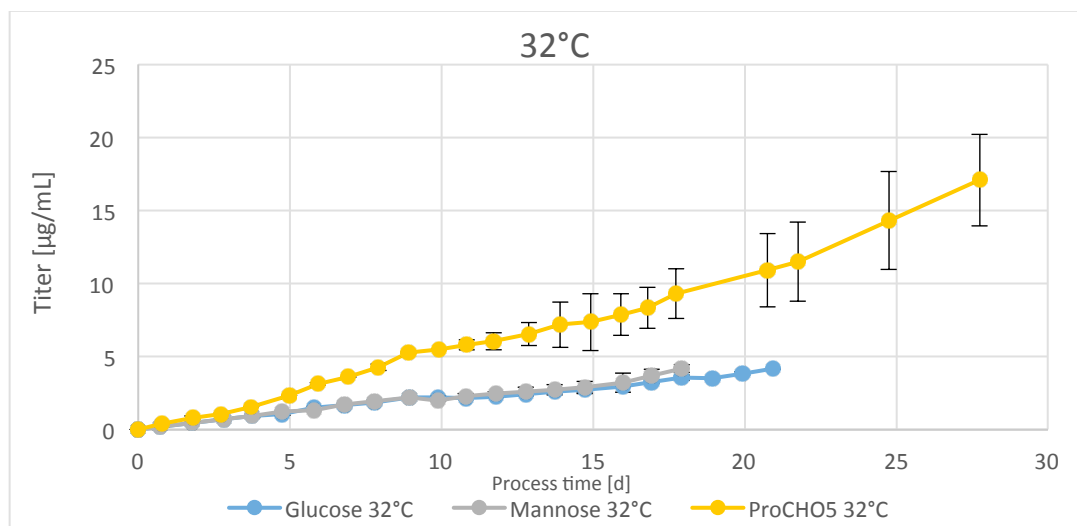


Figure 60: Daily titers of the shaking flasks incubated at 32°C as the average of the duplicates.

Table 18: All product related parameters as the average of the duplicates. D0 – Inoculation day, DX – Day of culture termination

Approach	Temp. [°C]	Flasks	qp day-to-day [pg/c/d]	qp DX - D0 [pg/c/d]	QP day-to-day [mg/d]	QP DX - D0 [mg/d]	STY day-to-day [mg/(L*d)]	STY DX - D0 [mg/(L*d)]
Glucose	37	2	1.67 ± 0.15	1.51 ± 0.11	0.11 ± 0.01	0.12 ± 0.01	1.33 ± 0.11	1.54 ± 0.12
	32	2	0.84 ± 0.04	0.55 ± 0.01	0.01 ± 0	0.01 ± 0	0.07 ± 0.01	0.20 ± 0
Mannose	37	2	1.43 ± 0.01	1.27 ± 0.01	0.09 ± 0	0.09 ± 0	1.06 ± 0	1.25 ± 0.01
	32	2	0.93 ± 0.20	0.64 ± 0.09	0.01 ± 0	0.01 ± 0	0.12 ± 0	0.23 ± 0.01
ProCHO5	37	2	1.54 ± 0.05	1.40 ± 0.05	0.13 ± 0.01	0.13 ± 0	1.47 ± 0.06	2.59 ± 0.02
	32	2	0.95 ± 0	0.96 ± 0.01	0.02 ± 0.02	0.01 ± 0	0.18 ± 0.04	0.62 ± 0.08

Table 19: All metabolism related parameters as the average of the duplicates. In case of qSugar and qGlutamine a positive value equals consumption. For qLactate, qGlutamate and qAmmonium a positive value means production.⁶

Approach	Temp. [°C]	Flasks	qSugar Bioprofiler [pg/c/d]	qSugar HPLC [pg/c/d]	qLactate Bioprofiler [pg/c/d]	qGlutamate Bioprofiler [pg/c/d]	qGlutamine Bioprofiler [pg/c/d]	qAmmonium Bioprofiler [pg/c/d]
Glucose	37	2	365 ± 1	359*	331 ± 35	7 ± 3	142 ± 5	15 ± 0
	32	2	301 ± 1	306*	128 ± 9	31 ± 5	82 ± 0	16 ± 0
Mannose	37	2	-	384*	365 ± 2	4 ± 1	133 ± 1	15 ± 0
	32	2	-	406*	181 ± 5	20 ± 1	86 ± 4	19 ± 2
ProCHO5	37	2	271 ± 9	245*	105 ± 25	21 ± 1	92 ± 5	8 ± 1
	32	2	236 ± 8	212*	59 ± 3	26 ± 4	42 ± 6	12 ± 1
*No standard deviation since not both shaking flasks were analyzed, but only one								

The silver staining clearly revealed, that this CHO cell population produced IgMs with a different isoform distribution: All shaking flasks indicated clearly visible bands for pentameric and hexameric IgMs. Additionally the flasks with D/H medium supplemented with either glucose or mannose revealed explicit tetrameric IgM bands and faint bands for IgM trimers. In this context it was shown, that mannose, as alternative sugar substrate, did not enhance the isoform distribution, but exhibited the same pattern as for glucose and the ProCHO5 medium. They all displayed explicit bands for IgM-hexamers, IgM-pentamers and the D/H medium additionally IgM-tetramers as well as faint bands for IgM-trimers (Figure 61).

⁶ See appendix 11.3 for detailed figures about the metabolic data for the batch F54.

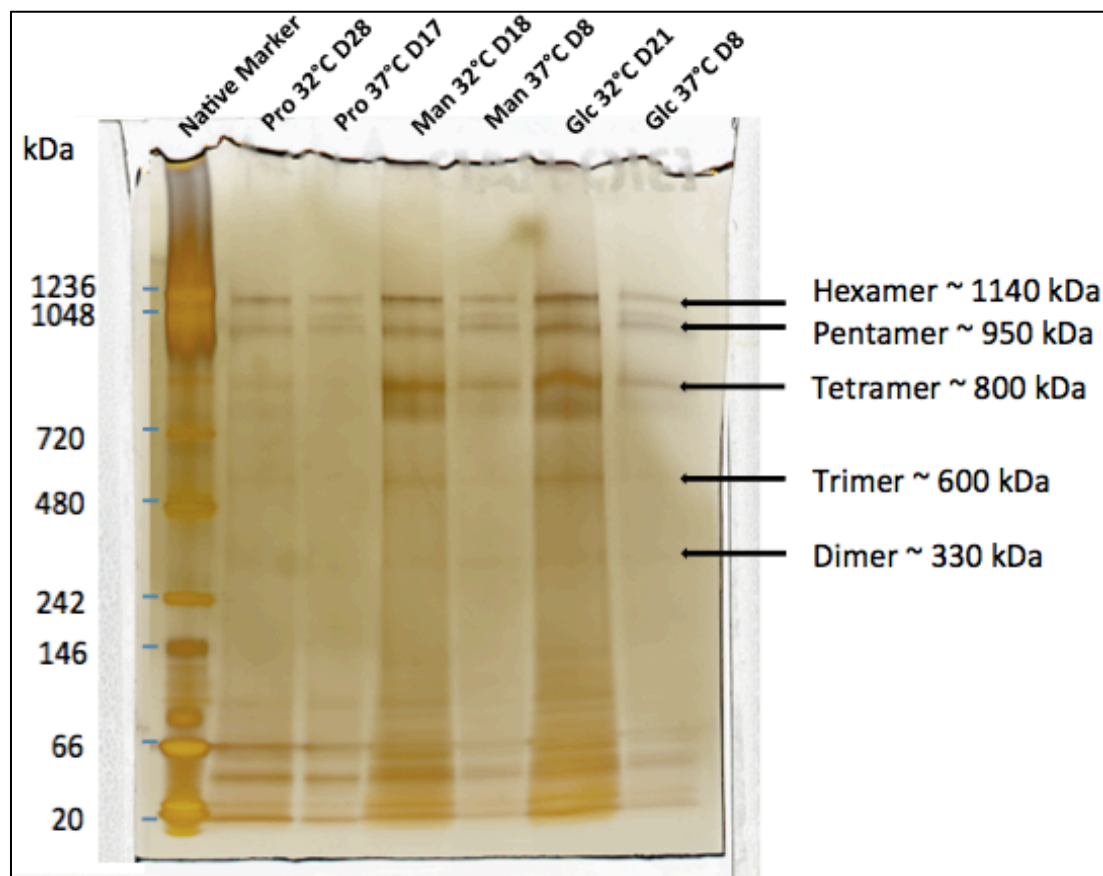


Figure 61: Result of the silver staining. For each sample 150 ng in 10 μ l were applied. Pro – ProCHO5 medium, Man – D/H medium supplemented with mannose, Glc – D/H medium supplemented with glucose.

Table 20: Summary of Batch F54. The specific growth rate μ is give for the exponential growth phase from the starting day until day 4.

Parameter	Glucose		Mannose		ProCHO5	
	37°C	32°C	37°C	32°C	37°C	32°C
Peak cell concentration [10^6 c/mL]	1.65 \pm 0.01	0.65 \pm 0.02	1.58 \pm 0.08	0.58 \pm 0.01	3.00 \pm 0.16	1.09 \pm 0.06
μ [1/d]	0.46 \pm 0.03	0.20 \pm 0.02	0.44 \pm 0.03	0.19 \pm 0.02	0.50 \pm 0.04	0.16 \pm 0.03
Titer [μ g/mL]	12 \pm 1	4 \pm 0	10 \pm 0	4 \pm 0	43 \pm 1	17 \pm 3
VCCD [10^6 c/mL]	7.94 \pm 0.05	7.55 \pm 0.29	7.66 \pm 0.01	6.59 \pm 0.90	31.1 \pm 1.16	17.8 \pm 2.93
Batch duration [d]	8	21	8	18	17	28

This batch experiment indicated a very high similarity in the performance of the cells in the D/H medium with glucose or mannose, respectively. Along with the superiority of the cells grown in ProCHO5 regarding the growth, these two outcomes are in accordance with the results of batch F52 (7.5). But in contrast to batch F52 the cells grown on ProCHO5 in this experiment revealed specific productivities in the range of the cells incubated in D/H medium with glucose/mannose.

The isoform distribution was not influenced by the application of mannose as carbon source.

7.8 Batch F56 – Parameter screening in DASGIP bioreactors of cell line A

This batch experiment was designed to primarily investigate the sheer forces, but also the impact of gassing, as potential factors for the bad performance of the cells in the DASGIP bioreactor in the batch F49. Therefore three different stirrer speeds and two different types of gassing were setup. While the L-sparger injects the gas at the bottom of the bioreactor directly into solution, the other method just aerates the headspace above the culture.

Key parameters:

Temperature [°C]:	37.0
pH:	7.00
Dissolved oxygen [% sat.]:	30
Gas-flow [L/h]:	1 (constant)
Volume [mL]:	600
Inoculum:	3×10^5 c/mL
Medium:	ProCHO5
T1:	L-Sparger + 80 rpm
T2:	L-Sparger + 60 rpm
T3:	L-Sparger + 160 rpm
T4:	Headspace + 80 rpm

The results indicated that the growth and the viability showed the best performance at the standard settings of 80 rpm and the L-sparger gassing directly into the cell suspension (Figure 62, Figure 63). The worst growth (specific growth rate of 0.40 d^{-1} in the exponential phase) and viability was observed with the gas input to the headspace (Figure 62, Table 21). Accordingly the pH was subject to much higher up- and downturns at this type of gas inflow (Figure 64), since it could be more precisely controlled by direct injection of carbon dioxide to the cell broth instead of the passive diffusion into solution via headspace. As already mentioned the stirrer speed of 80 rpm was superior (specific growth rate of 0.56 d^{-1} in the exp. phase), but interestingly the slight decrease to 60 rpm lead to worse growth (specific growth rate of 0.44 d^{-1} in the exp. phase) and viability when compared to the doubled stirrer speed of 160 rpm (specific growth rate of 0.51 d^{-1} in the exp. phase) (Figure 62, Figure 63, Table 21).

A closer look at the detailed gassing information (Figure 65) indicated that the bioreactor with the headspace aeration experienced higher fluctuations for the dissolved oxygen and needed far more oxygen and carbon dioxide in the course of the process, which revealed that this type of fumigation is much harder to handle.

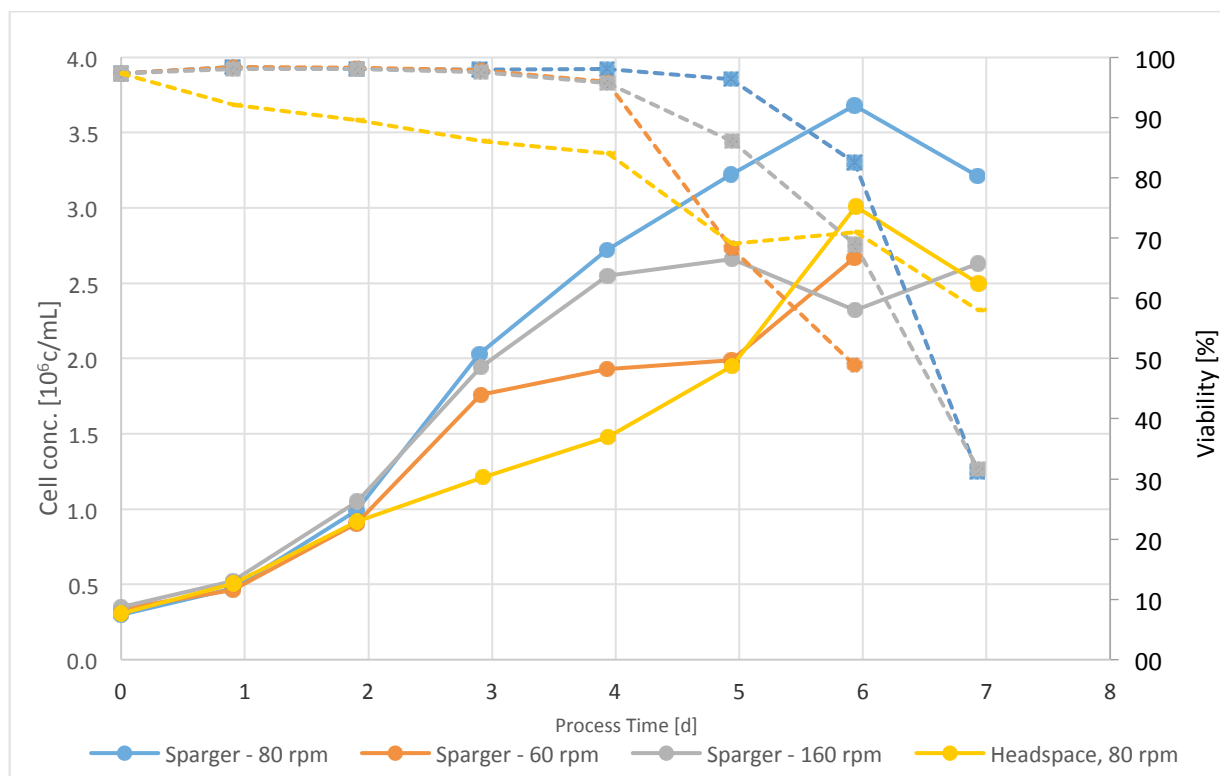


Figure 62: Daily cell concentrations and viabilities of the bioreactors.

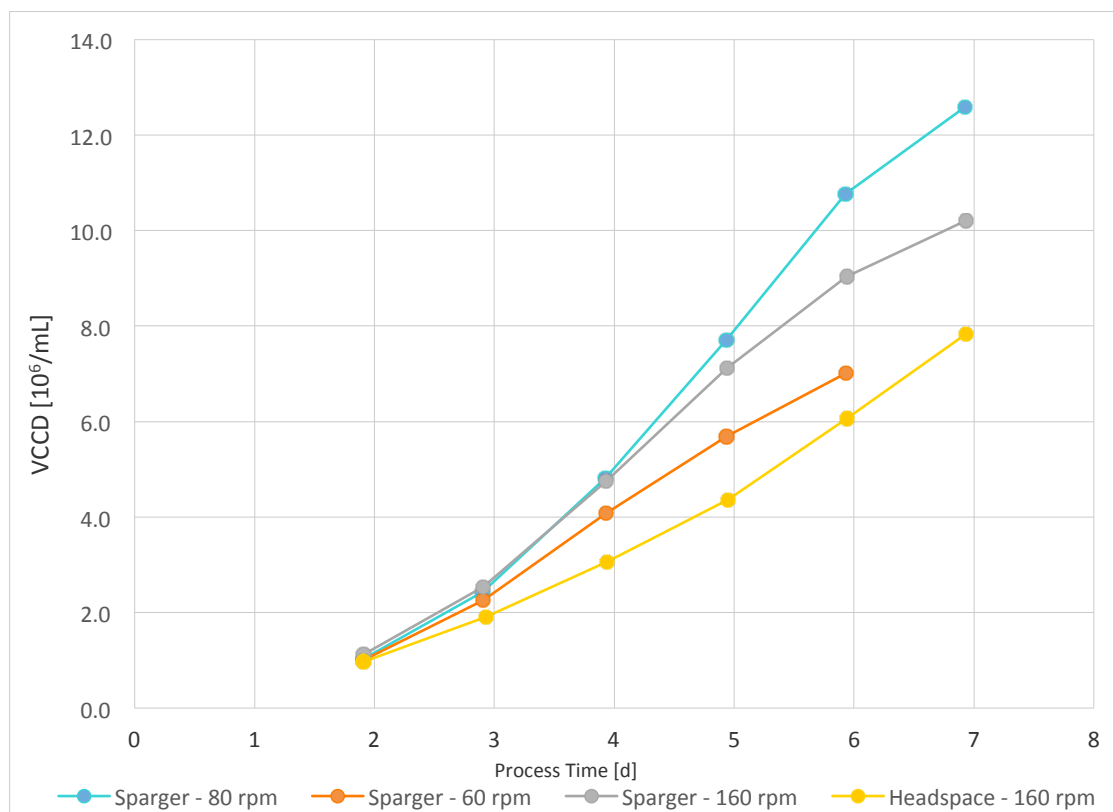


Figure 63: The viable cumulative cell days (VCCD) over the time of the batch experiment.

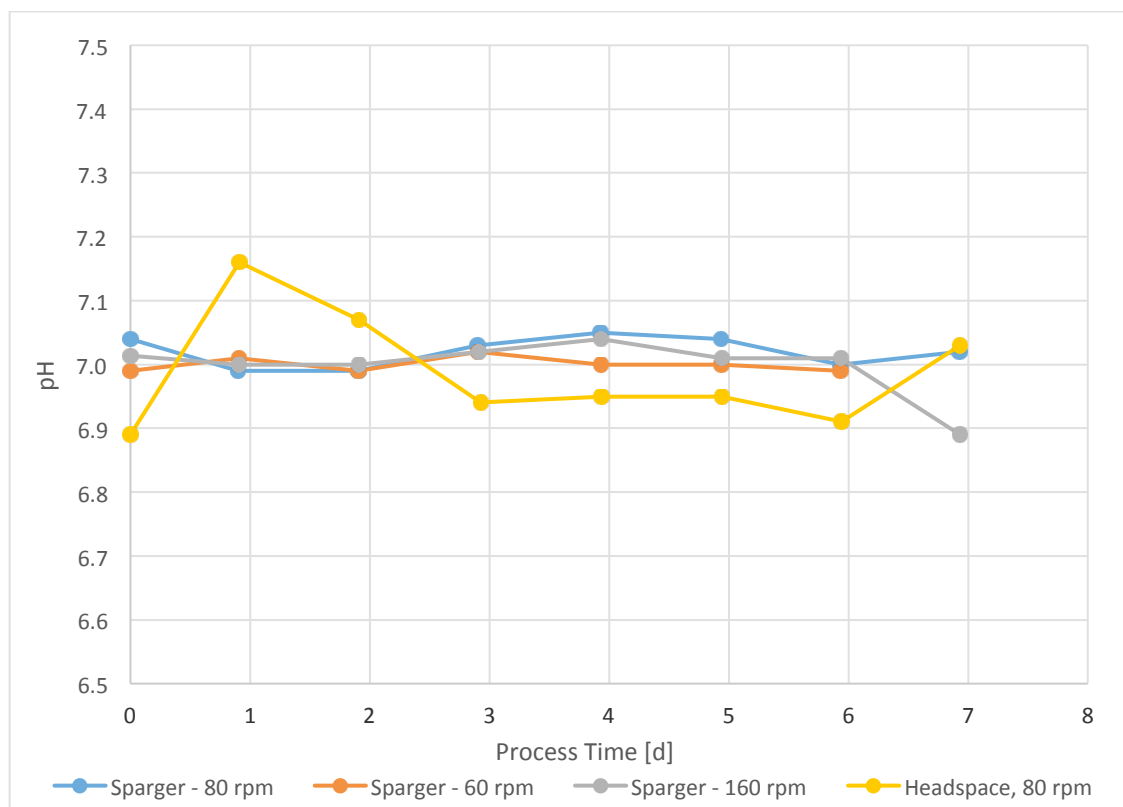


Figure 64: pH monitored over the whole process for each bioreactor.

Table 21: Summary of Batch F56. The specific growth rate μ is give for the exponential growth phase from the starting day until day 4. Because of the bad performance of the cells, the titers were not analyzed.

	Sparger – 80 rpm	Sparger – 60 rpm	Sparger – 160 rpm	Headspace, 80 rpm
Parameter				
Peak cell concentration [10^6 c/mL]	3.68	2.67	2.66	3.01
μ [1/d]	0.56	0.44	0.51	0.40
VCCD [10^6 c/mL]	12.6	7.02	10.2	7.83
Batch duration [d]	7	6	7	7

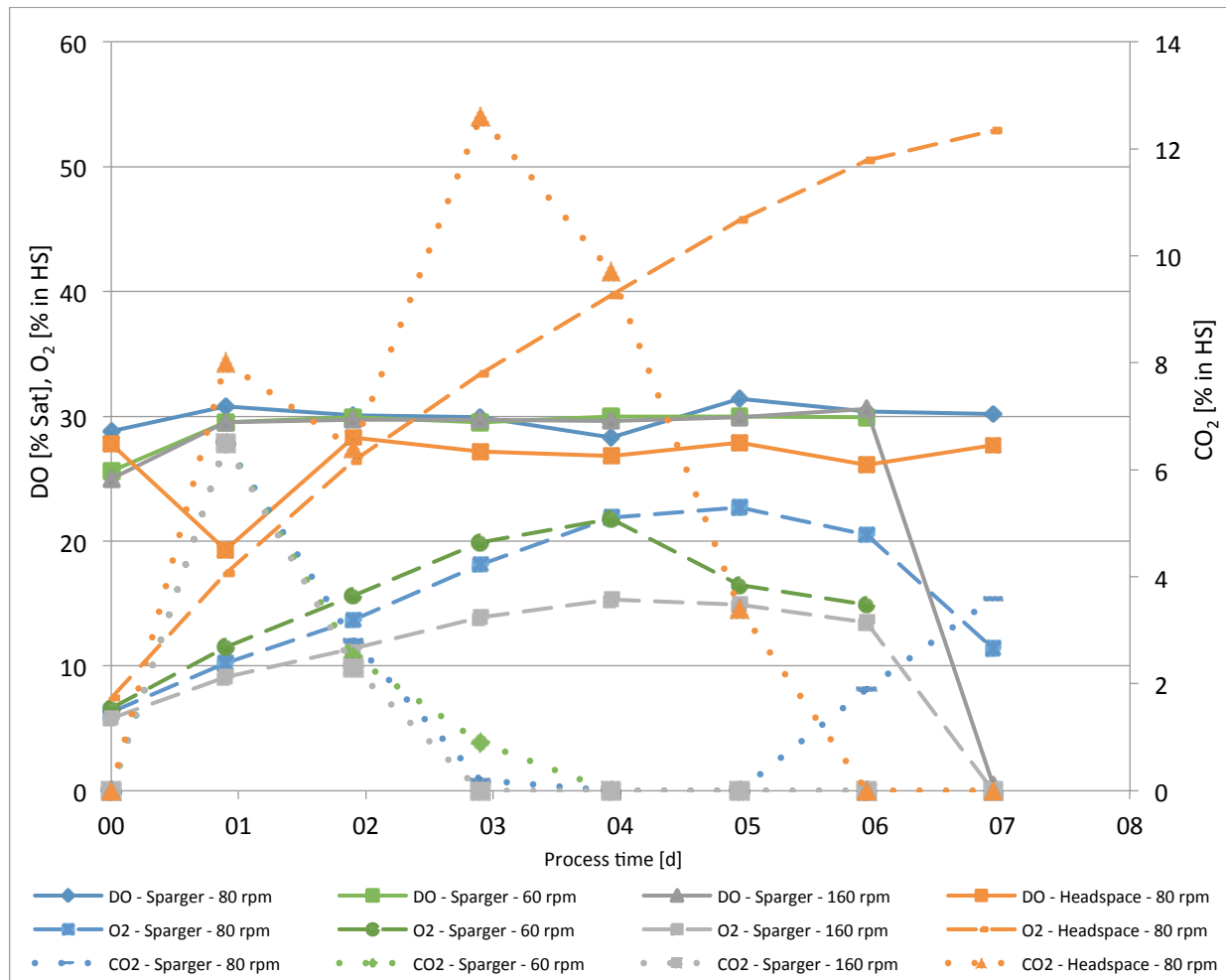


Figure 65: Detailed information about the dissolved oxygen [%saturation], O₂ and CO₂ concentration in the headspace of each bioreactor during the fermentation.

This batch experiment demonstrated that changes of the shear forces and the type of gassing had an impact on the performance of the cells, but also that these parameters could not explain the bad performance of the cells in the batch F49 (7.4).

8 Discussion

In the herein presented work, different sugar substrates such as fructose, mannose, galactose, sucrose and trehalose as possible alternatives to glucose were investigated on the performance of recombinant IgM antibody production process using CHO cells. The investigated parameters of relevance were cell growth, IgM antibody productivity as well as IgM quality in terms of isoform distribution. Additionally, the influence of temperature as an environmental parameter on the metabolic rates of recombinant CHO cell lines was studied.

8.1 Adaptation of cell lines to the alternative sugar substrates

Adaptation of the recombinant IgM producing cell line from glucose to galactose and mannose was successfully conducted within four passages (7.1). In this case, similar cell concentrations and viabilities were obtained without a long adaptation timespan of the cells (7.1). In comparison the adaption to other investigated alternative sugar sources such as fructose, sucrose and trehalose was not feasible. In these cases, the cell lines stopped growing and the viabilities dropped within a few passages (7.1). For the disaccharides trehalose and sucrose it is reported, that CHO cells were only able to grow on these substrates if the media they were suspended in contained the active serum enzymes for the hydrolysis of the disaccharides into their monomers (Scannel et al., 1982). A possible explanation for the cells being unable to grow on fructose may be that the ubiquitously expressed GLUT1 glucose transporter has no affinity for fructose. In a study conducted by another group (Wlaschin et al., 2007) CHO cells were engineered to stably express the GLUT5 fructose transporter, which has a higher K_m value for fructose compared to the ubiquitously expressed GLUT1 glucose transporter and thus lead to a more moderate sugar supply of the cells. The study compared the CHO cells grown on fructose and glucose at 3 g/L in a fed-batch process. It states that a 50% reduced sugar consumption and lactate production rate were observed and subsequently allowed an ~3 times increase in the maximum viable cell concentration in the fructose fed-batch process, although the specific growth rate was similar for the first 60-70 h in both cultures.

The applicability of mannose and galactose as a substrate for growth of CHO cells has been shown before by different groups (Berrios et al., 2011) (Altamirano et al., 2013). When adapted to mannose, the cells (CHO cells A and B) illustrated stable growth and viability (7.1). Galactose also proved itself as a feasible alternative substrate during the adaptation within four passages for the CHO cells A (7.1).

8.2 Determination of the optimal sugar concentration

After the adaptation phase the ideal sugar concentration (4 g/L, 6 g/L and 8 g/L) for batch growth of the recombinant IgM producing cell line was investigated in batch experiments (7.2). Despite different sugar concentrations were contained in the medium, similar IgM concentrations were measured when the cultures were harvested (Table 8). Moreover, the IgM isoform distribution was unaffected by the different sugar concentrations (Figure 26). The most promising concentrations for glucose, mannose and galactose were 6 g/L, since lower concentrations were depleted before the viability of the cultures dropped below 60%. Further, higher sugar concentrations could not be metabolized by the cells and also indicated 10-15% lower VCCDs (Table 8). As a consequence, all subsequent experiments were conducted with initial sugar concentrations of 6 g/L.

8.3 Sucrose and trehalose as supplements

Initial adaptation experiments using sucrose and trehalose for growing the recombinant cell line were not feasible. However, it is known that these sugars have an inherent protein stabilizing effect and are therefore frequently added during protein formulation (Cleland, et al. 2001) (Onitsuka, et al. 2014). Therefore, we reasoned that sucrose and trehalose may exert a potential influence on the IgM isoform distribution and added these sugars to the medium at different concentrations (0.1 g/L, 0.5 g/L, 1 g/L and 2 g/L) and performed batch cultures (7.3). With these experiments we found no beneficial impact on cell growth, process duration, IgM titers or the specific productivity of the CHO cells (Table 9). This was probably due to the fact that CHO cells cannot metabolize these sugars (as previously shown in our initial adaptation studies) (7.1). Despite the presence of sucrose and trehalose in the medium, the cell line almost exclusively produced pentamers and therefore we could not prove any positive effects on the isoform distribution (7.3).

8.4 Batch experiments and temperature reduction

In subsequently performed experiments we investigated the impact of environmental conditions on growth, productivity and IgM isoform distribution. An often applied principle during recombinant protein production is to cultivate cells at lower temperatures than 37°C (hypothermic conditions). Although the effects are cell line specific, hypothermic culture conditions have often been shown to reduce the cell metabolism while increasing culture viability, process duration and therefore also the recombinant protein yields (Bollati-Fogolín, et al. 2005). Therefore, we performed the batch experiments aimed at the comparison of galactose and mannose at 32°C in addition to the standard temperature of 37°C to determine the above described affects as well as to investigate the impact on protein quality. Furthermore these experiments were set up along with the cell lines grown in ProCHO5 medium containing

glucose for reasons of comparing the growth, viability, productivity and product quality at both temperatures with the D/H medium (7.4, 7.5, 7.7). The results of these fermentations illustrated that the substitution of glucose with mannose in the D/H medium did not seem to cause any differences in terms of growth and viability. In each experiment the cells peaked at very similar cell concentrations and demonstrated the same process time. Even the metabolism (specific consumption/production rates of metabolites), productivity and product quality (iso- and glycoforms distribution) were congruent between these two sugars throughout all performed batch experiments (7.5, 7.7). The ProCHO5 (w Glc) medium was shown to be superior to the D/H 1:1 (w/o Glc) medium regarding the growth for both CHO cell populations (VCCD of 30.1×10^6 per mL compared to 13.3×10^6 per mL for D/H + glc for CHO cells A; VCCD of 31.1×10^6 per mL compared to 7.94×10^6 per mL in case of CHO cells B), while revealing a lower specific glucose consumption (246 pg glucose/c/d compare to 372 pg glucose/c/d for CHO cells A; 271 pg glucose/c/d compared to 365 pg glucose/c/d for CHO cells B). Considering the productivity, the CHO cells A indicated a much lower specific productivity (4.02 pg IgM/c/d for ProCHO5 compared to 15.81 pg IgM/c/d for D/H + glc) and, despite much higher cell concentrations with 2.5 times higher peaked cell concentration compared to D/H + glc/man, also a 50% lower titer on the day of culture termination compared to D/H + glc/man. It seemed the cells made a shift from production to growth in the ProCHO5 medium. In contrast the CHO cells B did not exhibit a lower specific productivity and thus represented a higher titer based on the higher cell concentrations when grown on ProCHO5. Additionally the CHO cells B showed a much better viability and a longer process duration in the ProCHO5 medium (process time of 17 days compared to 8 days for D/H + glc) (7.5, 7.7). The major promising outcome of these experiments was that galactose, as alternative sugar substrate, in the CHO cell population A demonstrated specific productivities equivalent to glucose and mannose, while simultaneously showing a significantly reduced specific sugar consumption rate (50%) and specific lactate production rate (80%) accompanied by an increased specific ammonium production rate (80%) (Table 13).

The temperature reduction to 32°C lead in general to a clearly increased viability and hence prolonged process time (CHO cells A: 20 compared to 14 days for glucose, 18 compared to 14 days for mannose, 18 compared to 12 days for ProCHO5; CHO cells B: 21 compared to 8 days for glucose, 18 compared to 8 days for mannose, 28 compared to 17 days for ProCHO5), except for galactose, which illustrated a faster declining viability, but the same process time compared to the corresponding 37°C culture. At the same time the temperature reduction indicated a decrease in growth for both cell populations when compared to 37°C (VCCD CHO cells A: 50% lower for glucose and mannose, 75% lower for galactose and 66% lower for ProCHO5; VCCD CHO cells B: 10% lower for glucose and mannose, 50% lower for ProCHO5). In case of galactose the cell concentrations did not even rise, but rather declined from the starting day on (specific growth rate of -0.02 d^{-1} compared to 0.30 d^{-1} at 37°C). For glucose and mannose in D/H medium

and ProCHO5 medium the cells started to grow, but at a much lower specific growth rate (0.40 d^{-1} compared to 0.09 d^{-1} in the exponential phase for glucose in the CHO cell population A). For all sugars and both media it was observed that the decrease in the specific growth rate from the day of the peak cell concentrations occurred in a more moderate manner at 32°C . Moreover did the specific productivities show to be lower at 32°C (15.18 pg IgM/c/d compared to 9.78 pg IgM/c/d for glucose). It was only the CHO cells A in the ProCHO5 medium that demonstrated an increased specific productivity at 32°C (5.23 pg IgM/c/d compared to 4.02 pg IgM/c/d) (7.5, 7.7). The resulting deceleration of the metabolism causing the lower growth was also reported by other studies (Bollati-Fogolín et al., 2005) (Mason et al., 2014), while the latter study also states, that in contrast to our results the temperature reduction lead to increased specific productivities. Thus the effect of a temperature reduction regarding the productivity and product yield seem to be cell-line specific.

8.5 Investigation of the bad performance of cell line A in medium supplemented with galactose

Although minimizing its production could considerably reduce the negative impacts of lactate, the cells incubated with galactose demonstrated a worse performance on growth and process duration when compared to glucose and mannose (7.5). This might be, because despite the mentioned harmful acidic property of lactate in the introduction, it might to some extent also contribute to the pH of a culture not to become basic. During cultivation of galactose containing shaking flasks at $7\%\text{ CO}_2$ it was observed that the optical pH indicator (phenol red) in the medium did not turn orange (acidic) to the same extent as the shaking flasks with glucose, mannose or ProCHO5. The missing orange turn indicated a basic pH in the galactose flasks. Thus we suspected the basic pH due to the missing impact of lactate on the pH value as a possible reason for the bad performance of cell line A grown on galactose. To decrease the pH we studied the application of $20\%\text{ CO}_2$ instead of $7\%\text{ CO}_2$ in the headspace of the cultures grown on galactose. The results indicated a better viability when cultivated at 32°C , but no improvement of the viability at 37°C and growth on both temperatures (7.6).

8.6 Product quality – isoform distribution and glycosylation

Analysis of harvested culture supernatants of cell line A regarding product quality showed that neither galactose and mannose nor the temperature reduction changed the isoform distribution of the recombinantly expressed IgMs (7.5). Also, in case of the CHO cell population B it was demonstrated that mannose and the temperature reduction did not improve the isoform distribution towards the pentamer production (7.7). In case of galactose this was most likely due to the fact that the isoform distribution already showed a very high pentamer proportion under standard conditions for CHO cell population A that could not further be optimized.

However, analysis of the recombinantly expressed IgM quality by mass spectrometry revealed glycosylation differences as a consequence of the medium as well as sugar substrate. When the CHO cells were grown in the presence of galactose a new glycoform (GnGnF) that was not seen with glucose or mannose as substrate was observed while the glycoform NaNaAF disappeared. Additionally the addition of galactose demonstrated to have AAF as the most abundant glycoforms with 60%, in contrast to glucose and mannose that predominantly exhibited the glycoforms NaAF (about 36%) and NaNaF (about 30%) (7.5). The glycoforms produced by the human body commonly end with neuraminic acid (Na, also sialic acid (SA)) or fucose (F). The sialylation is of special importance because it is a charged moiety and thus fundamentally affects the properties of the glycan chain (Brooks 2004). Deductive of this information, the glycoforms with a sialic acid at the end of each branch are more likely to trigger immunological tolerance in the human body. Therefore the glycoforms generated by the cells that were grown on D/H medium supplemented with glucose and mannose are possibly more valuable (Figure 47). A review by McAtte (McAtte et al., 2014) describes the role of the central carbon metabolism in controlling the quality of secreted biotherapeutic proteins. While it mainly states that the production of the unwanted metabolite ammonium has a negative effect on the glycosylation by preventing the optimal activity of the sialyltransferase enzymes in the Golgi apparatus, information about the direct impact of alternative sugar substrates on the glycosylation needs to be further researched.

8.7 Mannose and galactose as alternative substrates

As a consequence of the batch experiments, galactose seemed to be taken up or metabolized in a slower manner and thus supposedly circumvented the accumulation of pyruvate. Thereby pyruvate could be more efficiently metabolized by channelling it into the pathway of the oxidative phosphorylation to a higher degree, instead of reducing it into lactate, as mentioned in the introduction. These results were also observed in several studies (Altamirano et al., 2013) (Jiménez et al., 2011). According to these studies the bad performance was due to the low uptake rate of galactose. This explanation would also be in consent with our results of the decreased specific galactose consumption rate compared to glucose and mannose (Table 13, Table 16).

Also has another group shown that CHO cells can use mannose as an alternative to glucose (Berrios et al., 2011). They replaced glucose with mannose in a continuous culture of CHO cells producing t-PA and observed an increase in biomass (15-20%) and a lower specific sugar consumption rate (20-25%) accompanied by an increase in the specific lactate production rate (25-35%). Their results are in contrast to our results, since we did not observe any mentionable alteration by applying mannose as alternative sugar substrate (Table 13, Table 19). Thus regarding the consumption of mannose as alternative substrate there also seemed to be a cell-line dependent effect.

8.8 Batch experiments in the DASGIP module

For large-scale production of IgM antibodies cultivation of the recombinant cell lines in bioreactors is needed. Given that the bioreactors were a more sophisticated system than shaking flasks, we expected the cells to perform better in the bioreactors. In a pre-experiment we investigated growth of the CHO cell line A in DASGIP bioreactors and compared the performance to shake flasks (7.4). We found that the cells revealed a worse performance in the D/H 1:1 (w/o Glc) + glc/gal/man and ProCHO5 medium when compared to the corresponding shaking flasks (7.4). The cell peak concentrations in the DASGIP bioreactors were about 50% lower for glucose and galactose and 70% lower for mannose and ProCHO5. The lower viabilities lead to shorter process time of just 8 days compared to 12 days for glucose, 4 days compared to 9 days for galactose, 5 compared to 12 days for mannose and 6 compared to 12 days for ProCHO5 (Table 11).

In a follow-up experiment we investigated the stirrer speed or aeration to address possible bottlenecks (7.8). Therefore only the stirrer speed (standard setting was 80 rpm) was increased (160 rpm) and decreased (60 rpm), respectively, or the aeration was changed from L-sparger to headspace in order to investigate the impact of direct gassing into the cell suspension which does not occur during cultivation in shake flasks. The results demonstrated that these changes had a rather negative impact on the behaviour of the cells when compared to the standard settings and could not explain the bad performance of the cells in the pre-experiment. Maybe the cell line we used was sensitive to the shear forces that are particularly caused by stirrers. Another possible effect on culture performance, although not analysed, could be due to the pH. During shake flask incubation the cells are cultivated in a bioreactor with a constant atmosphere of 7% CO₂ which allows continuous pH changes. During cultivation in the DASGIP bioreactors the pH is constantly controlled and CO₂ or base (NaOH) is added to keep the pH constant at 7.00 pH units. Although the true impact remains to be determined, also the addition of base causes changes in medium osmolality and therefore may influence cell growth and productivity.

9 Future prospectives

A promising approach for further investigation would be metabolic engineering of the galactose pathway, to take advantage of the minimized lactate production and aim for prolonged growth and process time. The study conducted by Jiménez et al (Jiménez, Wilkens und Gerdtzen 2011) investigated this idea, by experimenting with CHO cells, which have been genetically engineered to overexpress the galactose transporter Slc2a8 (GLUT8) and the galactokinase GalK1, the enzyme regulating the limiting step of the galactose catabolism. Their results indicate that these cells achieve prolonged viability when grown on a combination of glucose and galactose, with a metabolic shift towards lactate consumption, which is triggered when galactose starts to get consumed.

Another interesting concept would be to investigate if there is a way such as metabolic engineering to successfully grow CHO cells on one of the protein stabilizing disaccharides sucrose or trehalose. Although the “stabilizing sugars” did not impact the IgM isoform distribution in our experiments, their potential influence on cell metabolism as well as product glycosylation certainly would be an interesting task for future experiments.

Last but not least further testing is necessary to discover why the CHO cells did not show superior performance in the bioreactors and make them successfully grow there for scale-up of future production processes.

10Bibliography

Altamirano, Claudia, Julio Berrios, Mauricio Vergara, and Silvana Becerra. "Advances in improving mammalian cells metabolism for recombinant protein production." *Electronic Journal of Biotechnology* , 2013.

Berrios, J., C. Altaminaro, N. Osses, and R. Gonzalez. "Continuous CHO cell cultures with improved recombinant protein productivity by using mannose as carbon source: Metabolic analysis and scale-up simulation." *Chemical Engineering Science* 66, no. 11 (2011): 2431-2439.

Bollati-Fogolín, M., G. Forno, M. Nimtz, H.S. Conradt, M. Etcheverrigaray, and R. Kratje. "Temperature Reduction in Cultures of hGM-CSF-expressing CHO cells: Effect on productivity and product quality." *Biotechnology Progress* 21, no. 1 (2005): 17-21.

Brooks, S.A. "Appropriate Glycosylation of Recombinant Proteins for Human Use." *Molecular Biotechnology* 28, no. 3 (2004): 241-255.

Butler, Michael. "Animal cell cultures: recent achievements and perspectives in the production of biopharmaceuticals." *Appl Microbiol Biotechnol*, 2005: 283-291.

Cleland, J.L., et al. "A specific molar ratio of stabilizer to protein is required for storage stability of a lyophilized monoclonal antibody." *Journal of pharmaceutical sciences* 90 (03 2001): 310-321.

Cruz, H.J., C.M. Freitas, P.M. Alves, J.L. Moreira, and M.J.T. Carrondo. "Effects of ammonia and lactate on growth, metabolism, and productivity of BHK cells." *Enzyme and Microbial Technology* 27, no. 1-2 (2000): 43-52.

Eisen, Herman N. "Affinity enhancement of antibodies: How low-affinity antibodies produced early in immune responses are followed by high-affinity antibodies later and in B-cell responses." *Cancer Immunology Research* 2 (2014): 381-392.

Jayapal, Karthik P., Katie F. Wlaschin, Wei-Shou Hu, and Miranda G. S. Yap. "Recombinant Protein Therapeutics from CHO cells - 20 Years and Counting." *CHO Consortium*, 2007.

Jiménez, Natalia, Camila Wilkens, and Ziomara Gerdtsen. "Engineering CHO cell metabolism for growth in galactose." *BMC proceedings* 5 (2011): 119.

Kim, Jee Yon, Yeon-Gu Kim, and Gyun Min Lee. "CHO cells in biotechnology for production of recombinant proteins: current state and further potential." *Appl Microbiol Biotechnol*, 2012: 917-930.

Lai, Tingfeng, Yuansheng Yang, and Say Kong Ng. "Advances in Mammalian Cell Line Development Technologies for Recombinant Protein Production." *Pharmaceuticals*, 2013: 579-603.

Mader, A., V. Chromikova, and R. Kunert. "Recombinant IgM expression in mammalian cells: A target protein challenging biotechnological production." *Advances in Bioscience and Biotechnology* 4 (2013): 38-43.

Mason, M., B. Sweeney, K. Cain, P. Stephens, and S.T. Sharfstein. "Reduced Culture Temperature Differentially Affects Expression and Biophysical Properties of Monoclonal Antibody Variants." *Antibodies* 3 (2014): 253-271.

McAtte, A.G., N. Templeton, and J.D. Young. "Role of Chinese hamster ovary central carbon metabolism in controlling the quality of secreted biotherapeutic proteins." *Pharmaceutical Bioprocessing* 2 (2014): 63-74.

Onitsuka, M., et al. "Trehalose suppresses antibody aggregation during the culture of Chinese hamster ovary cells." 117, no. 5 (2014): 632-638.

Rachel Legmann, Julie Melito, Ilana Belzer, David Ferrick. "Analysis of glycolytic flux as a rapid screen to identify low lactate producing CHO cell lines with desirable monoclonal antibody yield and glycan profile." *BMC proceedings*, 2011: 94.

Scannel, John, and M.J. Morgan. "The regulation of carbohydrate metabolism in animal cells:Isolation of starch- and maltose-utilizing variants." *Bioscience Reports* 2, no. 2 (1982): 99-106.

Schneider, Markus, Ian W. Marios, and Urs von Stockar. "The importance of ammonia in mammalian cell culture." *Journal of Biotechnology* 46, no. 3 (1996): 161-185.

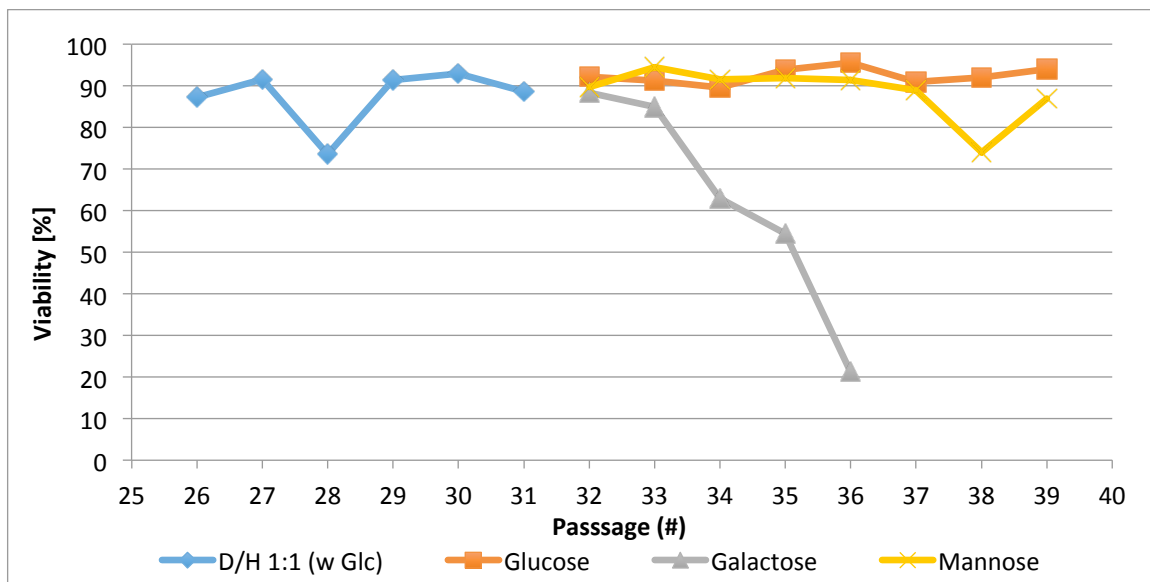
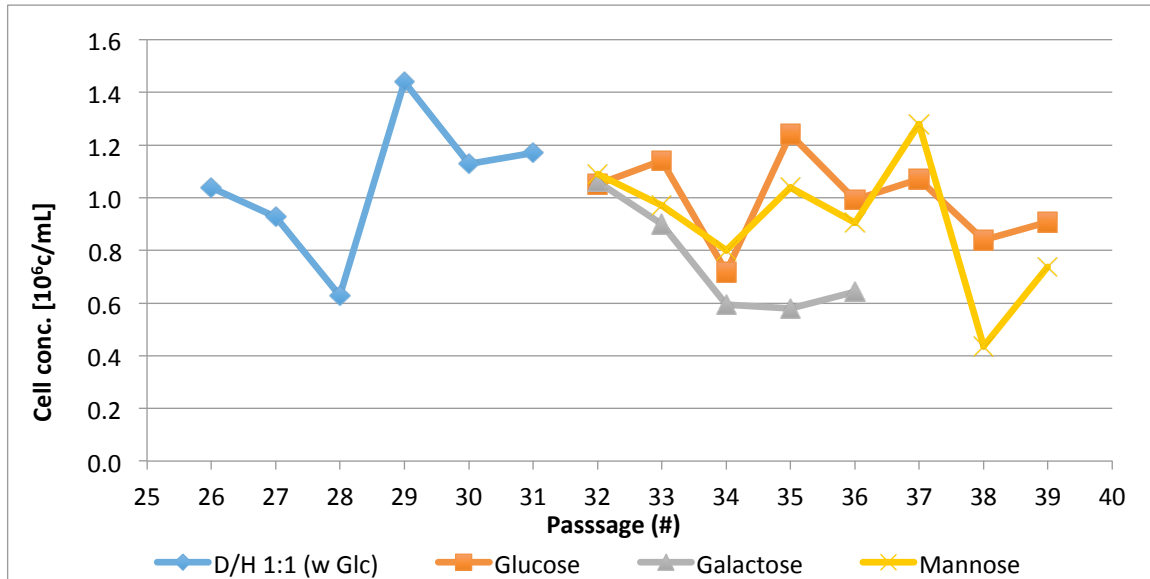
Verma, R., E. Boleti, and A.J.T. George. "Antibody engineering: Comparison of bacterial, yeast, insect and mammalian expression systems." *Journal of Immunological Methods* 216, no. 1-2 (1998): 165-181.

Wlaschin, K.F., and W.-S. Hu. "Engineering cell metabolism for high-density cell culture via manipulation of sugar transport." *Journal of Biotechnology* 131, no. 2 (2007): 168-176.

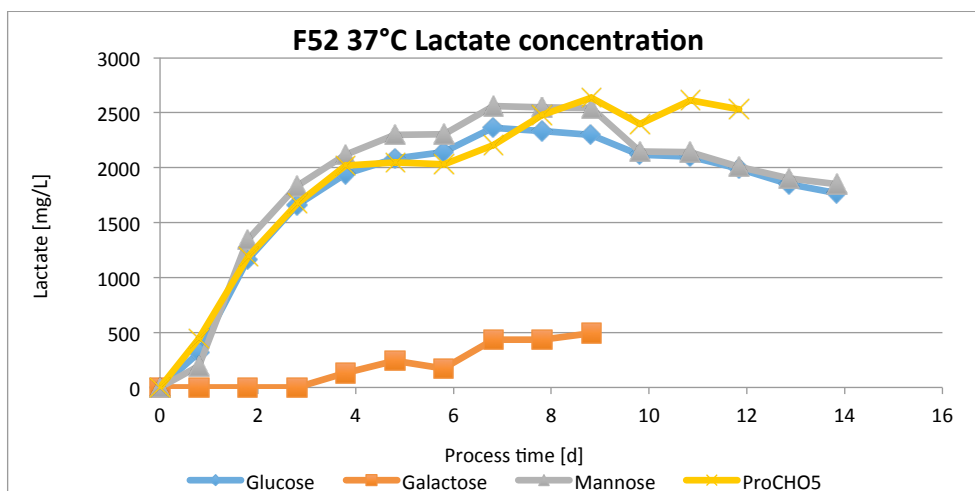
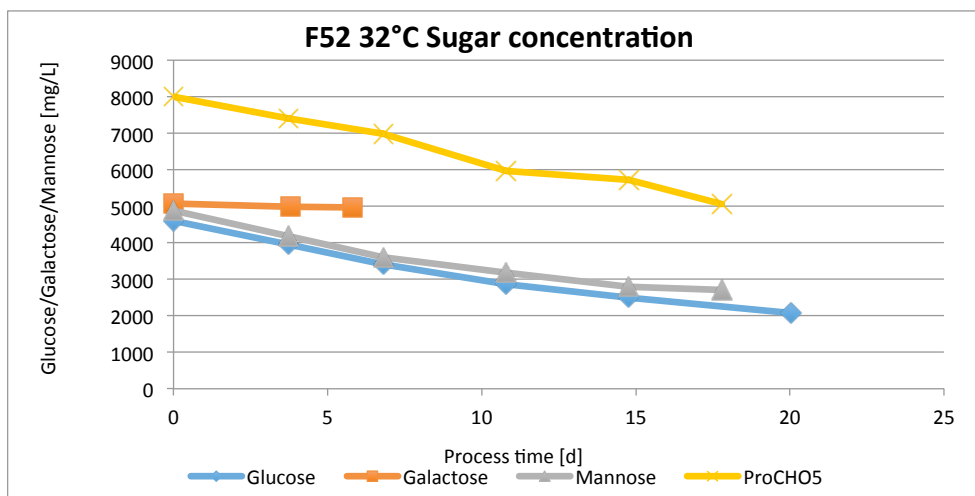
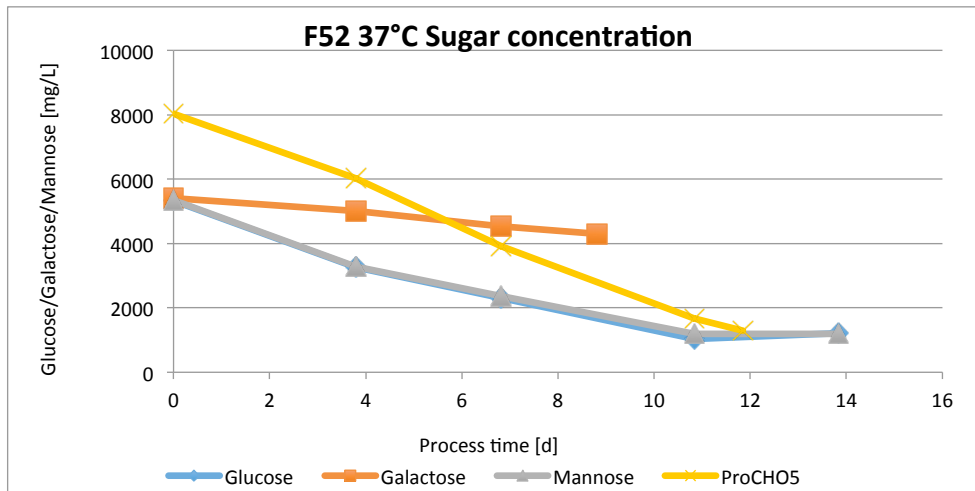
Wood, C, M.A. Boss, Kenten J.H., J.E. Calvert, N.A. Roberts, and J.S. Emtage. "The synthesis and in vivo assembly of functional antibodies in yeast." *Nature*, 1985: 446.

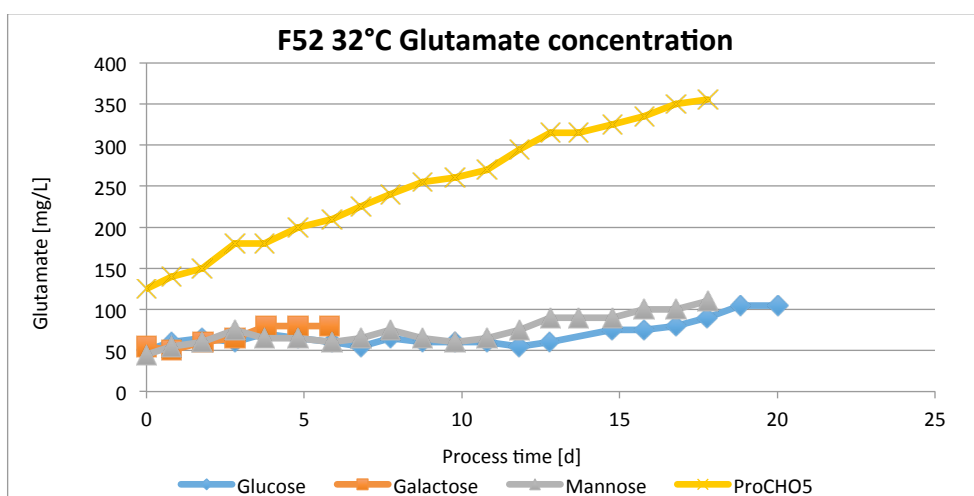
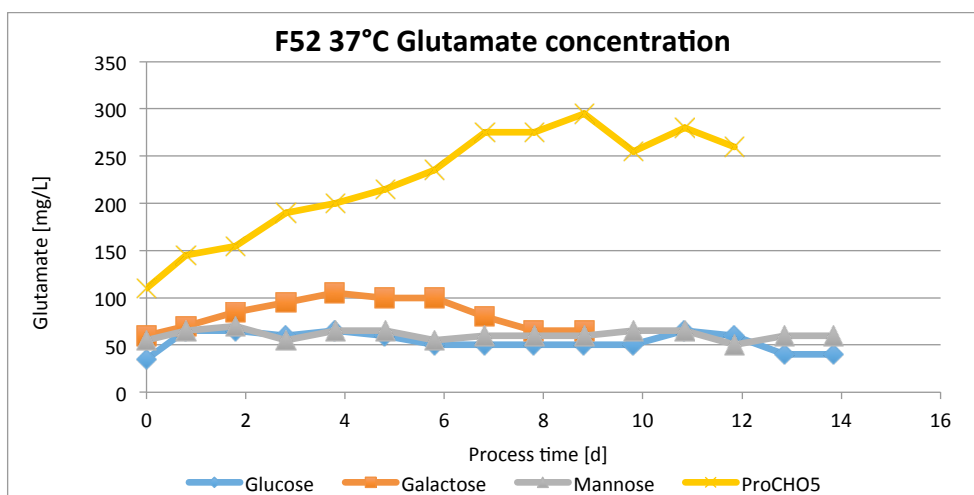
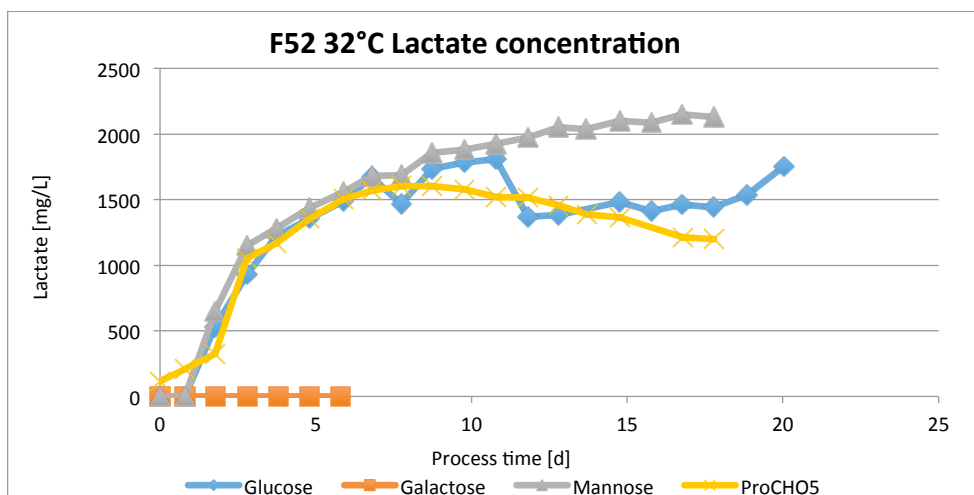
11Appendix

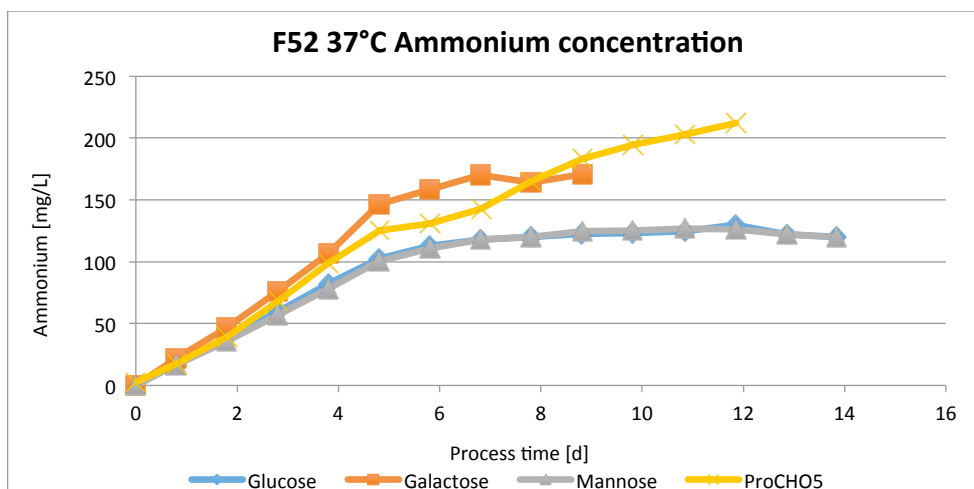
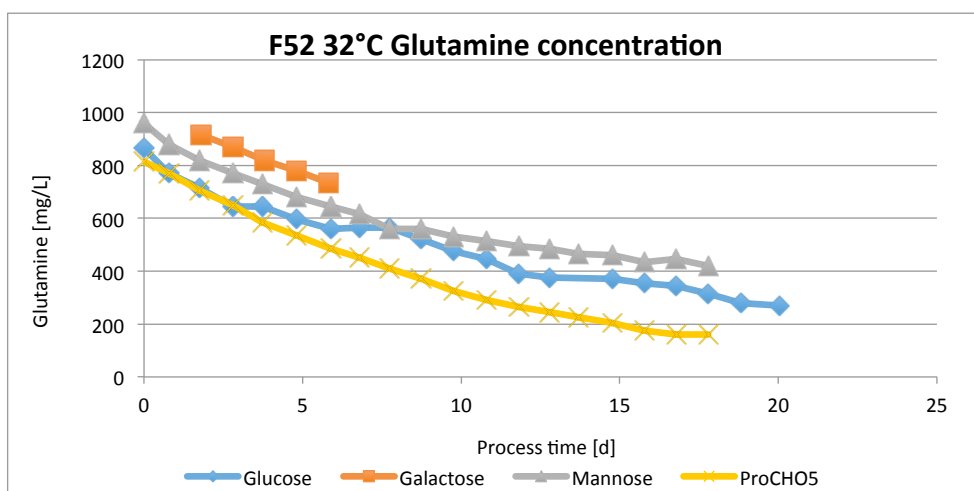
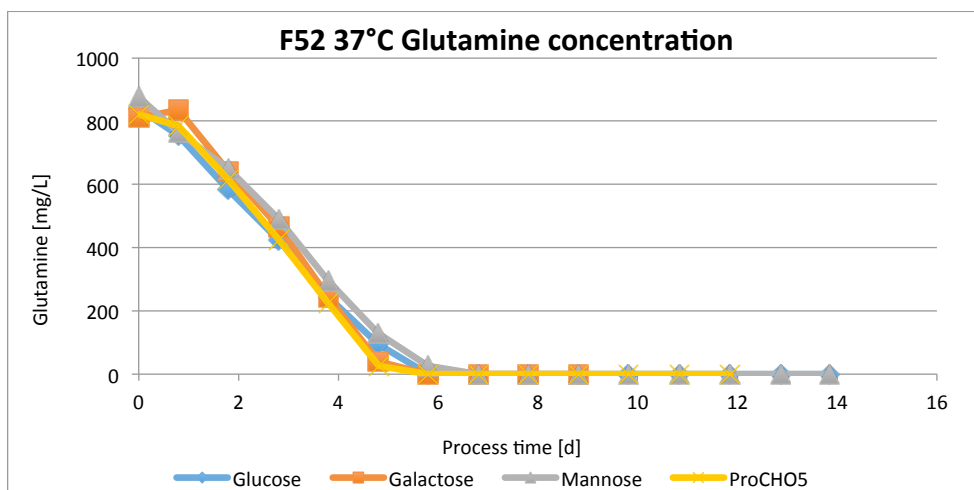
11.1Adaption of CHO cells (B) to alternative sugar substrates

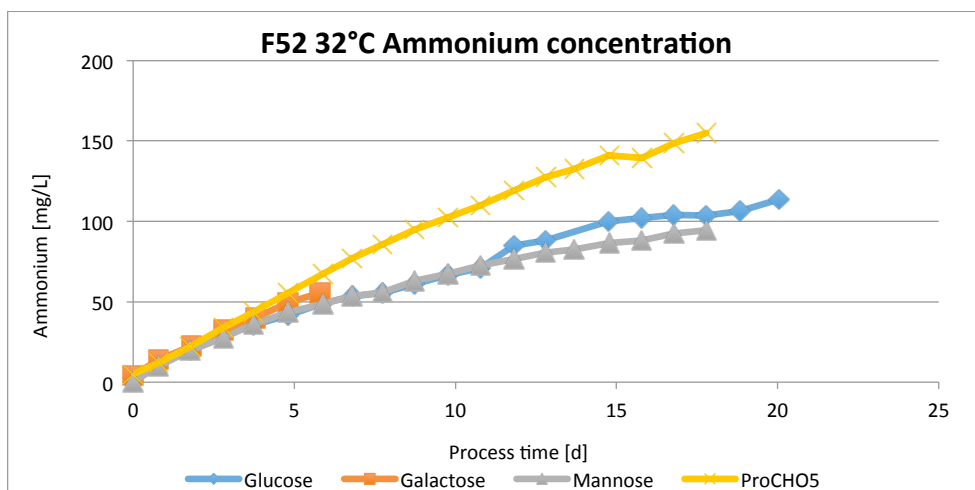


11.2 Metabolic data for the batch F52

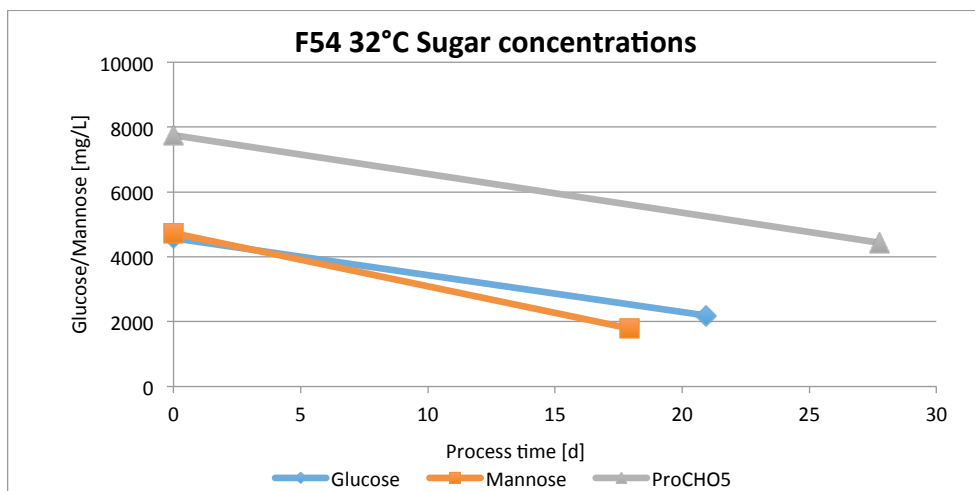
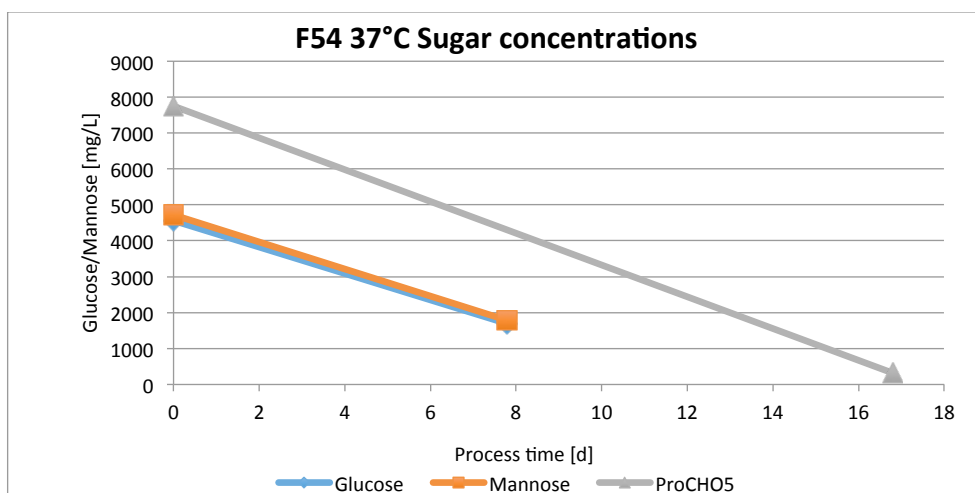


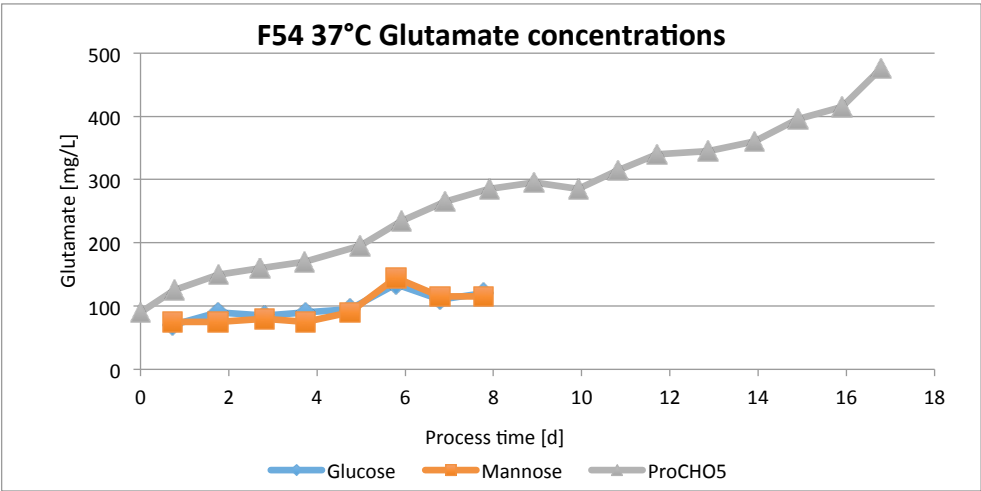
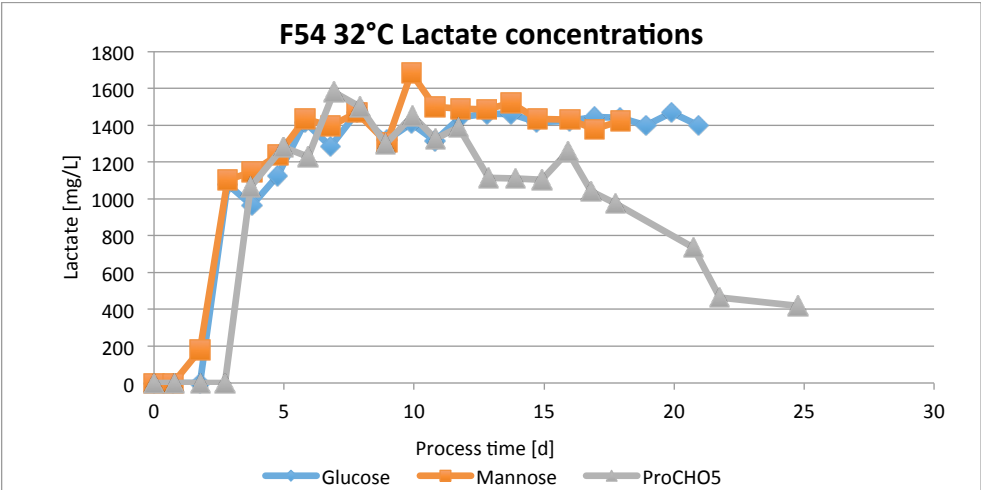
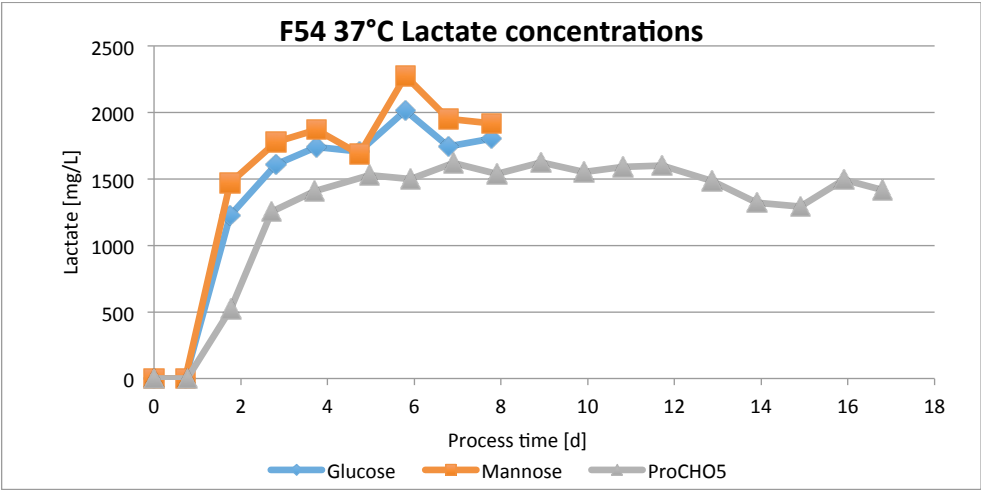


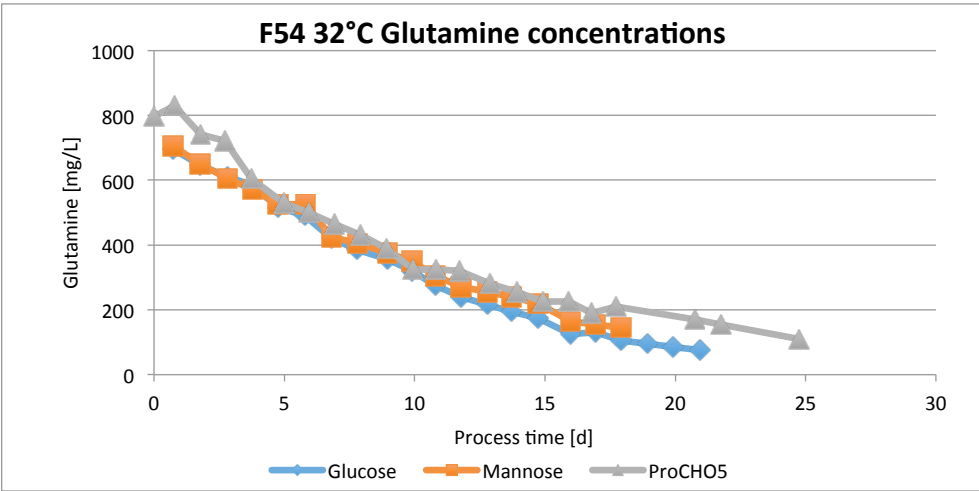
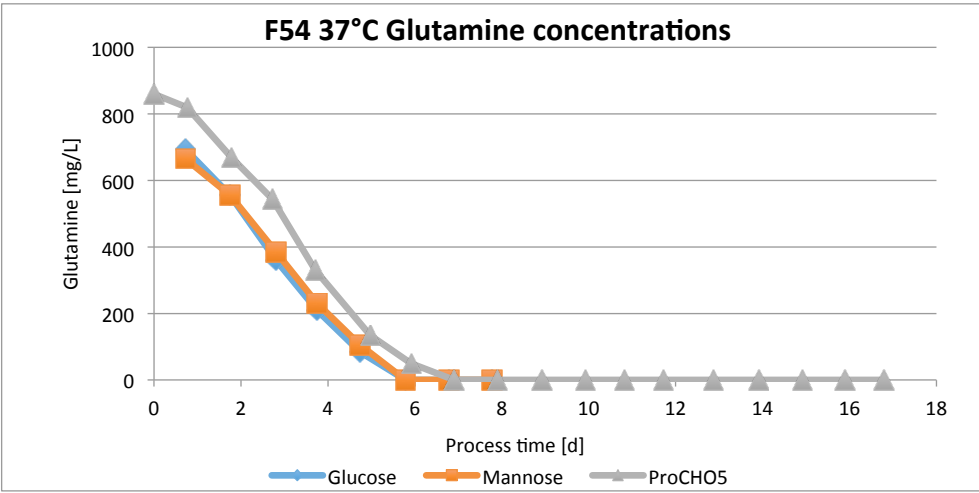
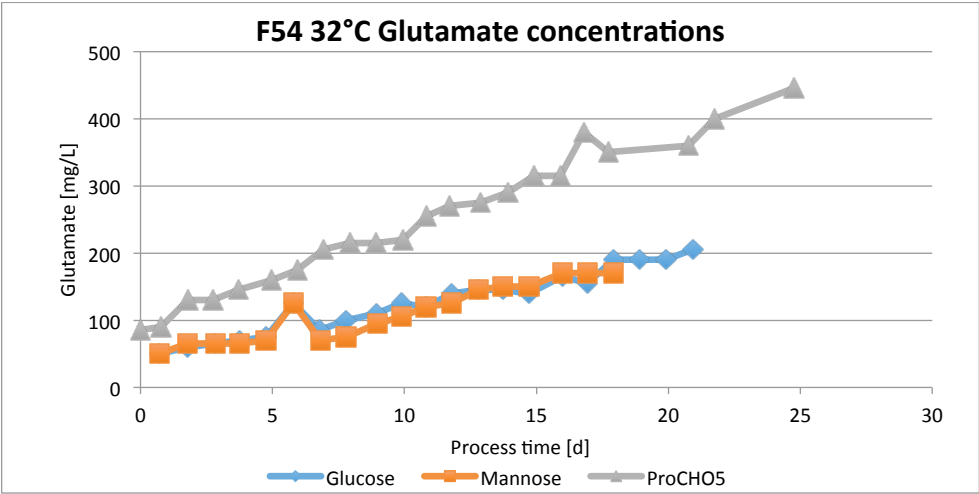


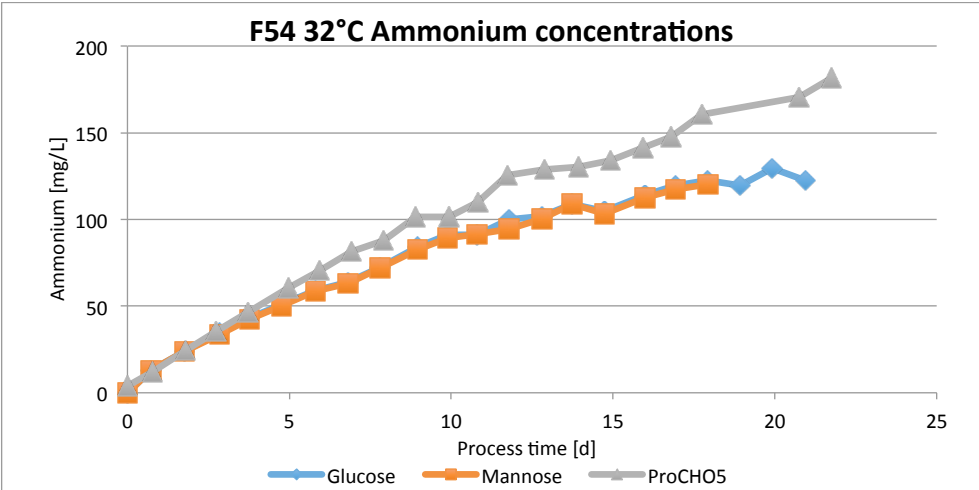
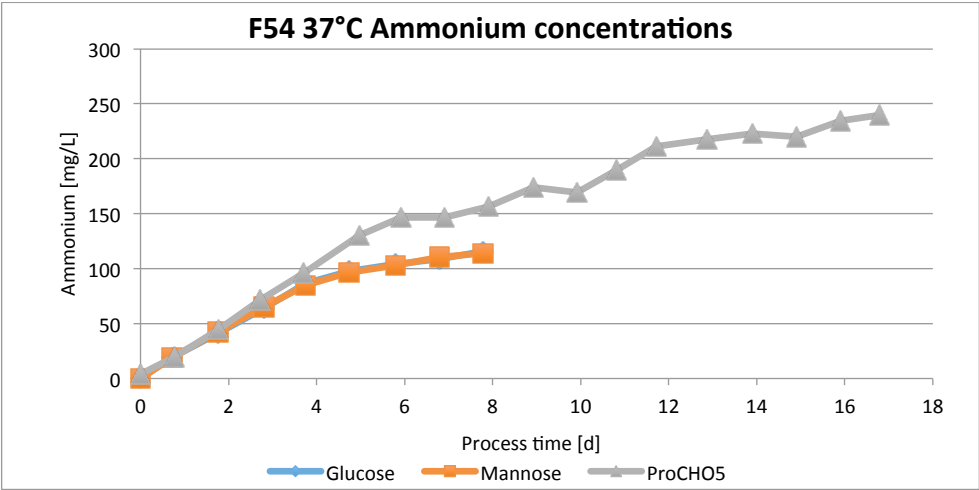


11.3 Metabolic data for the batch F54









11.4 Silver Staining

Fixation Solution: 50% Ethanol / 10% Acetic Acid in H₂O

Incubation Solution: 150 mL Ethanol

1.75 g Na₂S₂O₃*5H₂O (Sodiumthiosulfate pentahydrate)

56.4 g Na-acetate*3H₂O / 34 g waterfree Acetate

Fill up to 500 mL with H₂O

Add freshly 62.5 µL Glutaraldehyd (4°C) / 25 mL

Silver Solution (4°C): 0.25 g AgNO₃ in 500 mL H₂O

Add freshly 5 µL Formaldehyd (4°C) / 25 mL

Develop Solution: 12.5 g Na₂CO₃ in 500 mL H₂O

Add freshly 5 µL Formaldehyd (4°C) / 25 mL

Stop Solution: 0.05 M EDTA in H₂O

Fix 1 hour or overnight in Fixation Solution

Incubate 20 min in Incubation Solution

Wash 3 x 5 min in H₂O

Incubate 15 min in Silver Solution (4°C)

Wash briefly with H₂O

Develop until bands are seen with Develop Solution

Wash briefly with H₂O

Stop reaction in Stop Solution (15 - 60 min)

Store in 10% Glycerol at 4°C

Gel conservation:

Incubate gel 20 min in Drying Solution (Invitrogen)

Briefly incubate 2 membranes in Drying Solution and place one on each side of the gel

Fix in frame and store at room temperature 1-2 days

11.5 Cell-bank information sheets

472	
Zelllinie: <u>CHO-2G12</u> Code: <u>CHO 2G12-IgM/9D8/4D10</u>	
Zellfamilie: <u>CHO rekombinant</u> Datum: <u>11.10.2011</u> Bearbeiter: <u>Veronika Chromikova</u> Passage/Gen.: _____ ATK <input type="checkbox"/> Produktion/ZZ: _____ Position: <u>A</u> <u>3/9</u> <u>51 - 56</u> Amp. Zahl: <u>6</u>	
ZELLTYP CHO DG44 <hr/> Herkunft <hr/> Marker DHFR, G418 <hr/> Kulturbedingungen 37°C / 7% CO ₂ <hr/> Medium ProCHO5 + 4 mM L-Gln + 0,5 mg/ml G418 + 0,096 µM MTX <hr/> Opt. Pass.verh. <u>ca 1:3</u> <input checked="" type="checkbox"/> Suspension <input type="checkbox"/> Adhärenz	Auftaukontrolle / Entnahmen 06.10.2014 Nr. 2 David Reinhart 15.01.2014 Nr. 3 Veronika Chromikova 08.08.2013 Nr. 4 Reinhard Beyer 28.01.2013 Nr. 5 Veronika Chromikova 23.04.2012 Nr. 6 Veronika Chromikova
Anmerkungen	
05.03.2015 Unterschrift:	

611

Zelllinie: <u>CHO-2G12IgM germline variante</u>	
Code: <u>CHO 2G12-IgM_GL/1F11/6D8</u>	
Zellfamilie: <u>CHO rekombinant (DG44)</u>	
Datum: <u>17.05.2013</u> Bearbeiter: <u>Alexander Mader</u>	
Passage/Gen.: _____	<div>ATK <input type="checkbox"/></div>
Produktion/ZZ: _____	
Position: <u>A</u> <u>3/9</u> <u>27 - 30</u> Amp. Zahl: <u>4</u>	
ZELLTYP CHO DG44	Auftaukontrolle / Entnahmen 06.10.2014 Nr. 2 David Reinhart 15.01.2014 Nr. 3 Veronika Chromikova 08.08.2013 Nr. 4 Reinhard Beyer
Herkunft Transfektion von Stefan Bauernfried 18.12.2012 (PEI) / Subklonierung A.Mader April/Mai 2013	
Marker DHFR, G418	
Kulturbedingungen 37°C / 7% CO2	
Medium ProCHO5 + 4 mM L-Gln + 0,5 mg/ml G418 + 0,096 µM MTX	
Opt. Pass.verh. <u>ca 1:4-1.5</u>	
<input checked="" type="checkbox"/> Suspension <input type="checkbox"/> Adhärent	
Anmerkungen 	

05.03.2015

Unterschrift:

473

Zelllinie: <u>CHO-HB617</u>	
Code: <u>CHO HB617/3E11/5G7</u>	
Zellfamilie: <u>CHO rekombinant</u>	
Datum: <u>13.11.2011</u>	Bearbeiter: <u>Veronika Chromikova</u>
Passage/Gen.: _____	ATK <input type="checkbox"/>
Produktion/ZZ: _____	
Position: <u>A</u> <u>3/9</u> <u>61 - 66</u> Amp. Zahl: <u>6</u>	
ZELLTYP CHO DG44	Auftaukontrolle / Entnahmen 06.10.2014 Nr. 2 David Reinhart 15.01.2014 Nr. 3 Veronika Chromikova 08.08.2013 Nr. 4 Reinhard Beyer 28.01.2013 Nr. 5 Veronika Chromikova 23.04.2012 Nr. 6 Veronika Chromikova
Herkunft	
Marker DHFR, G418	
Kulturbedingungen 37°C / 7% CO2	
Medium ProCHO5 + 4 mM L-Gln + 0,5 mg/ml G418 + 0,096 µM MTX	
Opt. Pass.verh. <u>ca 1:3</u>	
<input checked="" type="checkbox"/> Suspension <input type="checkbox"/> Adhärent	
Anmerkungen	

05.03.2015

Unterschrift:

11.6 Glycosylation analysis-report

Department for Chemistry, Division of Biochemistry

DI Clemens Gruber, Dr. Friedrich Altmann

Vienna, Jan 27, 2015

Analysis report

Analysis of recombinantly produced IgM grown on different carbon sources

Aim

1. identify sequence (three possible IgM sequences)
2. identify glycosylation

Samples

Gal, Pro, Glc and Man

Analyses performed

LC-ESI-MS of tryptic and GluC peptides with data mining using GPM and manual searches

MATERIAL AND METHODS

Peptide analysis

The relevant protein bands were cut out and digested in gel. The proteins were S-alkylated with iodoacetamide (in gel) and digested with modified trypsin (Promega) or GluC (Roche) and trypsin.

About 1 µg of each digest was loaded on a BioBasic C18 column (BioBasic-18, 150 x 0.32 mm, 5 µm, Thermo Scientific) using 0.1% formic acid as the aqueous solvent. A gradient from 95% solvent A and 5% solvent B (Solvent A: 65 mM ammonium formate buffer pH 3, B: 100% acetonitrile) to 32% B in 35 min was applied, followed by a 15min gradient from 32% B to 75% B that facilitates elution of large peptides, at a flow rate of 6 µL/min. Detection was performed with a QTOF MS (Bruker maxis 4G ETD) equipped with the standard ESI source in positive ion, DDA mode (= switching to MSMS mode for eluting peaks). MS-scans were recorded (range: 150-2200 Da) and the 6 highest peaks were selected for fragmentation. Instrument calibration was performed using ESI calibration mixture (Agilent).

The analysis files were converted (using Data Analysis, Bruker) to mgf files, which are suitable for performing a MS/MS ion search with GPM. GPM is a web-based, open source user interface for analyzing and displaying protein identification data. The interface creates a series of web browser page views of tandem mass spectrometry data that has been assigned to protein sequences.

Sequences:

>IgM_David_AK1

QVQLVQSGAEMKPGASVKVCKASGYTFSFAMHWVRQAPGQRLEWMGWINAGNGNTKYSQKFQGRITITRDTASTAYMDLSSLRSEDTAVYYCARNLNYYDI
LTGLDAFDIWGQGTMTVSSGGASAPTLFPLVSCENSPSDTSSVAVGCLAQDFLPDSITFSWKYKNNSSDISSTRGFPSVLRGGKYAATSQVLLPSKDVMQGTDEHVV
CKVQHPNGNKEKNVLPVIAELPPKVSFVPPRDGFFGNPRKSKLICQATGFSPRQIQVSWLREGKQVGSVTTDQVQAEAKESGPTTYKVTSTLTIKESDWLSQSMFT
CRVDHRLTFFQKNASMCVPDQDTAIRVFAIPPSFASIFLTSTKLTCLVDTLTYDSVTISWTRQNGEAVKTHTNISESHPNATFSAVGEASICEDDWNNGERFTCTVT
HTDLPSPKQTSRPGKVALRRPDVYLLPPAREQLNLRRESATITCLVTGFSPADVFVQWMQRGQPLSPERYVTSAPMPEPQAPGRYFAHSILTVSEEEWNTGETYTCVV
AHEALPNRVTERTVDKSTGKPTLYNVS LVMSDTAGTCY

>IgM_David_AK2

EVQLVESGGGLVKAGGSLILSCGVSNFRISAHTMNWVRRVPGGGLWVASISTSSYRDYADAVKGRFTVSRDDLEDFVYLQMHKMRVEDTAIYYCARKGSDRLSDN
DPFDAGWPGTMTVSPGASAPTLFPLVSCENSPSDTSSVAVGCLAQDFLPDSITFSWKYKNNSSDISSTRGFPSVLRGGKYAATSQVLLPSKDVMQGTDEHVVCKVQ
HPNGNKEKNVLPVIAELPPKVSFVPPRDGFFGNPRKSKLICQATGFSPRQIQVSWLREGKQVGSVTTDQVQAEAKESGPTTYKVTSTLTIKESDWLSQSMFTCRVDH
RGLTFQKNASMCVPDQDTAIRVFAIPPSFASIFLTSTKLTCLVDTLTYDSVTISWTRQNGEAVKTHTNISESHPNATFSAVGEASICEDDWNNGERFTCTVTHTDLP
PLKQTSRPGKVALRRPDVYLLPPAREQLNLRRESATITCLVTGFSPADVFVQWMQRGQPLSPERYVTSAPMPEPQAPGRYFAHSILTVSEEEWNTGETYTCVVAHEALP
NRVTERTVDKSTGKPTLYNVS LVMSDTAGTCY

>IgM_David_AK3

EVQLVESGGGLVKAGGSLILSCAASNFRISAHTMNWVRRAPGGGLWVASISTSSYRDYADAVKGRFTVSRDDAENFVYLQMNLSRVEDTAIYYCARKGSDRLSDN
DPFDAGWPGTMTVSPGASAPTLFPLVSCENSPSDTSSVAVGCLAQDFLPDSITFSWKYKNNSSDISSTRGFPSVLRGGKYAATSQVLLPSKDVMQGTDEHVVCKVQ
HPNGNKEKNVLPVIAELPPKVSFVPPRDGFFGNPRKSKLICQATGFSPRQIQVSWLREGKQVGSVTTDQVQAEAKESGPTTYKVTSTLTIKESDWLSQSMFTCRVD
HRLTFFQKNASMCVPDQDTAIRVFAIPPSFASIFLTSTKLTCLVDTLTYDSVTISWTRQNGEAVKTHTNISESHPNATFSAVGEASICEDDWNNGERFTCTVTHTDLP
SPLKQTSRPGKVALRRPDVYLLPPAREQLNLRRESATITCLVTGFSPADVFVQWMQRGQPLSPERYVTSAPMPEPQAPGRYFAHSILTVSEEEWNTGETYTCVVAHEAL
PNRVTERTVDKSTGKPTLYNVS LVMSDTAGTCY

[N-glycosylation sites] [unique peptide sequence used for identification]

RESULTS

Sequences identified

In all samples unique peptides originating from the IgM sequences AK1 and AK3 were identified. Interestingly the concentrations/ratios of these differ. In the following tables the ratios of the unique peptides ASGYTFSSFAMHWVR (AK1) and AGGSLILSCAASNFR (AK3) are shown. Note that the cysteine of AGGSLILSCAASNFR occurs in two different variants (carbamidomethylated-CAM or with acrylamide adducts-PAM).

GAL	RT [min]	Area	Intens.	Chromatogram	Ratio (AK1/AK3)
Pep AK1	23.6	2706506	88212	BPC 873.9060±0.05 +All MS	3.948
Pep AK3 CAM	33.1	685517	30510	BPC 769.3930±0.05 +All MS	3.9 x more HB617

GLC	RT [min]	Area	Intens.	Chromatogram	Ratio (AK1/AK3)
Pep AK1	23.5	2652031	85608	BPC 873.9060±0.05 +All MS	0.278
Pep AK3 CAM	27.8	8489346	287557	BPC 762.3850±0.05 +All MS	3.6 x more GL
Pep AK3 PAM	28	1059891	40498	BPC 769.3930±0.05 +All MS	

PRO	RT [min]	Area	Intens.	Chromatogram	Ratio (AK1/AK3)
Pep AK1	23.5	1529390	47747	BPC 873.9060±0.05 +All MS	0.029
Pep AK3 CAM	27.9	47096837	1558635	BPC 762.3850±0.05 +All MS	34.5 x mehr GL
Pep AK3 PAM	28.1	6503909	222024	BPC 769.3930±0.05 +All MS	

MAN	RT [min]	Area	Intens.	Chromatogram	Ratio (AK1/AK3)
Pep AK1	23.6	2767219	86351	BPC 873.9060±0.05 +All MS	0.281
Pep AK3 CAM	28	8697545	300809	BPC 762.3850±0.05 +All MS	3.6 x mehr GL
Pep AK3 PAM	28.2	1151550	41942	BPC 769.3930±0.05 +All MS	

Glycosylation

In the following tables the glycan distribution of glycopeptide 3 (THTNISE) is shown. The monoisotopic peak and four isotope peaks are considered as well as two different charge states (2-times and 3-times charged).

GLC	RT [min]	Area	Intens.	%
NaNaNNaF	6.3	40873	2780	0.32
NaNaAF	6.3	1002591	32993	7.84
NaNaF	6.4	3761291	152589	29.43
NaAF	6.4	4592649	187345	35.93
AAF	6.4	2869409	119447	22.45
AGnF	6.4	515701	22986	4.03

GAL	RT [min]	Area	Intens.	%
NaNNaF	7	194001.3	6853	3.26
NaAF	7	698202.4	20974	11.74
AAF	7	3388660	115089	60.26
AGnF	7.1	1051752	32416	17.68
GnGnF	7.2	420332.2	13913	7.07

PRO	RT [min]	Area	Intens.	%
NaNNaF	6.8	69698	3860	1.18
NaAF	6.8	939240	34155	15.91
AAF	6.9	2598076	107281	46.82
AGnF	6.9	1258730	39548	21.33
GnGnF	7	870994	29957	14.76

MAN	RT [min]	Area	Intens.	%
NaNNaNNaF	6.5	26204	1576	0.18
NaNNaAF	6.5	1168370	29350	8.01
NaNNaF	6.6	4658595	198109	31.92
NaAF	6.6	5263830	222045	36.07
AAF	6.6	2874174	128616	21.10
AGnF	6.7	398075	14913	2.73